

Alma Mater Studiorum- Università di Bologna

**DOTTORATO DI RICERCA IN**

**SCIENZE BIOLOGICHE, BIOCOMPUTAZIONALI,  
FARMACEUTICHE E FARMACOLOGICHE**

Ciclo 33

**Settore Concorsuale:** 05/A1 - BOTANICA

**Settore Scientifico Disciplinare:** BIO/15 - BIOLOGIA FARMACEUTICA

**NEW APPROACHES TO PLANT-BASED DRUG DISCOVERY**

**Presentata da:** Mariacaterina Lianza

**Coordinatore Dottorato**

Maria Laura Bolognesi

**Supervisore**

Ferruccio Poli

**Esame finale anno 2021**

## Abstract

Natural products have been used to treat or prevent human or animal diseases since time immemorial. Although the value of natural products is widely recognised, plant-based drug discovery presents several challenges. New methods are needed for the rapid analysis of plant extracts, with minimal consumption of starting plant material, resources and time. Moreover, techniques enabling the extrapolation of many types of information with a single analysis are required.

Considering the challenges of plant-based drug discovery, new approaches for the study of plant extracts and the identification of the active metabolites are presented in this thesis.

Among the most recent techniques, metabolomics coupled with chemometrics is particularly outstanding. The goal of metabolomics is the comprehensive study of the low molecular weight molecules within an organism, by comparing data from many samples through multivariate analysis.

In this thesis the metabolomic-chemometric approach was applied in a screening of thirty-six plant extracts for antibacterial activity. The PCA model, built on the data of biological activity, cytotoxicity, polyphenol and flavonoid content, enabled the identification of the most promising extracts and provided an insight that allowed several considerations and inputs for future studies. The same technique was used to reap phytochemical variations of *Arbutus unedo* leaves samples, collected under different conditions. The hydroalcoholic leaves extract of *A. unedo* resulted endowed with antibacterial activity in the screening mentioned above. The metabolomic-chemometric approach led to the identification of the most diverse samples which were found to exhibit different antibacterial activities, demonstrating that the composition and biological activity of plant extracts are highly dependent on the conditions under which samples are collected. Moreover, one of the compounds responsible for antibacterial activity, namely kaempferol-3-O-rhamnoside, was identified.

One of the major issues of plant-based drug discovery is avoiding the cost and time-consuming isolation of compounds already known in literature. The rapid identification of known molecules is referred to dereplication approach. Amaryllidaceae alkaloids are a group of secondary metabolites with a wide range of biological activities and structural variety, to date more than 600 alkaloids were characterized. The most occurring alkaloids are widely known both for chemical structure and bioactivities, hence, these metabolites were selected for the development of a dereplication protocol. The method allowed the characterization of the bulb extract of *Urceolina peruviana* working directly on the fractions of the extract without resorting to purification processes, saving time and resources. Only the fraction containing an alkaloid whose NMR profile was absent in the databases was purified. This alkaloid presented a peculiar structure, with two nitrogen atoms. The new alkaloid was named 6-dehydroxy-6-acetamido-nerinine.

# NEW APPROACHES TO PLANT-BASED DRUG DISCOVERY

<b>1.INTRODUCTION</b> .....	<b>1</b>
<b>1.1 Natural products in plant-based drug discovery</b> .....	<b>1</b>
<b>1.2 Challenges of plant-based drug discovery</b> .....	<b>4</b>
<b>2. AIMS OF THE THESIS</b> .....	<b>5</b>
<b>3. PLANTS AS SOURCE OF ANTIBACTERIAL AGENTS</b> .....	<b>6</b>
<b>3.1 Introduction</b> .....	<b>6</b>
<b>3.1.1 Metabolomic-Chemometric approach</b> .....	<b>8</b>
<b>3.1.2 NMR-based metabolomics</b> .....	<b>8</b>
<b>3.1.3 Data analysis</b> .....	<b>9</b>
<b>3.2 SCREENING OF THIRTY-SIX SARDINIAN PLANTS FOR ANTIBACTERIAL ACTIVITY...</b>	<b>13</b>
<b>3.2.1 Introduction</b> .....	<b>13</b>
<b>3.2.2 Material and methods</b> .....	<b>14</b>
<b>3.2.3 Results and discussion</b> .....	<b>19</b>
<b>3.2.4 Conclusions</b> .....	<b>29</b>
<b>3.3 ARBUTUS UNEDO L., A SOURCE OF ANTIBACTERIAL AGENTS. PHYTOCHEMICAL AND BIOACTIVITY VARIATIONS OF SAMPLES COLLECTED UNDER DIFFERENT CONDITIONS.</b> .....	<b>30</b>
<b>3.3.1 Introduction</b> .....	<b>30</b>
<b>3.3.2 Materials and methods</b> .....	<b>31</b>
<b>3.3.3 Results and discussion</b> .....	<b>34</b>
<b>Phytochemical variation of <i>A. unedo</i> leaves extracts collected in different conditions.</b> .....	<b>34</b>
<b>Bioactivity variations of <i>A. unedo</i> leaves extracts</b> .....	<b>40</b>
<b>Characterization of the active metabolites</b> .....	<b>43</b>
<b>3.3.4 Conclusions</b> .....	<b>47</b>
<b>4 RAPID IDENTIFICATION OF AMARYLLIDACEAE ALKALOIDS IN BULB EXTRACT OF URCEOLINA PERUVIANA (C. Presl) J.F. Macbr</b> .....	<b>48</b>
<b>4.1 Introduction</b> .....	<b>48</b>
<b>4.1.1 Dereplication</b> .....	<b>50</b>
<b>4.1.2 Amaryllidoideae subfamily and Amaryllidaceae alkaloids</b> .....	<b>51</b>
<b>4.1.3 <i>Urceolina peruviana</i> (C. Presl) J.F. Macbr</b> .....	<b>53</b>
<b>4.2 Material and methods</b> .....	<b>54</b>
<b>4.3 Results and discussion</b> .....	<b>57</b>
<b>Alkaloid extraction</b> .....	<b>57</b>

<b>Fractionation of extract by Centrifugal Partition Chromatography in pH-zone refining mode ...</b>	<b>60</b>
<b>UPLC-HRMS analysis of alkaloid extract and CPC fractions.....</b>	<b>63</b>
<b>Identification of Amaryllidaceae alkaloids by dereplication.....</b>	<b>66</b>
<b>Structure elucidation of the new alkaloid.....</b>	<b>75</b>
<b>NMR data of identified alkaloids .....</b>	<b>76</b>
<b>4.4 Conclusion.....</b>	<b>86</b>
<b>5 CONCLUSIONS.....</b>	<b>87</b>
<b>REFERENCES .....</b>	<b>88</b>

# 1.INTRODUCTION

## 1.1 Natural products in plant-based drug discovery

Natural products from plants have been the basis of treatment of human diseases since the existence of human civilization. Crude and semi-pure extracts administered as tinctures, teas, poultices, powders and other herbal formulations, represented the only medications available to treat human and domestic animal illnesses until the 19<sup>th</sup> century. In 1805, the isolation of morphine from Opium and the advancement of the receptor theory of drug action revolutionized the thinking in the use of drugs and lead to the beginning of a totally new era in pharmacology since pure, isolated chemicals, instead of extracts, became the standard treatments for diseases. Hence, many bioactive compounds, responsible for the effects of crude extracts, were isolated and their chemical structure was elucidated<sup>1</sup>. Natural products from plants with biological activity are secondary metabolites. Differently from primary metabolites, these molecules are not essential for plant life, they are the products of the secondary metabolism that is generally activated as response to the environment, for adaptation and defence. Hence, temperature, humidity, light intensity, supply of water, minerals, pathogens, the presence of others growing species strongly influence the production of these compounds by plants<sup>2</sup>. From the chemical point of view, the secondary metabolites can be classified into three main groups: terpenes, phenols and N (Nitrogen) and S (Sulphur) containing compounds<sup>3</sup>. Terpenes form the biggest group of secondary metabolites, this group is very heterogeneous both from a structural and functional point of view. They all derive from isopentenyl diphosphate (IPP) and its isomer dimethylallyl diphosphate (DMAPP), defined as isoprene units. Depending on the number of isoprene units, they are chemically classified in monoterpenes, sesquiterpenes, diterpenes, triterpenes and polyterpenes<sup>4</sup>. They are part of both primary and secondary metabolism, in fact metabolites such as quinones, chlorophylls, carotenoids and steroids are essential for maintaining the basic functions of the plant cell, conversely, terpenes with ecological functions, e.g. pollination, defence against herbivores or pathogens and allelopathic molecules are classified as secondary metabolites<sup>5,6</sup>. Phenols are secondary metabolites characterized by a benzene bearing one or more hydroxyl groups. They all derive from shikimic acid pathway and they are considered to provide many of the healing properties of plant extracts. Flavonoids, coumarins, tannins, lignins and anthocyanins belong to this group. Many functions of phenolic compounds have yet to be elucidated, however it is clear they are produced in the highest quantities under stressful conditions. It has been proven that many flavonoids protect plants from UV radiation by acting as antioxidants<sup>7</sup>, many polyphenols defend against the attack of microorganisms by acting as antibacterial, antifungal and

antiviral<sup>8</sup>, tannins make the plant less attractive to herbivores, while anthocyanins play an important role in the development of flowers and fruits<sup>3,9</sup>.

Sulphur containing compounds, such as glucosinolates and alliinins, defend plants by releasing volatile compounds and regulating the absorption of sulphur from the soil<sup>10</sup>. Finally, Nitrogen containing compounds include alkaloids, non-protein amino acids, cyanogenic glycosides, glucosinolates and other molecules<sup>11</sup>. Among them, alkaloids were the first secondary metabolites to be isolated and used as pure substances due to their wide structural variety and remarkable bioactivities. Morphine, quinine, vinblastine are some examples of potent alkaloids commonly used in medicine for their analgesic, antimalarial and anticancer activity, respectively<sup>12</sup>.

Hence, plant secondary metabolites are an invaluable source of active ingredients.

However, over the last twenty years the interest in plant-based drug discovery has fallen, certainly as a result of the impact and hopes for other drug discovery methodologies such as the combinatorial chemistry and the high throughput screening (HTS)<sup>13</sup> which favour the use of synthetic products rather than natural products<sup>14</sup>. Nevertheless, the results obtained from the use of large synthetic compound libraries were unsatisfactory, since the number of new discovered drugs fell. Actually, while in 1990 the number of approved drugs by the Food and Drug Administration (FDA) was forty-five, in 2010 only twenty-one molecules were placed on the market<sup>15</sup>. Therefore, in recent years plant-based drug discovery has recovered its value. The chemical diversity offered by natural products is superior to that of synthetic libraries, plants bioactive compounds are produced to interact with biological systems thus they are already predisposed to interact with ligands, moreover they are generally well tolerated. Newman and Cragg reported all the new therapeutic agents approved from January 1981 to September 2019<sup>16</sup> (Fig. 1). The paper showed that the 23.5% of the new drugs is represented by unmodified natural products (N, 3.8%), botanicals “defined mixtures” now recognized as drug entities (NB, 0.8%) and by derived from natural products (ND, 18.9%), generally semisynthetic compounds from natural molecules. Moreover, among the synthetic approved drugs many compounds were “natural product mimic” (S\*/NM and S/NM) or inspired by a natural pharmacophore (S\*). Conversely, the totally synthetic drugs (S) represented only the 24.6% of the approved compounds.

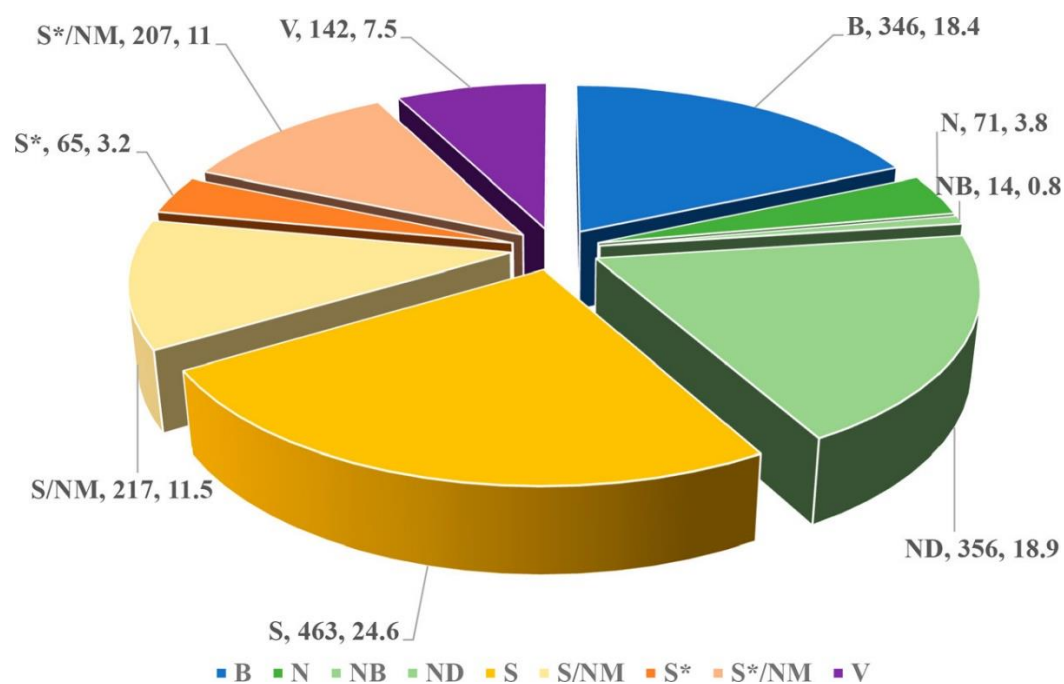


**Figure 1:** All new approved drugs from 01 January 1981 to 30 September 2019; n = 1881. “B”: Biological; usually a large (>50 residues) peptide or protein either isolated from an organism/cell line or produced by biotechnological means in a surrogate host. “N”: Natural product. “NB”: Natural product “Botanicals”. “ND”: Derived from a natural product, usually a semisynthetic modification. “S”: Totally synthetic drug, often found by random screening/modification of an existing agent. “S\*”: Made by total synthesis, but the pharmacophore is/was a natural product. “V”: Vaccin. “S\*/NM” and “S/NM”: natural product mimic. Newman and Cragg, 2020.

Definitely, plant-based drug discovery continues to be an important source of compounds both to be employed as they are and to be used as lead for the production of semi-synthesis molecules.

## 1.2 Challenges of plant-based drug discovery

The chemical variability associated with natural products is higher than with synthetic products, this is particularly important in lead research, hence, plant-based drug discovery cannot be replaced<sup>17</sup>. However, there are several difficulties and disadvantages in dealing with plant-based drug discovery. First of all, finding plant material can be very hard, this phase is often accompanied by a controversial time-consuming bureaucracy, as in the case of protected species or plants found in foreign countries for which different authorisations are required. Another problem is represented by the amount of plant material required to carry out experiments. Actually, secondary metabolites are produced in low concentration by plants, therefore, to extract large quantities of them it is necessary to start from an abundant source material. Others discouraging factors are the complexity of natural products chemistry and the repeated isolation already known metabolites<sup>18</sup>. The processes for the isolation of pure molecules from plant extracts are time-consuming and expensive, the recurrent isolation of molecules known both as chemical structure and biological activity was one of the main reasons that led Pharmaceutical Industries to invest in other sources of lead compounds in recent past years<sup>19</sup>. The scientific community is requested to propose solutions to the abovementioned problems. Hence, it is necessary to develop new techniques for the study of plant extracts that require the minimum consumption of resources, both in terms of starting plant material and reagent consumption. Moreover, there is a need for methods that avoid the isolation of already known molecules, i.e. dereplication protocols. With this aims, new approaches to plant-based drug discovery will be discussed. Specifically, the metabolomic-chemometric approach for the search of antibacterial agents and the elaboration of a dereplication protocol for Amaryllidaceae alkaloids will be reported.

## 2. AIMS OF THE THESIS

Based on the challenges of plant-based drug discovery, the aims of this thesis concerned the study of plant extracts and the research of bioactive metabolites through modern techniques that can satisfy the needs of the scientific community. In particular, the adopted methodologies focused to reduce the starting quantity of plant material, to obtain multiple information with a single analysis and to reduce investigation time and costs.

Hence, this thesis had two main objectives:

- The application of the metabolomic-chemometric approach as guide for the identification of new sources of antibacterial agents in a screening of thirty-six Sardinian plant species and for the analysis of *Arbutus unedo* hydroalcoholic leaves extract,
- The elaboration of a dereplication protocol for Amaryllidaceae alkaloids for the characterization of *Urceolina peruviana* bulb extract.

### 3. PLANTS AS SOURCE OF ANTIBACTERIAL AGENTS

#### 3.1 Introduction

Plants secondary metabolites have been and continue to be studied since they have shown evident and varied biological activities<sup>16,20</sup>. In particular, in fighting infections plants secondary metabolites showed positive effects, actually there are many worldwide ethnobotanical uses that testify to the antibacterial effect of plant extracts<sup>21-23</sup>. Unfortunately, the indiscriminate use of antibiotics on both humans and animals and by food-producing industries has led to increasing resistance from bacteria. In fact, bacteria have developed defence mechanisms against the action of the commonly used drugs, therefore the antibiotics which have always been successful used to treat infections nowadays can fail. The World Health Organization reported that the rate of resistance to ciprofloxacin, an antibiotic commonly used to treat urinary tract infections, varied from 8.4% to 92.9% for *Escherichia coli* and from 4.1% to 79.4% for *Klebsiella pneumoniae* in countries reporting to the Global Antimicrobial Resistance and Use Surveillance System (GLASS). *Escherichia coli* and *Klebsiella pneumoniae* cause urinary tract infections and pneumonia, respectively. High levels of resistance to the most commonly used drugs such as cephalosporins, carbapenems and fluoroquinolones have been reported for these bacteria<sup>24,25</sup>. Particularly worrying is also the increasing drug resistance of *Staphylococci* bacteria, which are characterised by high virulence and rapid transmission from person to person<sup>26,27</sup>. In fact, methicillin-resistant *S. aureus* (MRSA) and *S. epidermidis* (MRSE) are one of the main causes of airway and epidermis infections<sup>28,29</sup>. In this situation, finding new therapeutic agents is urgent. The secondary metabolites of plants are once again excellent candidates because of their small size, their ability to interact with biological systems, their high tolerability, low side effects and their great chemical variety that only nature can offer. Plants metabolites exert their antibacterial action in different ways: they can lead to the disruption of bacterial membrane inhibiting bacterial efflux pumps<sup>30</sup>, they can interfere with bacteria quorum sensing<sup>31</sup>, they can impede the intermediary metabolisms as well as the DNA and RNA synthesis or function<sup>32</sup>. Moreover, many plant extracts, although they do not kill bacteria directly, can be successfully used in combination to antibiotics to expand the antimicrobial spectrum, reduce the antibiotic dose with the consequent limitation of toxic effects and prevent antibacterial resistance<sup>33</sup>. As shown in Figure 2, from January 1981 to September 2019, 162 molecules were approved as antibacterial, 89 of these, i.e. almost the 55%, were natural

products (N) or derived from natural products (ND), one drug, the brodimoprin approved in 1993, was a synthetic modification of a pharmacophore from a natural product (S\*/NM), while 36 therapeutic agents (22.2%) were totally synthetic (mainly quinolone-based).

Metabolites from plants possess a great potential in fighting infections. Based on this, a part of this thesis is dedicated to the research of plant extracts with antibacterial activity. This goal was achieved through a new approach for the study of plant extracts namely Metabolomics coupled to Chemometrics.

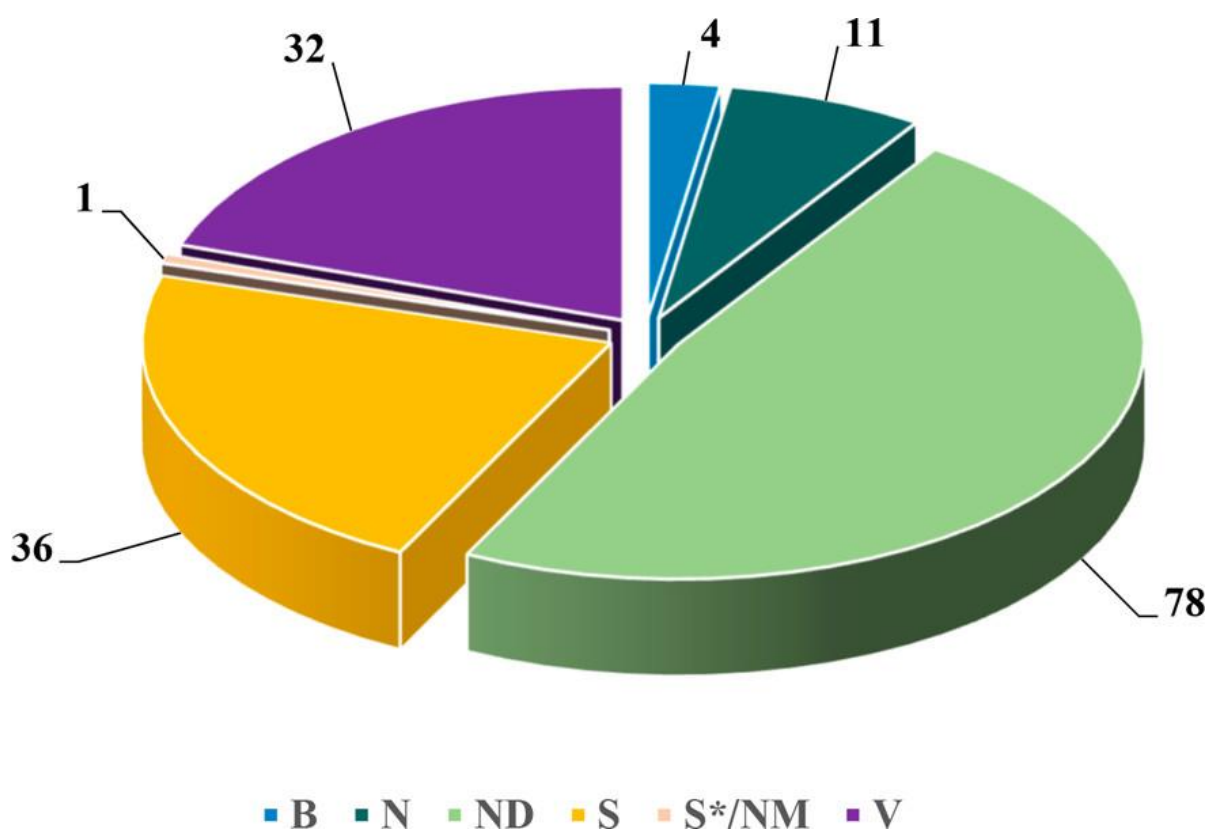


**Figure 2:** Approved antibacterial drugs by source from 01 January 1981 to 30 September 2019. “B”: Biological. “N”: Natural product. “ND”: Derived from a natural product, usually a semisynthetic modification. “S”: Totally synthetic drug, often found by random screening/modification of an existing agent. “S\*/NM”: Made by total synthesis, but the pharmacophore is/was from a natural product. “V”: Vaccin. Newman and Cragg 2020.

### **3.1.1 Metabolomic-Chemometric approach**

The term metabolomics refers to the area of scientific research that deals with the study of the metabolome of an organism<sup>34</sup>. The metabolome consists of all the metabolites produced by the organism, hence metabolomics aim at measuring all metabolites in a determined time and under certain conditions both in qualitative and quantitative aspects<sup>35</sup>. The metabolites of metabolomics are small molecules with a molecular weight between 30 and 3000 Da, that means that polymeric molecules such as DNA, RNA and proteins are not covered.

A metabolomic study can have a targeted or an untargeted approach. The first approach is used when the interest of the research deals with specific classes of metabolites, conversely the untargeted approach focus on a general view of the metabolome. Generally, the untargeted approach is employed to generate a hypothesis that is then confirmed with a targeted approach<sup>36</sup>. To achieve this goal numerous metabolic fingerprints are acquired and then compared through multivariate analysis to detect the differences between them, hence a large number of samples are required<sup>35</sup>.

The applications of metabolomics are plentiful and involve many different fields, it has been used for diagnosis of disease<sup>37</sup>, evaluation of drug toxicity<sup>38</sup>, food quality control<sup>39</sup> and for the analysis of complex mixtures such as the plant extracts<sup>40</sup>. Several techniques can be employed for metabolomics studies, the most common and powerful are Nuclear Magnetic Resonance (NMR) and Mass Spectrometry (MS) coupled to separation techniques, including Gas Chromatography (GC-MS), Liquid Chromatography (LC-MS) and Ultra Performance Liquid Chromatography (UPLC-MS)<sup>41</sup>.

In the following studies the metabolomic-chemometric approach was applied for the analysis of plant extracts with an untargeted approach by the employment of NMR.

### **3.1.2 NMR-based metabolomics**

NMR is one of the most suitable technique for the metabolomic-chemometric approach.

NMR allows the detection of different classes of plant metabolites simultaneously, without resorting to sample pre-treatment (e.g. derivatization). This technique is non-destructive, hence the sample can be recovered after the analysis. Moreover, NMR signals are proportional to the molar concentration making possible the comparison among the metabolites, thus their amount in a mixture can be

determined. NMR is a great technique for structure elucidation, therefore some compounds present in the sample can be directly recognized<sup>42</sup>. Like every technique, also NMR have some limitations, the most limitative is the sensitivity. Actually, NMR requires more amount of sample in comparison to other analytical techniques (e. g. Mass Spectrometry). However, the evolution of NMR hardware is improving this aspect more and more, the use of cryoprobes has greatly enhanced the signal-to-noise ratio in NMR analysis, while the production of microprobes allows to analyse samples of a few microlitres<sup>43</sup>. Another limitation related to <sup>1</sup>H-NMR is the signals overlapping, plant extracts are generally complex like their NMR spectra. The multidimensional NMR spectroscopy can help to bypass this problem, possessing higher resolution than one-dimensional analysis<sup>44</sup>.

NMR-based metabolomics has been successfully applied to correlate bioactivities of plant extracts with their phytochemical diversity<sup>45,46</sup>, for quality control of species with nutraceutical and pharmacological interest<sup>47,48</sup>, for authentication of herbal medicines<sup>49</sup>, for quality control of herbal products<sup>50</sup>, to correlate genetic variations with metabolites expression<sup>51</sup> and to detect metabolic changes in response to the environment<sup>52,53</sup>.

### 3.1.3 Data analysis

A typical metabolomics study consists of three fundamental phases: the metabolomic fingerprint of a large number of samples is obtained, the metabolomic profiles are compared in order to capture the differences among them, the data are interpreted to generate a hypothesis.

In order to be able to compare metabolomic profiles through multivariate analysis, the data must be processed. In the case of NMR-based metabolomics the pre-processing procedures to be carried out on <sup>1</sup>H-NMR spectra usually involves: baseline correction, alignment, binning, normalization and scaling<sup>54,55</sup>. The baseline correction implies the correction of any baseline distortion in the <sup>1</sup>H NMR spectra, this is generally an automated procedure. However, this operation is not enough to be sure that the same signals of different spectra are aligned, i.e. that they fall at the same chemical shift value. Changes in temperature, pH, instrumental factors, etc. can cause the shift of NMR signals, hence another operation is required, namely alignment.

The alignment consists in setting the internal reference signal (e.g. Trimethylsilylpropanoic acid) of each spectrum at 0 ppm (Fig. 3).

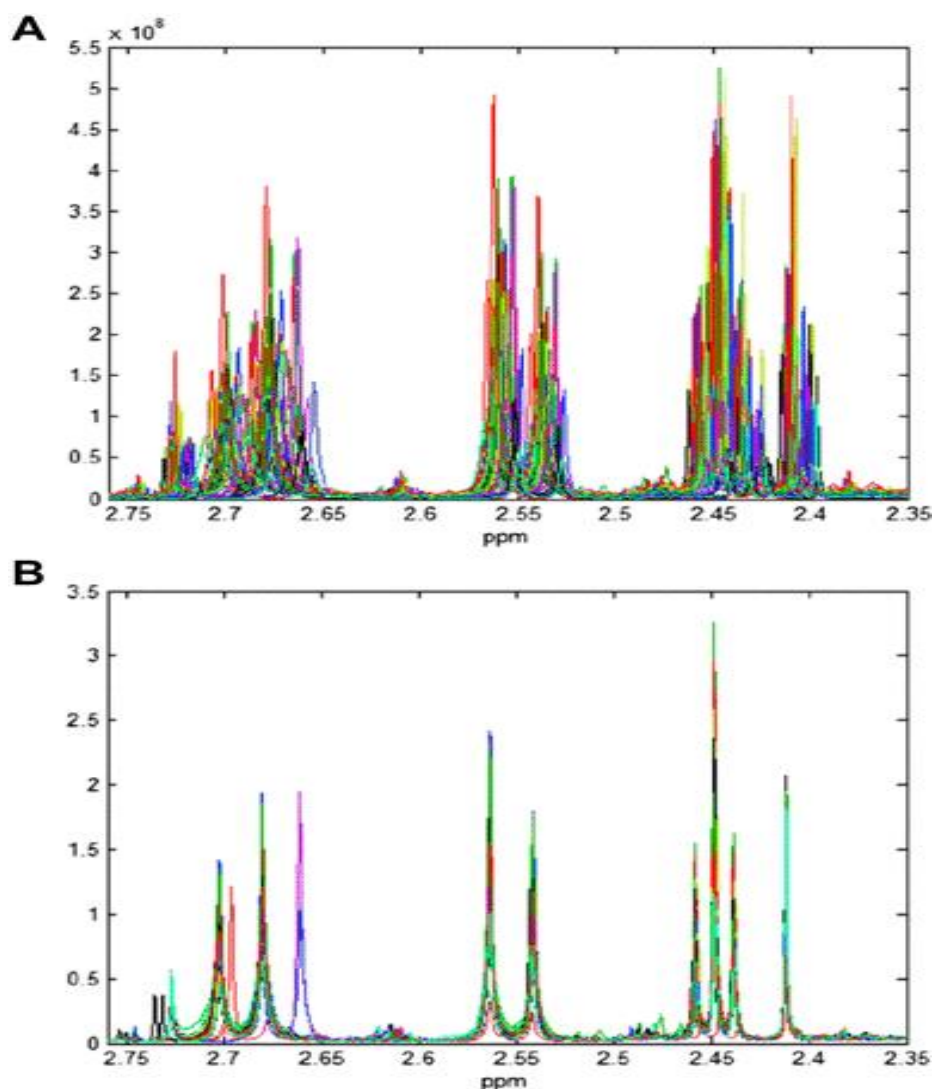


**Figure 3:** Example of NMR spectra before (A) and after (B) baseline correction and alignment

The baseline correction and the alignment remove the global shift in the NMR spectra, however, there may be local shifts that are not corrected by these operations.

The binning serves precisely to remedy these inaccuracies in chemical shifts, for the digitalization of NMR data in numeric values and for reducing the complexity of the data set. At this step solvents signals must be removed from the spectra. In the binning operation each spectrum is divided into bins (buckets) typically of 0.02 or 0.04 ppm (Fig. 4). It may happen that when binning is carried out a signal is divided between adjacent bins, in this case corrections are needed. For each bucket the sum of signals intensities is calculated and normalized. There are several alternatives to perform the normalization, the most used are the normalization by the area of the reference standard peak and by the sum of the total intensities.

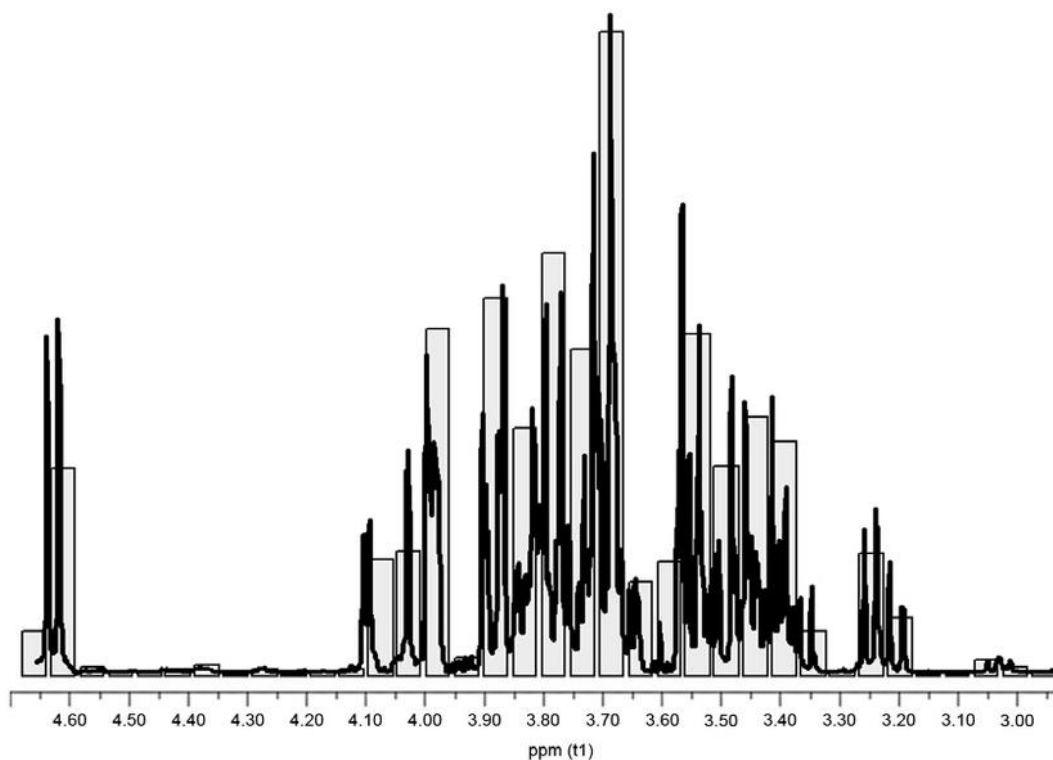


*Figure 4: Example of binning operation on  $^1\text{H-NMR}$  spectra*

To carry out these operations several software can be employed, for example AMIX-TOOLS (Bruker Topspin), ACD NMR Manager (ACD Labs) and MNova (Mestrelab)<sup>56</sup>. Independently of the software used, the binning leads to the conversion of NMR data into a format that can be used for subsequent statistical analysis (PCA, PLS etc.), this format is the ASCII file.

The  $^1\text{H-NMR}$  spectrum of a plant extract displays signals of many metabolites whose intensity is proportional to their concentration. Hence, the less abundant metabolites, that are often produced by the secondary metabolism of plants, are represented by less intense signals, conversely metabolites from primary metabolism show more intense signals. The most abundant signals have more influence on statistical analysis, such as PCA or PLS, to overcome this problem the scaling is carried out.

Several scaling methods can be employed to make all variable comparable to each other: Centering scaling, Unit Variance (UV) scaling, Pareto scaling, Vast scaling, Level scaling<sup>55</sup>. Each method applies a different mathematical equation and has disadvantages and advantages. In the pareto scaling the scaling factor is the square root of the standard deviation, this method is effective in reducing the influence of more abundant signals, hence is particularly suitable for the treatment of plant extract data. The data pre-processing is followed by multivariate analysis. The data can be analysed with two main approaches: the unsupervised and the supervised multivariate analysis.

The unsupervised analysis is used to obtain a general view of the data and understand possible relations among the samples and the variables that determine the arrangement of the statistical model.

Principal Component Analysis (PCA) and Hierarchical Clustering Analysis (HCA) are unsupervised multivariate analysis. PCA allows the simplification of the data set, in fact the variables are reduced in number and combined to form the principal components that define the layout of the score plot. In the score plot the samples with similar metabolomic fingerprint are close. This model is useful to identify trends in the data set.

Supervised multivariate analysis models are used to obtain informations on a specific class attribute which can be designated as Y variable. Partial Least Squares Discriminant Analysis (PLS-DA) and Orthogonal Projections to Latent Structure Discriminant Analysis (OPLS-DA) are examples of supervised models. PLS-DA and OPLS-DA allow to correlate the spectroscopic data to a class attribute facilitating the identification of metabolites<sup>49</sup>. However, since in these models there is a kind of forcing given by the imposition of a class attribute, the data may be overfitted, hence it is necessary to statistically validate the models for example by permutation test or cross validation<sup>57</sup>.

## **3.2 SCREENING OF THIRTY-SIX SARDINIAN PLANTS FOR ANTIBACTERIAL ACTIVITY**

### **3.2.1 Introduction**

The phenomenon of antibiotic resistance is becoming more and more common and raises many concerns. The search for new antibacterial agents becomes increasingly important. Plant extracts are a source of molecules with widely recognised antibacterial activity<sup>32,58</sup>. Their value is not only linked to the identification of new therapeutic agents but to the functioning of the extract with all its components which, although not antibacterial in themselves, can help the action of antibacterial molecules by inhibiting the resistance mechanisms of bacteria<sup>59,60</sup>.

The Italian island of Sardinia possesses extremely pronounced biodiversity due to its geographical isolation and the high geomorphological and geological diversification that results in a vastly varied and dynamic environment<sup>61,62</sup>. Sardinia is considered one of the most important biodiversity hot spots in the Mediterranean Basin<sup>63</sup>. In such an environment the production of secondary metabolites by plants is particularly stimulated, in fact, many endemic species can be found in Sardinia island, with peculiar phytochemical and genetic profiles<sup>64-66</sup>. Considering this background and that many Sardinian plants still need to be properly studied, thirty-six plant species from Sardinia, of which twelve endemics, have been selected and tested for their antibacterial activity both against Gram positive and negative bacteria. The most promising extract were also tested against fifteen clinical isolates with different antibiotic-resistance profiles. In addition, the content of polyphenols and flavonoids was measured and these data together with those of antibacterial activity and cytotoxicity were treated with multivariate analysis to assess possible correlations.

### 3.2.2 Material and methods

#### *Plant material*

Plant material was harvested in Sardinia (Italy) during a period of time covering both the years 2017 and 2018. The plants were identified by Dr. Cinzia Sanna and Prof. Andrea Maxia and the vouchers were deposited at the General Herbarium of the Department of Life and Environmental Sciences, University of Cagliari. The list of plants is reported in Table 1.

Plant name	Plant organ and sample label	Family	Place of collection	Collection date	Voucher
<i>Arbutus unedo</i> L.	Fruits (AuF)	Ericaceae	Jerzu	December 2017	Herbarium CAG 878
	Leaves (AuL)		Jerzu	December 2017	
<i>Asphodelus ramosus</i> L. subsp. <i>ramosus</i>	Rhizome (ArRh)	Asphodelaceae	Geremeas	April 2017	Herbarium CAG 1405
	Leaves (ArL)		Geremeas	April 2017	
<i>Carlina gummifera</i> (L.) Less.	Leaves (CgL)	Asteraceae	Cala Surya (Cardedu)	July 2018	Herbarium CAG 770
<i>Centaurea calcitrapa</i> L.	Aerial parts (CcA)	Asteraceae	Siliqua	June 2017	Herbarium CAG 781
<i>Centaurea horrida</i> Badarò*	Aerial parts (ChA)	Asteraceae	Capo Falcone	June 2017	Herbarium CAG 777
<i>Centaurea napifolia</i> L.	Aerial parts (CnA)	Asteraceae	Uta	June 2017	Herbarium CAG 784
<i>Cistus monspeliensis</i> L.	Aerial parts (CmA)	Cistaceae	Cala Surya (Cardedu)	April 2018	Herbarium CAG 135
<i>Cistus salviifolius</i> L.	Aerial parts (CsA)	Cistaceae	Cala Surya (Cardedu)	April 2018	Herbarium CAG 135/C

<i>Cynara cardunculus</i> L.	Aerial parts (CycA)	Asteraceae	Siliqua	April 2017	Herbarium CAG 790
<i>Cytinus hypocistis</i> (L.) L.	Aerial parts (CyhA)	Cytinaceae	Gesturi	May 2017	Herbarium CAG 1200
<i>Ferula arrigonii</i> Bocchieri*	Leaves (FaL)	Apiaceae	Tharros	April 2017	Herbarium CAG 612/A
	Roots (FaR)		Tharros	April 2017	
<i>Galactites tomentosa</i> Moench	Aerial parts (GtA)	Asteraceae	Jerzu	September 2018	Herbarium CAG 789
<i>Genista corsica</i> (Loisel.) DC*	Aerial parts (GcA)	Fabaceae	Seui	May 2017	Herbarium CAG 286
<i>Glechoma sardoa</i> (Bég.) Bég.*	Aerial parts (GsA)	Lamiaceae	Gennargentu	June 2017	Herbarium CAG 1104
<i>Hypericum hircinum</i> L. ssp <i>hircinum</i> *	Aerial parts (HhA)	Hypericaceae	Jerzu	June 2018	Herbarium CAG 232
<i>Hypericum scruglii</i> Bacch., Brullo & Salmeri*	Aerial parts (HsA)	Hypericaceae	Jerzu	June 2018	Herbarium CAG 239/C
<i>Lavandula stoechas</i> L.	Aerial parts (LsA)	Lamiaceae	Cala Surya (Cardedu)	April 2017	Herbarium CAG 1067
<i>Limonium morisianum</i> Arrigoni*	Aerial parts (LmA)	Plumbaginaceae	Jerzu	December 2017	Herbarium CAG 909/G
<i>Myrtus communis</i> L.	Fruits (McF)	Myrtaceae	Cala Surya (Cardedu)	December 2018	Herbarium CAG 514

	Leaves (McL)		Poggio dei Pini	April 2018	
<i>Pistacia lentiscus</i> L.	Fruits (PIF)	Anacardiaceae	Cala Surya (Cardedu)	December 2017	Herbarium CAG 280
	Leaves (PIL)		Cala Surya (Cardedu)	December 2017	
<i>Pistacia terebinthus</i> L. <i>ssp.</i> <i>terebinthus</i>	Leaves (PtL)	Anacardiaceae	Jerzu	June 2018	Herbarium CAG 279
<i>Plagius flosculosus</i> (L.) Alavi & Heywood*	Aerial parts (PfA)	Asteraceae	Iglesias	July 2017	Herbarium CAG 743
<i>Ptilostemon casabonae</i> (L.) Greuter*	Aerial parts (PcA)	Asteraceae	Gairo Taqisara	June 2018	Herbarium CAG 796
<i>Rosmarinus officinalis</i> L.	Aerial parts (RoA)	Lamiaceae	Alghero	May 2017	Herbarium CAG 1091
<i>Santolina corsica</i> Jord. & Fourr*	Aerial parts (ScA)	Asteraceae	Monte Albo	November 2017	Herbarium CAG 732/A
<i>Scolymus hispanicus</i> L. <i>subsp.</i> <i>hispanicus</i>	Aerial parts (ShA)	Asteraceae	Sarroch	June 2018	Herbarium CAG 812
<i>Silybum marianum</i> (L.) Gaertn.	Aerial parts (SmA)	Asteraceae	Uta	May 2017	Herbarium CAG 801
<i>Smilax aspera</i> L.	Aerial parts (SaA)	Smilacaceae	Geremeas	May 2017	Herbarium CAG 1414
<i>Stachys glutinosa</i> L.*	Aerial parts (SgA)	Lamiaceae	Gennargentu	June 2017	Herbarium CAG 1099

<i>Tanacetum audibertii</i> (Req.) DC*	Aerial parts (TaA)	Asteraceae	Gennargentu	August 2018	Herbarium CAG 737/A
<i>Thymus herba barona</i> Loisel.	Aerial parts (ThA)	Lamiaceae	Gennargentu	June 2017	Herbarium CAG 1065

**Table 1:** List of thirty-six Sardinian plants selected for this study. The table reports the update botanical names, the plant organ used, the labels, the families, the places and dates of collection and voucher numbers. \* indicates the endemic species of Sardinia. Mandrone et al. 2019<sup>67</sup>.

## Chemicals

All chemicals were purchased from Sigma-Aldrich (Milan, Italy)

## Preparation of the extracts

Thirty mg of dried and powdered plant material were extracted with 1.5 mL of MeOH/H<sub>2</sub>O (1:1) and sonicated for 30 minutes. After 20 min of centrifugation (1700 × g) the supernatant was dried for two hours in vacuum concentrator (speedVac, Savant, Italy). To ensure the removal of all water, the samples were subsequently freeze-dried.

## Total phenolic and flavonoid assays

For determination of total phenolic content, the extracts were solubilized in water at different concentrations (from 0.05 to 0.2 mg/mL). 50 µL of these stock solutions were added to 250 µL of Folin-Ciocalteu reagent (diluted 1:10) and 500 µL of H<sub>2</sub>O. The calibration curve was constructed with the same chemicals replacing the 50 µL of extract with 50 µL of gallic acid (solubilized in MeOH 80%) at different concentrations (from 10 to 200 µg/mL). After 5 minutes of incubation, 800 µL of sodium carbonate solution (Na<sub>2</sub>CO<sub>3</sub> 20%) were added to all samples and the microplate was left at 40 °C for 30 minutes, then the absorption at 760 nm was recorded. The total phenolic content was calculated as mg GAE (gallic acid equivalent)/g of extract (dried weight) by interpolation to the calibration curve. For total flavonoid content assay the calibration curve was constructed using 50 µL of rutin (solubilized in DMSO) at different concentrations (from 1 to 100 µg/mL) mixed with 450 µL of MeOH and 500 µL of AlCl<sub>3</sub> (2% v/v of MeOH). 50 µL of extracts, solubilized in water at concentration from 0.05 to 0.2 mg/mL, were mixed to the same reagents. After 15 minutes of incubation at room temperature, adsorption at 430 nm was measured. The total flavonoid content was calculated as mg RE (rutin equivalent)/g of extract (dried weight) by interpolation in the calibration curve. The assays were carried out in triplicate.

### **Multivariate data analysis**

PCA was performed processing the data by UV (United variance) scaling method. SIMCA P+ software (v. 15.0, Umetrics, Sweden) was employed for developing the multivariate analysis model.

### **Antibacterial assay**

To carry out the antibacterial assay the extracts were dissolved in water and tested at concentration of 200 µg/mL against four reference strains namely *Staphylococcus aureus* ATCC 25293, *Staphylococcus epidermidis* (ATCC 12228), *Escherichia coli* (ATCC 25922) and *Klebsiella pneumoniae* (ATCC 9591) obtained from the American Type Culture Collection. The most promising extracts were also tested against 15 clinical isolates collected at the Microbiology Unit, St. Orsola Malpighi University Hospital, Bologna, Italy. These 15 clinical isolates were composed of five *S. aureus* strains, three of which methicillin-resistant (MRSA), five *S. epidermidis*, of which three methicillin-resistant (MRSE) and five *K. pneumoniae*, of which two carbapenemase-producing (KPC-producing *K. pneumoniae*). The methicillin and carbapenem resistance were established according to the EUCAST criteria. The antibacterial assays were carried out according to the method proposed by Bonvicini *et al.*<sup>68,69</sup>. Briefly, Mueller Hinton broth (Sigma-Aldrich, St. Louis, USA) was used to prepare the bacterial suspensions, after incubation with the extracts at 37°C for 24 h the OD<sub>630 nm</sub> was measured in the microplate reader Multiskan Ascent (Thermo Fisher Scientific Inc., Waltham, USA). Both negative and positive control were included in the analysis and the growth percentage was calculated as relative to the positive control. The extracts showing inhibition of bacterial growth superior to 70% were selected for the calculation of their IC<sub>50</sub>. GraphPad Prism version 5.00 for Windows (GraphPad Software, San Diego California, USA) was employed for performing one-way ANOVA test followed by Dunnett's multiple comparison test with the aim of detecting significant differences among samples activities.

### **Cell viability assay**

The cytotoxicity of the extracts was tested on African green monkey kidney cells (Vero ATCC CCL-81). The cells grew at 37 °C with 5% of CO<sub>2</sub> in Eagle's Minimal Essential Medium (MEM) (Sigma-Aldrich, St. Louis, MO, USA) with 10% fetal bovine serum (FBS) (Carlo Erba Reagents, Milan, Italy), 100 U/mL penicillin and 100 µg/mL streptomycin. After washing with PBS (phosphate-buffered saline), a monolayer of cells was incubated with 100 µL of serially 2-fold dilution of plant extracts for 48 h. Cell viability was determined by WST8-based assay (CCK-8, Cell Counting Kit-8, Dojindo Molecular Technologies, Rockville, MD, USA), standard medium as positive control was included in the analysis. After washing with PBS, 100 µL of fresh medium with 10 µL of CCK-8

solution were added under constant temperature of 37°C. After two hours of incubation the OD<sub>450/630 nm</sub> was measured. Cell viability was expressed as relative percentage to the control. A dose-response curves was edited and used to calculate the CC<sub>50</sub> values by interpolation.

### 3.2.3 Results and discussion

In order to find novel sources of antibacterial agents, thirty-six hydroalcoholic extracts of Sardinian plants were tested against the bacteria responsible for the most common infections, namely *Staphylococcus aureus*, *Staphylococcus epidermidis* among Gram-positive bacteria, *Klebsiella pneumoniae* and *Escherichia coli* among Gram-negative bacteria.

The same extracts were also tested on mammalian epithelial cells to assess their cytotoxicity.

The analyses were carried out testing the extracts at concentration of 200 µg/mL. The extracts that, at this concentration, determined a bacterial growth less than 30% compared to the positive control (100% bacterial growth) were considered active and selected for further analysis. Thirteen out of the thirty-six extracts showed a marked antibacterial activity against one or more reference strains (Table 2). In particular, ten extracts namely *A. unedo* leaves extract (AuL), *Cistus monspeliensis* aerial parts extract (CmA), *Cistus salviifolius* aerial parts extract (CsA), *Cytinus hypocistis* aerial part extract (CyhA), *Limonium morisanum* aerial part extract (LmA), *Myrtus communis* fruit extract (McF), *Myrtus communis* leaves extract (McL), *Pistacia lentiscus* leaves extract (PIL), *Pistacia terebinthus* L. ssp. *terebinthus* leaves extract (PtL) and *Thymus herba barona* aerial parts extract (ThA) resulted active against both the Gram-positive bacteria. Conversely, *Pistacia lentiscus* fruit extract (PIF), *Rosmarinus officinalis* aerial part extract (RoA) and *Smilax aspera* aerial part extract (SaA) only inhibited the growth of *S. aureus*. Regarding the activity against Gram-negative bacteria the best results were obtained against *K. pneumoniae*, whose growth was significantly inhibited by six extracts namely AuL, CmA, CyhA, McL, PIL and PtL. Against *E. coli* only two extracts, CyhA and PtL, showed promising activity.

Sample lable	<i>S. aureus</i>	<i>S. epidermidis</i>	<i>E. coli</i>	<i>K. pneumoniae</i>
	ATCC 25293	ATCC 12228	ATCC 25292	ATCC 9591
AuL	16 ± 3	2 ± 3	58 ± 5	29 ± 5
CmA	8 ± 3	5 ± 5	66 ± 6	18 ± 4
CsA	11 ± 6	3 ± 4	47 ± 4	37 ± 10
CyhA	5 ± 4	3 ± 4	34 ± 14	19 ± 1
LmA	9. ± 4	10 ± 5	69 ± 12	44 ± 6
McF	19 ± 5	12 ± 7	69 ± 7	64 ± 6
McL	5 ± 8	4 ± 6	55 ± 8	26 ± 11
PIF	26 ± 9	49 ± 15	77 ± 8	42 ± 3
PIL	9 ± 8	7 ± 13	47 ± 5	24 ± 7
PtL	4 ± 5	3 ± 3	33 ± 6	17 ± 3
RoA	13 ± 6	74 ± 7	97 ± 6	89 ± 2
SaA	30 ± 11	111 ± 15	73 ± 13	76 ± 4
ThA	13 ± 3	21 ± 15	106 ± 10	90 ± 1

**Table 2.** Bacterial growth of the reference strains treated with the 13 most active extracts at 200 µg/mL. Data are mean values and standard deviation obtained in two independent experiments performed in triplicate. Percentage values are relative to the positive control (100% of growth). Mandrone et al. 2019.

The thirty-six extracts were subjected to cytotoxicity tests. These data are important in determining the effective antibacterial activity of a sample, reducing the misleading ("false") positive results due to the cytotoxicity. As shown in Figure 5, eight out of thirty-six extracts strongly reduced mammalian cell metabolism to below 30%. Six out of these eight extracts resulted active in the antibacterial investigation. These samples need further analysis to ensure that the activity is not due to a generalized toxicity.

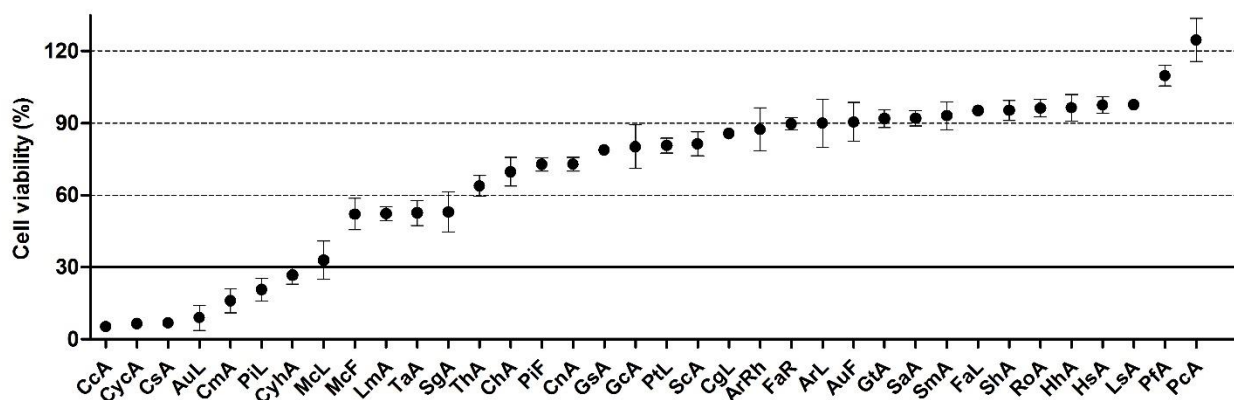


**Figure 5:** Vero cells viability after 72 hours of incubation with extracts at 200 µg/mL. Values are relative to the positive control (100% viability) and are expressed as means with standard deviations. Mandrone et al. 2019.

Multivariate analysis allows to take into account several types of data simultaneously. In this study, four types of data were collected for each sample: antibacterial activity, cytotoxicity, phenol content and flavonoid content. These data can be considered as the x-variables of a PCA data set. The PCA allows all these variables to be displayed in the scatter plot and to capture any correlations. The PCA model (Fig. 6) was constructed expressing the bioactivity and cytotoxicity data as % of inhibition and cell viability respectively at 200 µg/mL, the total polyphenols data were expressed as mg of gallic acid equivalents (GAE)/g of extract, while the flavonoids contents as mg of rutin equivalents (RE)/g of extract.

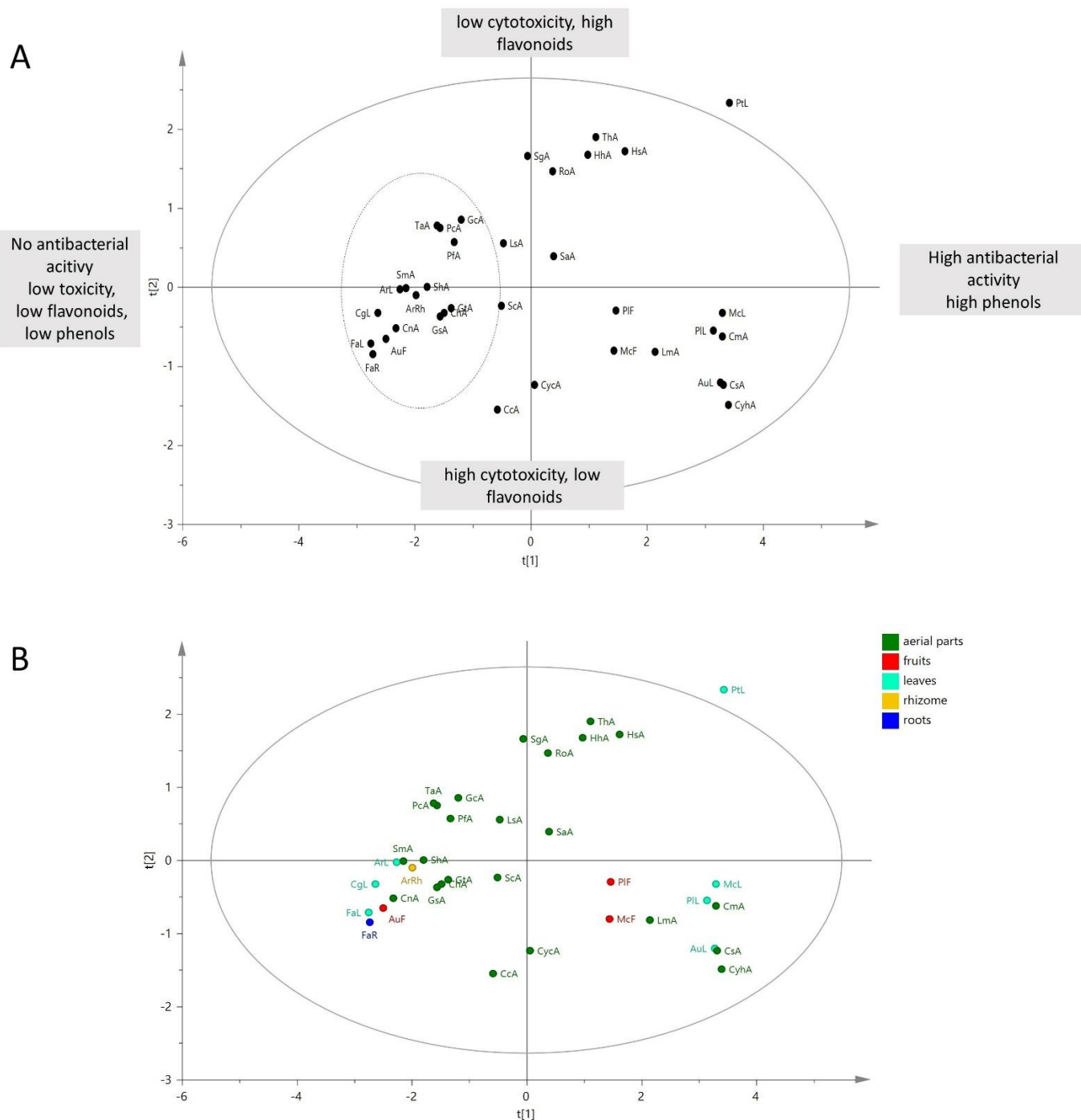


**Figure 6:** A) PCA-Loading Scatter Plot. The extracts with increasing antibacterial activity and phenolic content were placed along the positive component  $t[1]$  (PC1), while the extracts with increasing flavonoids content and decreasing cytotoxicity are discriminated along the component  $t[2]$  (PC2). The extracts clustered in the circle were not active, averagely cytotoxic and with scarce phenols and flavonoid content. B) PCA-Loading Scatter Plot coloured according the plant organ tested in the study. Mandrone et al. 2019

The PCA scatter plot showed that the extracts shifted to the positive side of the  $t[1]$  component (PC1), with high value of antibacterial activity, also possessed a high content of polyphenols, suggesting their possible involvement in antimicrobial activity. This deduction could be supported by the literature, in fact several polyphenols are known for the antibacterial properties. Particularly gallic

acid, caffeic acid and chlorogenic acid showed potent activity against *Staphylococcus* species and their mechanism of action was elucidated: gallic acid alters the adhesive properties of *S. aureus*, caffeic acid affects the stability of the bacterial membrane, while chlorogenic acid inhibits the biofilm formation of *S. epidermidis*<sup>70-72</sup>. Several phenolic compounds combinations were successfully tested against both *K. pneumoniae* and *E. coli* demonstrating a significant reduction in the viability of these pathogens and inhibition of biofilm formation<sup>73,74</sup>.

On the negative side of the PC1 axis, the extracts showing no activity on bacteria and low content of phenolic compounds and flavonoids were grouped together. On the positive side of PC1 and along the negative side of the t[2] component (PC2), extracts with the highest cytotoxicity and showing only moderate antibacterial activity were placed. Finally on the upper side of PC2 the extracts with medium antibacterial activity and very low cytotoxicity were clustered, these extracts resulted enriched in flavonoids content, hence their low toxicity could be due to the cytoprotective role that flavonoids exert<sup>75,76</sup>.

Among the thirty-six extracts several species belonged to the same genus. In particular, three species of *Centaurea* (*C. calcitrapa*, *C. napifolia* and *C. horrida*), two species of *Pistacia* (*P. lentiscus* and *P. terebinthus* ssp. *terebinthus*), two species of *Cistus* (*C. salvifolius* and *C. monspeliensis*) and two species of *Hypericum* (*H. scruglii* and *H. hircinum* ssp. *hircinum*) were analyzed. The arrangement of these samples in the PCA's scatter plot allowed to make further considerations. The samples of *Centaurea* genus (CcA, CnA and ChA) displayed similar results, in fact they were all placed on the bottom left part of the plot, where samples with increasing cytotoxicity, low content of both flavonoids and polyphenols and scarce or null activity clustered. However, while CnA and ChA were much closer in the graph, CcA appeared more distant, in fact its antibacterial activity was higher than that of CnA and ChA, moreover it was also more cytotoxic. Ultimately, the *Centaurea* genus proved to be scarcely interesting for this study. The two *Cistus* species, CsA and CmA, resulted very similar both in terms of bioactivities and in the content of polyphenols and flavonoids, as can be deduced from their position in the plot. The same trend was observed for the two *Hypericum* species (HsA and HhA) which showed high content of flavonoids, low cytotoxicity and moderate antibacterial activity and polyphenols content. The two *Pistacia* species (PIL and PtL) showed strong antibacterial activity and high polyphenol content, however they were different in flavonoid content and cytotoxicity. Actually, PtL resulted more enriched in flavonoids and showed very low cytotoxicity. These great properties differentiated PtL from all other samples, in fact in the PCA model it was identified as an outlier. Figure 5B shows the PCA plot coloured according the plant organ analysed in the study. No correlation emerged between the analysed properties (bioactivities and polyphenols and flavonoids content) and the tested plant organ. However, from this scatter plot an interesting data can be

achieved: the species *Myrtus communis* and *Pistacia lentiscus* showed similar features in the fruit extracts as in the leaves extracts, appearing close in the plot in both cases. Deeper studies are needed to determine the factors that caused this similarity.

The thirteen active extracts were further analysed to obtain the IC<sub>50</sub> values for the inhibition of the selected bacteria strains. The IC<sub>50</sub> corresponds to the concentration capable of inhibiting bacterial growth by 50%, considering the positive control (extract-free) as 100% growth. As shown in Table 3 only one extract, from *Cytinus hypocistis* aerial parts (CyhA), was active against all the tested bacteria. In addition to being the best extract against *E. coli* with an IC<sub>50</sub> of 74.9 µg/mL, CyhA also yielded the best results for the activity against both *S. aureus* and *K. pneumoniae* with IC<sub>50</sub> of 1.4 µg/mL and 28.5 µg/mL, respectively. Against *S. epidermidis* CyhA also showed a marked activity (IC<sub>50</sub> of 8.0 µg/mL) resulting the most potent extract after LmA (*Limonium morisanum* aerial parts) that yielded an IC<sub>50</sub> of 3.9 µg/mL. Overall, the extracts showed the best results against Gram-positive bacteria, yielding several IC<sub>50</sub> lower than 10 µg/mL. Precisely, these extracts were CmA, CsA, CyhA, LmA and McL for the inhibition of *S. aureus* and AuL, CyhA, LmA, McF and McL for the inhibition of *S. epidermidis*. Regarding the activity against the Gram-negative bacteria, the IC<sub>50</sub> values ranged between 28.5 µg/mL and 97.5 µg/mL for *K. pneumoniae*, while, in addition to CyhA, only one other extract, PIL, was able to inhibit the growth of *E. coli* with an IC<sub>50</sub> of 156.3 µg/mL. The different Gram-negative bacteria susceptibility can certainly be due to the presence of an additional bacterial membrane which is missing in Gram-positives bacteria and which makes the first ones impermeable to the passage of many molecules.

Sample lable	<i>S. aureus</i>	<i>S. epidermidis</i>	<i>E. coli</i>	<i>K. pneumoniae</i>
	ATCC 25293	ATCC 12228	ATCC 25292	ATCC 9591
AuL	31.9 [26.2-38.8]	10.0 [9.3-10.9]	n.d. <sup>§</sup>	93.8 [81.8-107.6]
CmA	5.3 [4.4-6.5]	12.4 [11.1-13.9]	n.d.	64.65 [57.0-73.2]
CsA	9.0 [7.9-10.4]	29.5 [26.4-32.9]	n.d.	97.5 [80.6-118.1]
CyhA	1.4 [0.9-1.9]	8.0 [7.5-8.5]	74.9 [57.9-96.9]	28.5 [22.8-35.6]
LmA	9.2 [6.8-12.3]	3.9 [2.5-6.1]	n.d.	n.d.
McF	15.4 [10.7-21.9]	8.8 [7.5-10.5]	n.d.	n.d.
McL	7.5 [6.0-9.3]	9.7 [8.9-10.9]	n.d.	37.0 [28.3-48.4]
PIF	144.5 [126.0-165.6]	n.d.	n.d.	n.d.
PIL	27.3 [21.6-34.5]	56.8 [48.1-67.2]	n.d.	48.0 [40.6-56.7]
PtL	62.9[48.6-81.4]	103.1 [92.6-109.0]	156.3[138.1-177.0]	49.0 [42.8-56.0]
RoA	99.2 [83.1-118.5]	n.d.	n.d.	n.d.
SaA	153.6 [129.1-182.7]	n.d.	n.d.	n.d.
ThA	63.3 [55.5-72.1]	150.0 [131.0-171.8]	n.d.	n.d.

**Table 3.**  $IC_{50}$  values ( $\mu\text{g}/\text{mL}$  of extract) for the thirteen active extracts. Data are reported as mean values and 95% confidence interval. Mandrone et al. 2019.

In order to assess the safety of the thirteen active extracts, dose-effect experiments on Vero cells were performed. The  $CC_{50}$  values and the selectivity index (SI) are reported in Table 4. The  $CC_{50}$  is defined as the extract concentration that reduced the cell viability by 50% when compared to untreated control, while selectivity index is calculated as the  $CC_{50}/IC_{50}$  ratio. The latter is a parameter that indicates the selective capacity of a sample, i.e. its ability to discriminate eukaryotic cells from bacterial cells. Once again, the best SIs were yielded against Gram-positive bacteria, the most selective extracts were CyhA, LmA and McL. Conversely, the extracts that resulted active against *K. pneumoniae* showed lower SI.

Sample lable	CC <sub>50</sub> (µg/mL)	SI
AuL	41.7 [35.0-49.7]	4.1 ( <i>S. epidermidis</i> )
CmA	88.2 [69.6-111.7]	16.5 ( <i>S. aureus</i> )
CsA	53.7 [43.5-66.3]	5.9 ( <i>S. aureus</i> )
CyhA	90.3 [75.2-108.3]	64.7 ( <i>S. aureus</i> ); 3.2 ( <i>K. pneumoniae</i> )
LmA	>200	>51.0 ( <i>S. epidermidis</i> )
McF	>200	>22.6 ( <i>S. epidermidis</i> )
McL	120.2 [92.9-155.6]	16.1 ( <i>S. aureus</i> ); 3.3 ( <i>K. pneumoniae</i> )
PIF	>200	>1.4 ( <i>S. aureus</i> )
PIL	84.2 [74.2-95.5]	3.1 ( <i>S. aureus</i> )
PtL	>200	4.1 ( <i>K. pneumoniae</i> )
RoA	>200	>2.0 ( <i>S. aureus</i> )
SaA	>200	>1.3 ( <i>S. aureus</i> )
ThA	>200	>3.2 ( <i>S. aureus</i> )

**Table 4.** Cytotoxicity of the thirteen active extracts against Vero cells. CC<sub>50</sub>, expressed as mean value at 95% confidence interval, and Selectivity Indexes (SI) are reported. Mandrone et al. 2019

Considering both antibacterial activity and cytotoxicity, the best extracts, namely CyhA, LmA and PtL, were selected for the assays against multi-resistant pathogens recovered from biological specimens. Specifically, the extracts were tested against clinical isolates of *S. aureus*, *S. epidermidis* and *K. pneumoniae*. The three extracts inhibited the growth of all the multi-resistant bacteria, yielding the same IC<sub>50</sub> recorded against the laboratory reference strains (Tab. 5). These data were statistically validated by ANOVA test followed by Dunnett's Multiple comparison.

<b>CyhA Vs <i>S. aureus</i></b>	<b>IC<sub>50</sub> (µg/mL)</b>	<b>Antibiotic-resistance profile</b>
ATCC 25293	1.4 [0.9-1.9]	
MSSA 1	1.6 [1.3-1.9]	CM <sup>S</sup> , E <sup>S</sup> , GMN <sup>S</sup> , LVX <sup>S</sup> , OX <sup>S</sup> , P <sup>R</sup> , TE <sup>S</sup> , SXT <sup>S</sup>
MSSA 2	2.8 [2.1-3.9]	CM <sup>R</sup> , E <sup>R</sup> , GMN <sup>S</sup> , LVX <sup>S</sup> , OX <sup>S</sup> , P <sup>S</sup> , TE <sup>S</sup> , SXT <sup>S</sup>
MRSA 1 <sup>§</sup>	2.6 [1.9-3.6]	GMN <sup>S</sup> , LVX <sup>R</sup> , OX <sup>R</sup> , P <sup>R</sup> , TE <sup>S</sup> , TEC <sup>S</sup> , SXT <sup>S</sup> , VA <sup>S</sup>
MRSA 2 <sup>§</sup>	3.2 [2.4-4.4]	GMN <sup>S</sup> , LVX <sup>R</sup> , OX <sup>R</sup> , P <sup>R</sup> , TE <sup>S</sup> , TEC <sup>S</sup> , SXT <sup>S</sup> , VA <sup>S</sup>
MRSA 3 <sup>§</sup>	1.9 [1.6-2.2]	CM <sup>R</sup> , E <sup>R</sup> , GMN <sup>S</sup> , LVX <sup>R</sup> , OX <sup>R</sup> , P <sup>R</sup> , TEC <sup>S</sup> , TE <sup>S</sup> , SXT <sup>S</sup> , VA <sup>S</sup>
<b>LmA Vs <i>S. epidermidis</i></b>		
ATCC 12228	3.9 [2.5-6.1]	
MSSE 1	2.6 [1.0-6.7]	CM <sup>S</sup> , E <sup>R</sup> , GMN <sup>S</sup> , LVX <sup>S</sup> , OX <sup>S</sup> , TE <sup>S</sup> , SXT <sup>S</sup>
MSSE 2	4.2 [2.1-8.3]	CM <sup>S</sup> , E <sup>S</sup> , GMN <sup>S</sup> , LVX <sup>S</sup> , OX <sup>S</sup> , P <sup>R</sup> , TE <sup>S</sup> , SXT <sup>S</sup>
MRSE 1 <sup>§</sup>	3.0 [2.1-8.4]	CM <sup>S</sup> , E <sup>R</sup> , GMN <sup>S</sup> , LVX <sup>S</sup> , OX <sup>R</sup> , P <sup>R</sup> , TE <sup>S</sup> , TEC <sup>S</sup> , SXT <sup>R</sup>
MRSE 2 <sup>§</sup>	6.7 [3.9-11.5]	CM <sup>S</sup> , E <sup>S</sup> , GMN <sup>S</sup> , LVX <sup>S</sup> , OX <sup>R</sup> , TE <sup>S</sup> , SXT <sup>R</sup> , VA <sup>S</sup> , TEC <sup>S</sup>
MRSE 3 <sup>§</sup>	3.7 [1.8-7.8]	CM <sup>S</sup> , DA <sup>S</sup> , E <sup>I</sup> , GMN <sup>S</sup> , LVX <sup>R</sup> , OX <sup>R</sup> , TE <sup>S</sup> , SXT <sup>S</sup> , VA <sup>S</sup> , TEC <sup>S</sup>
<b>PtL Vs <i>K. pneumoniae</i></b>		
ATCC 9591	49.0 [42.8-56.0]	
Kp 1	48.7 [42.0-56.5]	AK <sup>S</sup> , AMC <sup>R</sup> , CTX <sup>R</sup> , CFZ <sup>R</sup> , CIP <sup>R</sup> , FOS <sup>S</sup> , GMN <sup>S</sup> , TZP <sup>S</sup> , SXT <sup>R</sup>
Kp 2	46.1 [37.5-56.6]	AK <sup>S</sup> , AMC <sup>S</sup> , CTX <sup>S</sup> , CFZ <sup>S</sup> , CIP <sup>S</sup> , FOS <sup>S</sup> , GMN <sup>S</sup> , TZP <sup>S</sup> , SXT <sup>S</sup>
Kp 3	45.5 [34.7-59.7]	AK <sup>S</sup> , AMC <sup>S</sup> , CTX <sup>S</sup> , CFZ <sup>S</sup> , CIP <sup>S</sup> , FOS <sup>R</sup> , GMN <sup>S</sup> , TZP <sup>S</sup> , SXT <sup>S</sup>
KPC-Kp 1*	53.0 [42.2-66.5]	AK <sup>R</sup> , AMC <sup>R</sup> , AMP <sup>R</sup> , CFZ <sup>R</sup> , CIP <sup>R</sup> , EPM <sup>R</sup> , GMN <sup>S</sup> , MEM <sup>R</sup> , TZP <sup>R</sup> , SXT <sup>R</sup> , TGC <sup>I</sup> , CS <sup>S</sup>
KPC-Kp 2*	47.3 [44.0-56.9]	AK <sup>S</sup> , AMC <sup>R</sup> , AMP <sup>R</sup> , CFZ <sup>R</sup> , CIP <sup>R</sup> , EPM <sup>R</sup> , GMN <sup>R</sup> , MEM <sup>I</sup> , TZP <sup>R</sup> , SXT <sup>R</sup> , TGC <sup>S</sup> , CS <sup>S</sup>

**Table 5.** IC<sub>50</sub> values of the three selected extracts towards clinical isolates. Data are reported as mean values and 95% confidence interval. AK = Amikacin; AMC = Amoxicillin/Clavulanic Acid; AMP = Ampicillin; CM = Clindamicyn; CTX = Cefotaxime; CFZ = Ceftazidime; CIP = Ciprofloxacin; CS = Colistin; EPM = Ertapenem; E = Erythromycin; FOS = Fosfomycin; GMN = Gentamicin; LVX = Levofloxacin; MEM = Meropenem; OX = Oxacillin; P = Penicillin; SXT = Trimethoprim/Sulfamethoxazole; TE = Tetracycline; TEC = Teicoplanin; TZP = Piperacillin/Tazobactam, TGC = Tigecycline; VA = Vancomycin.

R = Resistant; S = Susceptible; I = Intermediate, according to the EUCAST guidelines

<sup>§</sup>*Staphylococcus* methicillin-resistant species

\*Carbapenemase-producing *K. pneumoniae*.

Mandrone et al. 2019.

The screening carried out in this study allowed to select *Cytinus hypocistis*, *Pistacia terebinthus* ssp. *terebinthus* and *Limonium morisianum* as potential sources of antibacterial molecules.

*Cytinus hypocistis* is a small perennial plant of Cytinaceae family. It normally grows on the roots of species belonging to the genus *Cistus* since it is a parasite plant. Researches on the ethnobotanical use of this plant revealed its astringent, skin soothing and anti-inflammatory properties<sup>77,78</sup>. The antibacterial activity of this plant was recently investigated<sup>79,80</sup>. These studies confirmed the activity against *S. aureus* and *S. epidermidis* while diverged on *K. pneumoniae* inhibition. This difference may be due to the different type of extraction method employed. The phytochemical composition is scarcely known, however Magiatis *et al.* reported the characterization of several hydrolysable tannins, mostly of the ellagitannin class, responsible for the antitumor activity against several cancer cell lines tested in their study<sup>81</sup>. Hydrolysable tannins demonstrated antimicrobial properties<sup>82</sup>, therefore it is likely that this class of secondary metabolites are involved in the activities reported in study.

*Pistacia terebinthus* ssp. *terebinthus* is a bushy shrub of Anacardiaceae family, widespread in several areas of Southern Europe. In Sardinia it grows in the calcareous areas of the east coast. In European traditional medicine this plant was widely used: the leaves to treat burns, the resin for respiratory diseases, the fruit for its anti-inflammatory and analgesic properties<sup>83,84</sup>. Several studies carried out on both the extract and the essential oil confirmed the anti-inflammatory, antioxidant, antibacterial and antifungal properties<sup>85-88</sup>. *Limonium morisianum* (Plumbaginaceae) is an endemic plant of Sardinia growing only in the calcareous mountains. Given its rarity, there is a scarce information in literature about ethnobotanical uses and phytochemistry. However, some recent studies reported the antiviral activity against Ebola and HIV-1 viruses and the inhibition of elastase and tyrosinase enzymes. Several flavonoids such as myricetin myricetin-3-*O*-(6"-galloyl)- $\beta$ -D-galactopyranoside and myricetin 3-*O*-rutinoside were identified in the aerial parts extract<sup>89-91</sup>.

### 3.2.4 Conclusions

In search for new antibacterial agents, thirty-six plant species growing spontaneously in Sardinia island were selected for *in vitro* antimicrobial assays. The hydroalcoholic extracts were tested against four reference strains, namely *Staphylococcus aureus* and *S. epidermidis* among Gram-positive bacteria, *Klebsiella pneumoniae* and *Escherichia coli* among Gram-negative bacteria. The extracts were also evaluated for their cytotoxicity on mammalian cells. These bioactivities data, together with the total polyphenols and flavonoids contents, were treated by multivariate analysis. PCA model highlighted the positive correlation between the polyphenols content and the antibacterial activity, while the flavonoids content was related to their cytotoxicity suggesting a cytoprotective role of these metabolites. Thirteen out of thirty-six extracts displayed antibacterial activity, thus the IC<sub>50</sub> values were determined. The best results were achieved for the inhibition of Gram-positive bacterial growth. Actually, all the thirteen extracts were active against *S. aureus* showing IC<sub>50</sub> between 1.4 and 153.6 µg/mL, ten out of them inhibited also *S. epidermidis* exhibiting IC<sub>50</sub> between 3.9 and 150.0 µg/mL. Regarding the activity against Gram-negative bacteria, only two extracts inhibited *E. coli* with IC<sub>50</sub> of 74.9 and 156.3 µg/mL, while seven extracts were effective in counteracting *K. pneumoniae* growth displaying IC<sub>50</sub> between 28.5 and 97.5 µg/mL. Considering both antibacterial activity and cytotoxicity, three out of the thirteen extracts, namely *Pistacia terebinthus ssp. terebinthus*, *Cytinus hypocistis* and *Limonium morisianum*, were selected for the biological assays against multi-resistance strains of *S. aureus*, *S. epidermidis* and *K. pneumoniae*. The extracts confirmed their activity on drug-resistant strains, thus proving to be excellent candidates for the preparation of herbal products or dietary supplements with antibacterial action as well as for further studies to identify the molecules responsible for the antimicrobial activity.

### **3.3 ARBUTUS UNEDO L., A SOURCE OF ANTIBACTERIAL AGENTS. PHYTOCHEMICAL AND BIOACTIVITY VARIATIONS OF SAMPLES COLLECTED UNDER DIFFERENT CONDITIONS.**

#### **3.3.1 Introduction**

Plant metabolism is strongly influenced by biotic and abiotic factors. It varies during a calendar year in response to the climate, moreover, a plant could be attacked by pathogens that lead to a rebalancing of its own metabolism. Usually, under stress conditions plants produce signal molecules that activate pathways leading to the synthesis of metabolites for adaptation<sup>92</sup>. All these factors mean that the same species under different conditions can have a different metabolism, i.e. it can produce different molecules or different quantities of the same molecules.

*Arbutus unedo* proved to be one of the most promising extracts endowed with antibacterial activity in the screening of 36 Sardinian plants. Although it was not the best extract in terms of IC<sub>50</sub>, its broad spectrum of action and its strong ability to grow in different areas and environments made it an excellent candidate for a metabolomic study to determine metabolic changes in leaves collected under different conditions and any resulting changes in the biological activities.

Actually, the hydroalcoholic leaves extract showed promising activity both against the Gram-negative bacterium *K. pneumoniae* and the Gram-positive bacteria *S. aureus* and *S. epidermidis*. Precisely, this extract yielded IC<sub>50</sub> of 93.8 µg/mL against *K. pneumoniae*, and 31.9 µg/mL and 10.0 µg/mL against *S. aureus* and *S. epidermidis*, respectively. In the cytotoxicity assay on mammalian cells the CC<sub>50</sub> was 41 µg/mL with a selectivity index (SI), calculated as the CC<sub>50</sub>/IC<sub>50</sub> ratio for the bacterial strain most susceptible to inhibition, i.e. *S. epidermidis*, of 4.1.

*Arbutus unedo* L., commonly known as the strawberry tree, is a small tree of 1.5-3 metres tall belonging to the family of Ericaceae. It is particularly widespread in the Mediterranean basin but also in the coastal regions of Ireland and Anatolia. In fact, this evergreen species can grow on different types of soils, at several altitudes and in coexistence with different plant species that inhabit the same environment, thus it can be found from the sea level until 1200 metres. During the autumn and the early winter it bears red or orange fruits and pinkish-white flowers which render the plant highly appreciated for its ornamental value<sup>93</sup>. The fresh fruits are commonly used to produce jams, marmalades and liquors, the high content of minerals and vitamins, especially vitamin C, make them also suitable for the production of food supplements<sup>94</sup>. Both the fruits and the leaves have been widely used in folk medicine, the first ones for diuretic, antiseptic and laxative purposes, while the leaves for the astringent, depurative and antihypertensive properties<sup>95</sup>.

Considering the broad antibacterial activities of the hydroalcoholic leaves extract and the strong ability of this species to grow in a variety of environments, *A. unedo* was selected for studying the metabolomic changes in the phytochemical profiles and biological activities of leaves collected under different conditions. Hence, metabolomic-chemometric approach was applied to compare *A. unedo* leaves metabolome from samples harvested in 10 different areas of Sardinia (Fig. 1) within 216 days covering three seasons, namely spring, summer and autumn, during two consecutive years (2017 and 2018). The  $^1\text{H-NMR}$  spectra of sixty hydroalcoholic extracts were recorded and treated with multivariate analysis to capture phytochemical differences. The samples which were found to be the most diverse were tested against three bacteria of the most common pathologies, namely *Staphylococcus aureus*, *Staphylococcus epidermidis* and *Klebsiella pneumoniae*. The biological data were statistically analysed to assess significant differences among samples bioactivities. Moreover, these extracts were also evaluated for cytotoxicity on mammalian cells to determine their safety. Finally, the most promising extract was submitted to bio-guided fractionation for the characterization of the metabolites responsible for antibacterial activity.

### 3.3.2 Materials and methods

#### Plant material

*Arbutus unedo* leaves were harvested by Dr. Cinzia Sanna, voucher specimens were deposited at the Herbarium of Cagliari. Leaves were collected over 216 days that covered three seasons (spring, summer and autumn) in ten different collection field of Sardinia island (Fig.1).

#### Chemicals

Deuterium oxide ( $\text{D}_2\text{O}$ , 99.90% D) was purchased from Eurisotop (Cambridge Isotope Laboratories, Inc, France). The standard 3-(trimethylsilyl)-propionic-2,2,3,3- $d_4$  acid sodium salt (TMSP) and all the solvents and chemicals were purchased from Sigma-Aldrich Co. (St. Louis, MO, USA).

#### Extracts preparation for NMR analysis and biological assays

For each sample thirty mg of dried and powdered leaves were extracted in 1.5 mL of MeOH/ $\text{H}_2\text{O}$  (1:1) by sonication for 30 min. After 20 min of centrifugation ( $1700 \times g$ ) the supernatant was dried for two hours in vacuum concentrator (speedVac, Savant, Italy). The samples were subsequently freeze-dried overnight to completely remove the residual  $\text{H}_2\text{O}$ , yielding the crude extracts.

For NMR analysis the extracts were prepared in D<sub>2</sub>O (containing 0.1 M phosphate buffer and 0.01% of TMSP standard) at concentration of 10 mg/mL.

For biological assays the extracts were dissolved in water and tested at concentration of 200 µg/mL.

### **Extract preparation for bio-guided fractionation**

Twelve g of dried and powdered leaves of *A. unedo* harvested at day 200 of the year 2017 in San Gregorio field (SG2017\_200) were extracted by sonication for 30 min with 600 mL of MeOH/H<sub>2</sub>O (1:1). Subsequently, the extract was centrifugated for 20 min (2469 x g) and filtered on Büchner funnel. Finally, it was dried under reduced pressure yielding the crude extract.

### **NMR analysis**

The extracts were solubilised in water-d<sub>2</sub> containing 0.01% of TMSP standard (trimethylsilylpropionic-2,2,3, 3-d<sub>4</sub> acid sodium salt) and analysed in NMR at a concentration of 10 mg/mL. For the NMR analysis a Varian R 14.4 T spectrometer (600 MHz for <sup>1</sup>H) equipped with Probe High-Field Triple Resonance was used. The experiments were recorded at 25 °C, using D<sub>2</sub>O for internal lock.

### **Multivariate data analysis**

The <sup>1</sup>H-NMR profiles of sixty hydroalcoholic extracts of *Arbutus unedo* leaves were processed to obtain the data in a properly format for multivariate analysis. Hence, for each <sup>1</sup>H-NMR spectrum baseline correction and alignment of standard signal (TMSP) at 0 ppm were carried out. After manually remotion of the eventual residual solvent, a bucket width of 0.04 ppm was chosen to perform the binning operation and the sum of signals intensities of each bin was normalized by the sum of the total intensities. Pareto scaling was used as scaling method and the processed data converted in ASCII file. The data processing was carried out using the NMR Mestrenova 12 software. The statical models (PCA) were developed using SIMCA P+ software (v. 15.0, Umetrics).

### **Bacterial strains and determination of antibacterial activity and cytotoxicity**

*Staphylococcus aureus* (ATCC 25293), *Staphylococcus epidermidis* (ATCC 12228), and *Klebsiella pneumoniae* (ATCC 9591) were obtained from the American Type Culture Collection. The cytotoxicity of the extracts was tested on African green monkey kidney cells (Vero ATCC CCL-81). The *in vitro* antibacterial activity and cytotoxicity were evaluated by the methods previously described.

### **Statistical analysis**

Statistical analysis was carried out using GraphPad Prism version 5.00 for Windows (GraphPad Software, San Diego California, USA). One-way ANOVA followed by Tukey Post-hoc test were performed to evaluate significance differences. The differences were statistically significant for  $p < 0.05$ .

### **Fractionation of SG2017\_200 extract**

The dried extract (3,50 g) was fractionated using Reveleris® X2 Flash Chromatography System with multiple wavelengths UV detector (BÜCHI Labortechnik AG Meierseggrasse 40 Postfach, Germany). The chromatographic separation was performed using a C<sub>18</sub> column (80 g). The sample was dissolved in a proper volume of methanol 70%. A gradient elution mode was used with H<sub>2</sub>O (solvent A) and MeOH (solvent B) at flow rate of 50 mL min<sup>-1</sup>. The extract was fractionated in four fractions of different polarity collected six minutes apart. Starting from 5% B, the gradient was linearly increased to 20% B in 3 min, keeping it constant for 3 min (first fraction), then it was increased to 30% B in 3 min maintaining it constant for 3 min (second fraction). The gradient was again linearly increased to 50% B in 3 min holding it constant for 3 min (third fraction). Finally, it was raised to 100% B in 3 min, keeping it constant for 3 min (fourth fraction).

### **Purification of fraction 3**

Eighty mg of fraction 3 were submitted to chromatographic separation using Reveleris® X2 Flash Chromatography System with multiple wavelengths UV detector (BÜCHI Labortechnik AG Meierseggrasse 40 Postfach, Germany). A C<sub>18</sub> column (4 g) was used for the separation and the extract was solubilized in a proper volume of MeOH 70%. A gradient elution mode was employed with H<sub>2</sub>O with 0,1% of TFA (solvent A) and MeOH with 0,1% of TFA (solvent B) at flow rate of 10 mL min<sup>-1</sup>. Starting from an isocratic elution at 10% B for 10 min, the gradient was linearly increased to 20% B in 1 min maintaining it constant for 20 min., then it was further raised to 30% B in 1 min keeping it constant for 10 min, the percentage of B reached the 50% in 1 min remaining unchanged for 10 min. Finally, the gradient was linearly increased to 70% B in 1 min holding it constant for 5 min. The UV detector was set at 220, 280 and 350 nm, being these the characteristic wavelengths of flavonoids, and the fractions were collected by UV peaks, obtaining fifteen sub-fractions.

### **NMR and MS spectra measurement for identification of the active metabolite**

<sup>1</sup>H NMR spectra, J-resolved (J-res), <sup>1</sup>H-<sup>1</sup>H homonuclear and inverse detected <sup>1</sup>H-<sup>13</sup>C correlation experiments were recorded at 25 °C on NMR instrument Varian Inova (Milan, Italy), 600 MHz operating at the <sup>1</sup>H frequency, equipped with an indirect triple resonance probe. For <sup>1</sup>H NMR profiling, relaxation delay was 2.0 s, observed pulse 5.80 μs, number of scans 256, acquisition time 16 min, and spectral width of 9595.78 Hz (corresponding to δ 16.0). A presaturation sequence (PRESAT) was used to suppress the residual H<sub>2</sub>O signal at δ 4.83 (power= -6dB, presaturation delay 2 s). ESI-MS analyses were performed by direct injection of MeOH solutions of the compounds using a WATERS ZQ 4000 (Milford, MA USA) mass spectrometer.

### **3.3.3 Results and discussion**

#### **Phytochemical variation of *A. unedo* leaves extracts collected in different conditions.**

With the aim to reap metabolomic variations, *A. unedo* leaves were collected under different conditions. Ten Sardinian fields were selected for sampling (Fig. 1), these areas differed in altitude, proximity to the sea, type of soil, moreover, since wild *A. unedo* trees were chosen for this study, each sampled species had a different surrounding, made up of other growing species. The sampling was carried out over a period of 216 days from April to November. In each field three samples were collected, one during the spring season, one in summer and one in autumn for two consecutive years (2017 and 2018), resulting in a total of sixty leaves samples.



- GT** = Gairo Taquisara
- PL** = Porcu e Iudu
- SA** = Sant'Antonio
- CS** = Cala Surya
- CO** = Campu Omu
- SG** = San Gregorio
- GU** = Gutturumannu
- PP** = Poggio dei Pini
- DO** = Domusnovas
- LR** = Località Rombi

*Figure 1: Map of collection fields in Sardinia island with corresponding labels*

NMR is one of the most appropriate techniques to capture differences in the metabolomic profiles of extracts since it provides a snapshot of the occurring metabolites whose signals are proportional to their relative concentrations.

Hence, the  $^1\text{H-NMR}$  spectra of the sixty hydroalcoholic extracts were treated with multivariate analysis to catch any differences in metabolic profiles. The PCA model in Figure 2 was developed using as X variables the NMR data properly processed.

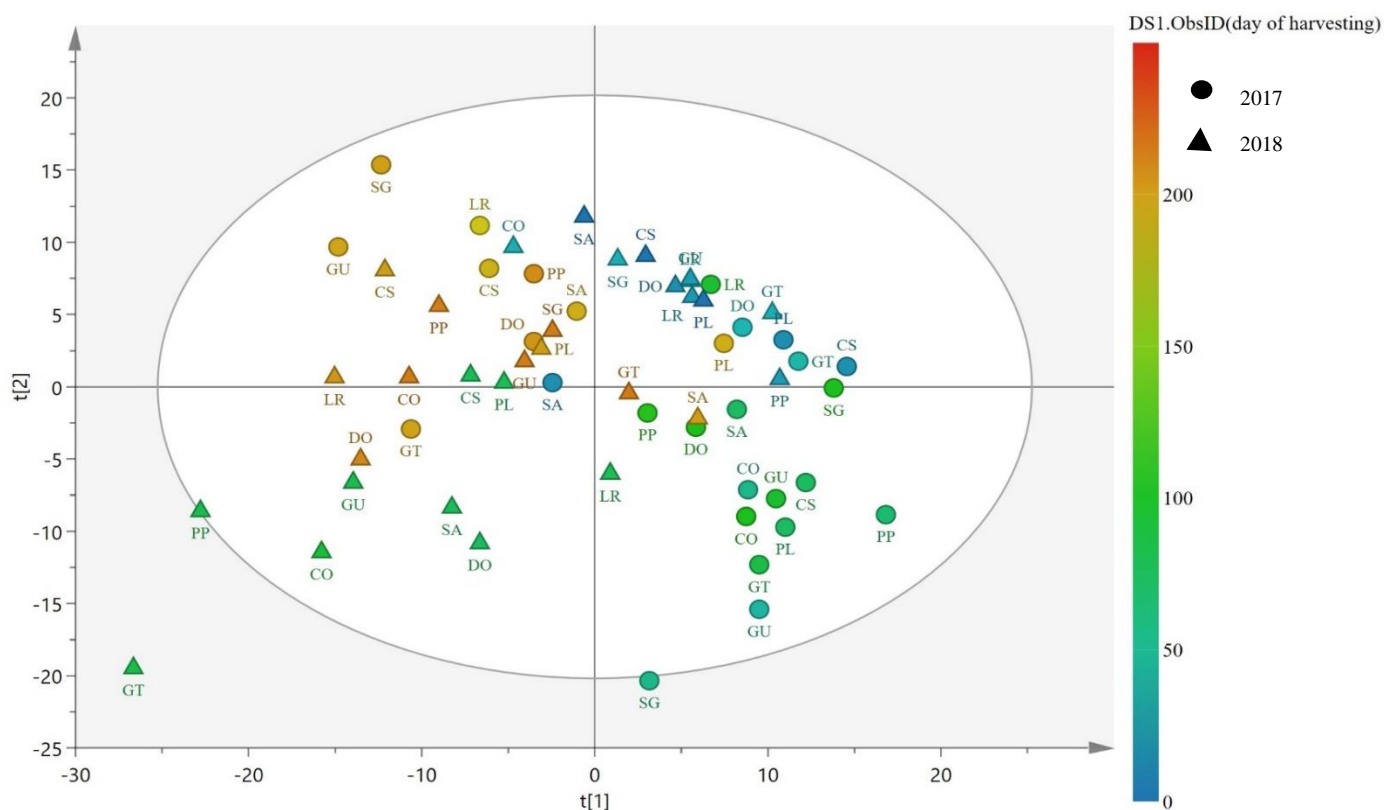


**Figure 2:** PCA scatter plot of sixty hydroalcoholic extracts of *A. unedo* leaves developed using the  $^1\text{H-NMR}$  signals as *X* variables, The labels correspond to the collection fields. Different colours indicate different days of harvesting (from day 0 to day 216), the dots represent samples collected in 2017 while the triangles represent the samples harvested in 2018.

The PCA scatter plot showed samples distribution along the main components (PC1 and PC2) according to their NMR profiles. Samples appearing close in the plot possessed a similar NMR spectrum. The colour scale on the right of the plot represents the collection period from day 1 to day 216: samples collected in the first days during the spring season were coloured in blue, the colour turns green around the sixtieth day of harvesting with the beginning of the summer months and then turns yellow and finally red for the samples collected in the autumn months. Samples collected in the same period tended to show a similar phytochemical profile but no defined clusters were formed in the PCA model precisely because not only seasonality influences the expression of metabolites but many other factors contribute to stimulating plant metabolism.

By comparing the  $^1\text{H-NMR}$  spectra, some signals that determined the arrangement of the samples in the scatter plot were identified. Figure 3 shows the magnification of the NMR spectrum between 0 and 8 ppm of two representative samples.

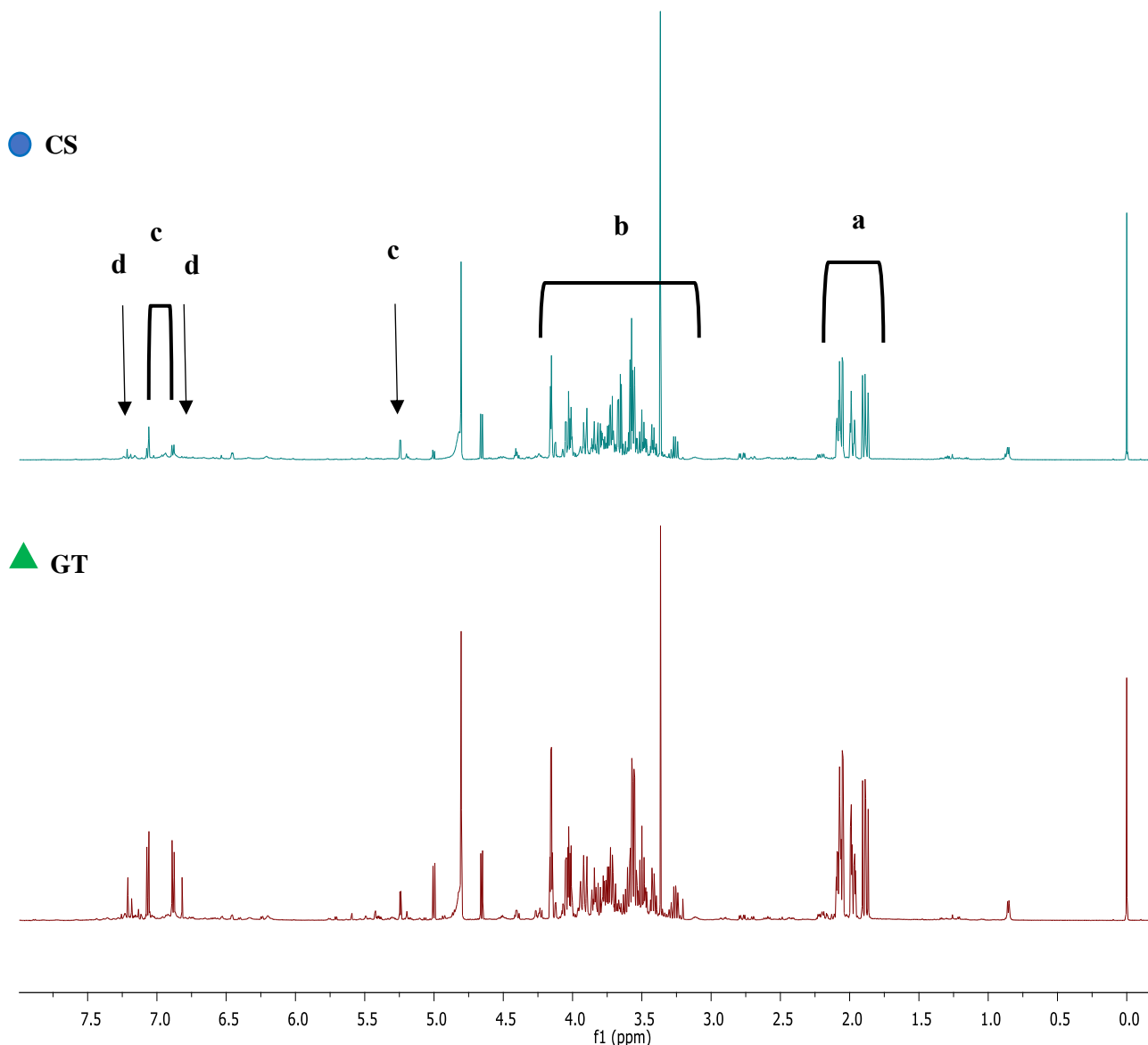


**Figure 3:** Comparison between  $^1\text{H-NMR}$  profile of two representative samples. a: quinic acid, b: sugars region, c: arbutin, d: flavonoids.

Substantial differences among the samples concerned the expression of carbohydrates, which in the NMR spectrum typically resonate between 3.0 and 4.5 ppm. Since sugars signals were much more abundant than those of secondary metabolites, they greatly influenced samples distribution in the PCA model. The application of pareto scaling as scaling method in data processing serves to reduce this effect<sup>35</sup>. Another highly variable zone in the NMR spectra was around 2.0 ppm. In this zone the quinic acid signals were detected, hence the expression of quinic acid resulted different depending on the samples. Finally, marked differences were reaped in the zone between 6.5 and 7.5 ppm. In this part of the NMR spectrum characteristically resonate aromatic compounds such as many secondary metabolites. Actually, some typical signals belonging to flavonoids, mainly kaempferol and myricitrin derivatives, were identified. In the same area some signals of the well-known active

ingredient of *A. unedo*, namely arbutine also resonate. The AA'BB' hydrogens system of aglycone part was identified around 7.0 ppm, while some signals belonging to the sugar portion were individuated around 5.0 ppm.

Sugars are essential for the life of a plant, they derive directly or indirectly from chlorophyll photosynthesis and provide the energy needed to grow and develop. Sugars regulate seed germination, promote flowering and are implicated in senescence<sup>96-98</sup>. In addition to being structural and reserve molecules, they are involved in many metabolic processes where they act as substrate or metabolic intermediaries. In recent years it has been demonstrated that sugars also act as signal molecules by controlling the activation of metabolic pathways in conjunction with phytohormones<sup>99</sup>. Moreover, sugars are also involved in the responses to stress caused by pathogens, cold, drought, lack of elements such as iron and phosphorus in the soil<sup>97,100</sup>. Due to their countless functions, sugars concentrations and compositions constantly change in plant tissues. These variations take place during the day and night, during subsequent developmental stages and every time that an external factor disturbs the life of the plant<sup>101</sup>, as confirmed by the data of this study.

Quinic acid is a product of the shikimate pathway, a metabolic pathway peculiar of plants and microorganism that provides the precursors of plant secondary metabolites. Specifically, quinic acid originates from reduction of 3-dehydroquinic acid (DHQ), an intermediate that is generated during the second of the seven reactions that lead to the formation of Chorismic acid from which the aminoacids L-Phe, L-Tyr, and L-Trp are formed<sup>102</sup>. It is plausible that the accumulation and metabolism of quinic acid affects the production of the shikimate pathway molecules thus, the expression of the secondary metabolites<sup>103</sup>. Quinic acid gives rise to its derivatives through esterification reactions, for example chlorogenic acid originates from esterification of quinic acid with caffeic acid. Moreover, quinic acid can form part of alkaloids structures as in the case of quinine. Several studies report the variation of this metabolite content in various plant organs. For example, it was observed that iron deficiency in the soil led to changes in the expression of organic acids and also of quinic acid<sup>104</sup>. In a study on metabolic changes of *Quercus suber* leaves, the authors observed that quinic acid concentration was high in recently formed leaves (in spring) and continued to be one of the most abundant metabolites until the end of the summer when its concentration started to decrease. Conversely, the sugars content resulted low in young leaves and increased slowly during the warmer months until the beginning of autumn when the sugars maximum concentration was detected<sup>105</sup>. In this study many metabolic profile of *A. unedo* leaves followed a similar trend. However it was not possible to correlate metabolic changes with seasonality since the samples analysed in this study were harvested from different plants and under different conditions, hence numerous factors influenced the expression of metabolites.

Arbutin (*p*-hydroxyphenyl- $\beta$ -D-glucopyranoside) is a phenol glucoside that occurs in several species mainly belonging to Ericaceae and Saxifragaceae family<sup>106</sup>. Since arbutin is an inhibitor of tyrosinase, an enzyme responsible for skin pigmentation, this metabolite is widely employed by cosmetics industry as skin-whitening agent<sup>107,108</sup>. Moreover, arbutin exhibited antioxidant properties, acting as a cytoprotective agent for erythrocytes and skin fibroblasts<sup>109,110</sup>. This metabolite is also endowed with anti-inflammatory activity by modulating interleukin-6, interleukin-10 and TNF- $\alpha$  levels during inflammation<sup>111</sup>. Arbutin anticancer activity was also evaluated, this metabolite demonstrated positive effects on skin cancer and bladder cancer by regulation of malignant tumorigenesis and cancer cells proliferation, respectively<sup>108,112</sup>. Arbutin is officially recognised for the treatment of urinary infections, in fact, EMEA directives recommend the administration of 400–800 mg/day of arbutin in 2–3 doses for solving urinary bacterial infections<sup>113</sup>. Several studies confirmed that in *A. unedo* leaves arbutin expression, as well as polyphenols and flavonoids concentration, vary in relation to the plant and to the period of the year in which sampling is carried out. Nenadis *et al.* reported flavonoids and polyphenols variations under different UV and precipitations conditions, they noted lowest concentration values in spring and highest in autumn and winter<sup>114</sup>. Maleš *et al.* measured the monthly concentrations of quercitrin, hyperoside, and chlorogenic acid, they found highest concentrations of hyperoside and quercitrin in January, whereas for chlorogenic acid the highest amounts were detected in June, July and October<sup>115</sup>. Žlabur *et al.*, confirmed that location strongly influenced the physical-chemical composition of both fruits and leaves of *A. unedo* harvested in different coastal regions of Croatia<sup>116</sup>.

## Bioactivity variations of *A. unedo* leaves extracts

In the screening of the thirty-six Sardinian plants, *S. aureus*, *S. epidermidis* and *K. pneumoniae* resulted susceptible to *A. unedo* leaves extract. For assessing whether metabolomic changes also led to variations in the bioactivity panel, some samples were selected for antibacterial assays. The PCA model guided the choice of samples, in fact, the extracts representing the different metabolic profiles were selected for the biological tests (Fig. 4).

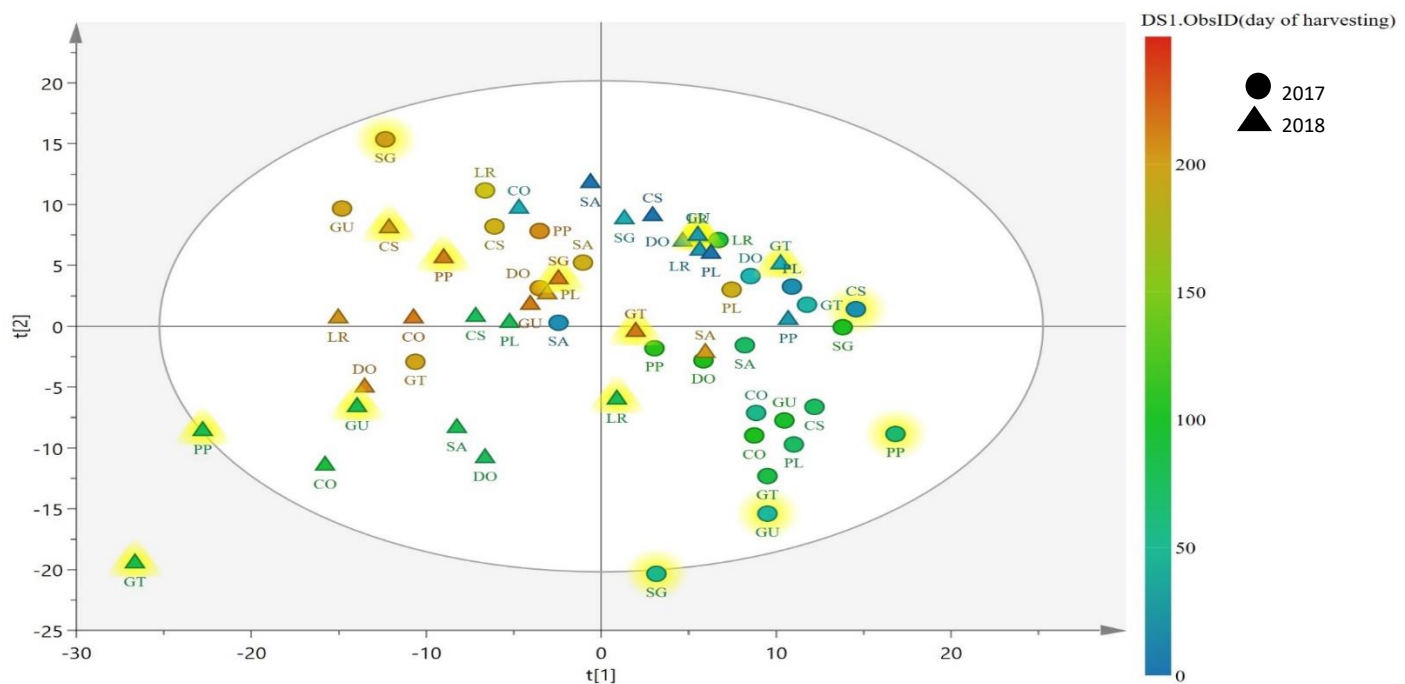


**Figure 4:** Principal Component Analysis (PCA) of *A. unedo* extracts. The symbols marked by yellow colour represent the samples selected for the antibacterial assays.

For each sample, the  $IC_{50}$  values for the inhibition of bacterial growth were calculated and submitted to the statistical analysis to verify significant differences among the antimicrobial activities (Fig. 5, 6, 7).

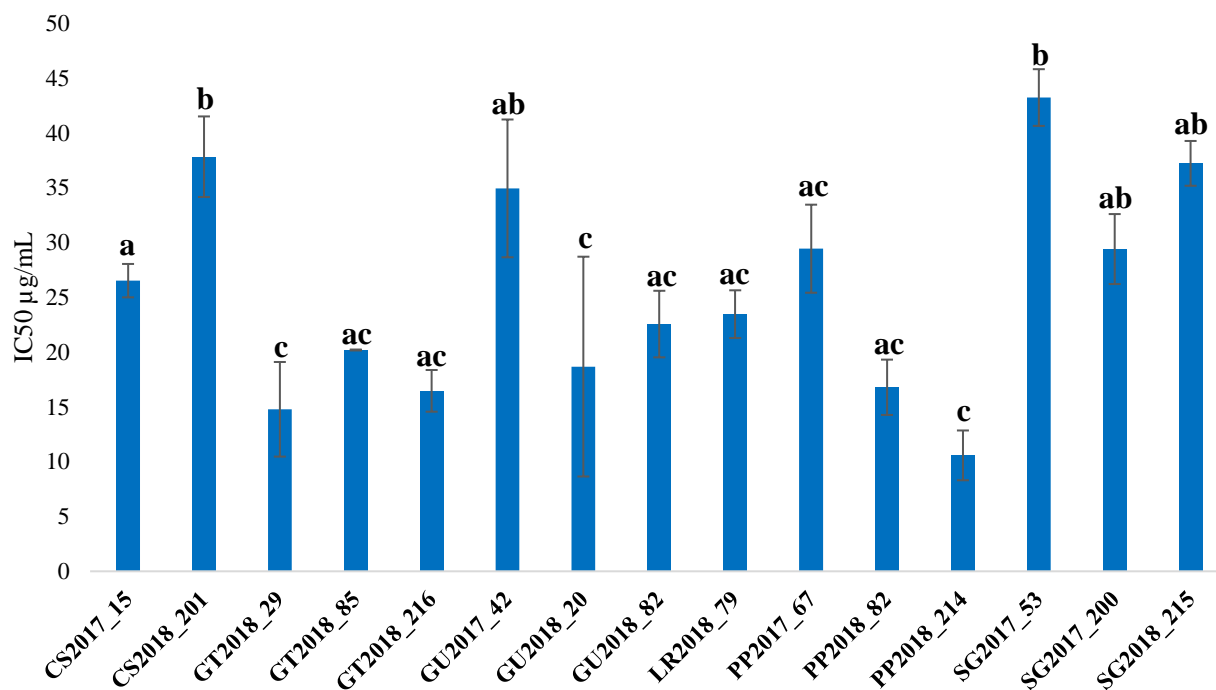


**Figure 5:** Antibacterial activity of the fifteen selected samples against *S. aureus*. Each label reports the collection field, the year and the day of harvesting. The IC<sub>50</sub> values were expressed in µg/mL. Each histogram carries a letter referring to the statistical analysis.

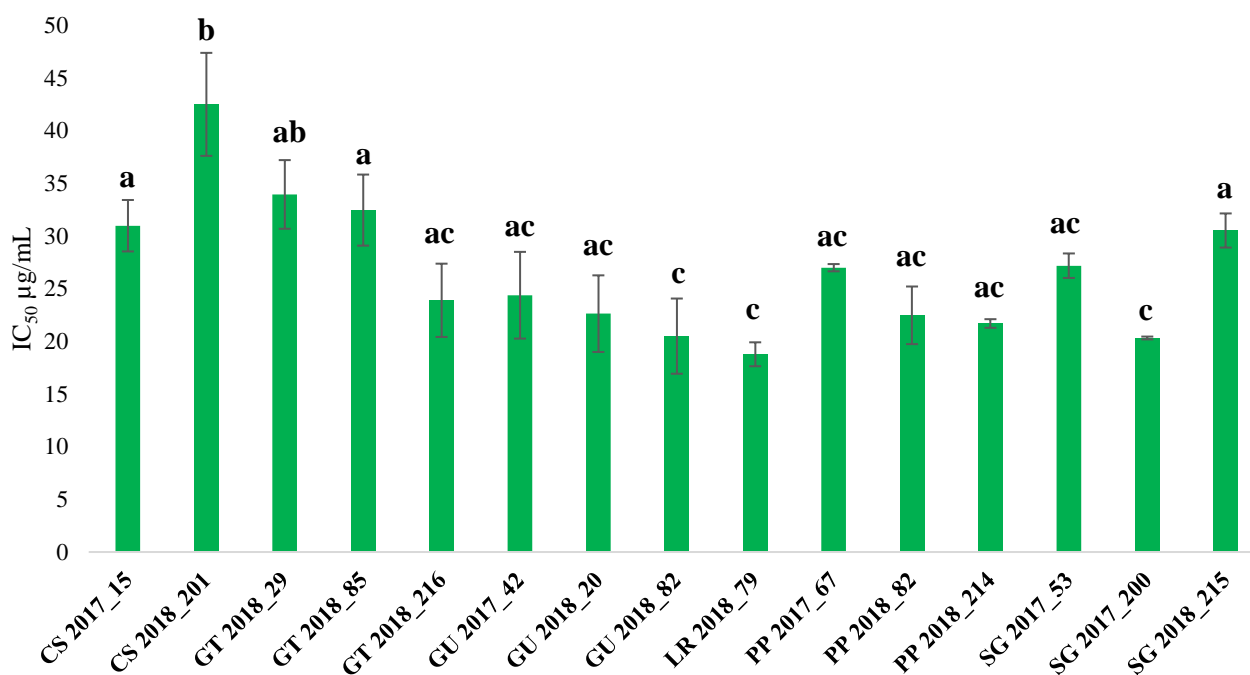


**Figure 6:** Antibacterial activity of the fifteen selected samples against *S. epidermidis*. Each label reports the collection field, the year and the day of harvesting. The IC<sub>50</sub> values were expressed in µg/mL. Each histogram carries a letter referring to the statistical analysis.

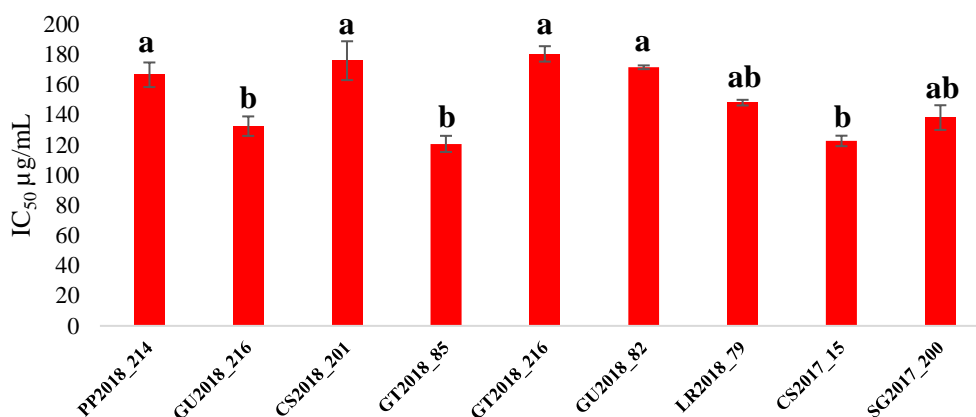


**Figure 7:** Antibacterial activity of the active samples against *K. pneumoniae*. Each label reports the collection field, the year and the day of harvesting. The IC<sub>50</sub> values were expressed in µg/mL. Each histogram carries a letter referring to the statistical analysis

The samples showed significant differences in biological activity yielding different IC<sub>50</sub>s.

For the antibacterial activity against *S. aureus* the IC<sub>50</sub>s ranged from 10.58 µg/mL to 43.2 µg/mL, for *S. epidermidis* from 18.77 µg/mL to 42.49 µg/mL while for *K. pneumoniae* from 120.7 µg/mL to 175.9 µg/mL. All the extracts were active on *staphylococci* species, conversely against *K. pneumoniae* only nine out of fifteen extracts resulted effective.

The fifteen extracts were also evaluated for cytotoxicity on mammalian cells. The data are reported in Table 1.

SAMPLE	Day of harvesting	CC <sub>50</sub> µg/mL	S.D.
PP 2018	82	120.9	3.2
GT 2018	85	252.3	9.2
GU 2018	82	139.2	11.5
CS 2018	201	102	1.7
SG 2018	215	140.2	9.0
PP 2018	214	112.3	10.0
GT 2018	29	171	2.6
GT 2018	216	120.8	5.1
GU 2018	20	231.6	6.1
LR 2018	79	161.1	7.3
CS 2017	15	162.8	9.9
GU 2017	42	139.6	5.6
PP 2017	67	189.7	2.8
SG 2017	53	148.1	12.0
SG 2017	200	224.7	9.7

**Table 1:** Cytotoxicity of the fifteen extracts against Vero cells. The CC<sub>50</sub> values were expressed as mean value and standard deviation (SD) of three independent experiments

The extracts cytotoxicity ranged between 102  $\mu\text{g/mL}$  and 252  $\mu\text{g/mL}$ . Hence, regarding the activity against *S. aureus* and *S. epidermis* all the extracts resulted safe, showing  $\text{IC}_{50}$ s lower than  $\text{CC}_{50}$ s. On the contrary, for *K. pneumoniae* growth inhibition most of the extracts resulted active at cytotoxic concentrations, thus the activity may be due to a generalized toxicity.

### **Characterization of the active metabolites**

After noting that metabolic changes also involved changes in biological activity, the NMR profiles of the most promising samples were analysed to select the best extract for bio-guided fractionation, with the aim to characterize the metabolites responsible for the biological activities.

Since the screening of the thirty-six Sardinian plants suggested the involvement of polyphenols and flavonoids for antibacterial activity, the extract showing the most abundant signals in the area between 6 and 8 ppm of  $^1\text{H}$  NMR spectrum, typical of these metabolites, was selected. This extract, namely SG2017\_200, showed marked activity on both *Staphylococci* with an  $\text{IC}_{50}$  of 20.3  $\mu\text{g/mL}$  against *S. epidermidis* and 29.4  $\mu\text{g/mL}$  against *S. aureus*. This extract resulted also active against *K. pneumoniae*, with an  $\text{IC}_{50}$  of 138.2  $\mu\text{g/mL}$ , lower than the  $\text{CC}_{50}$  value which was 224,7  $\mu\text{g/mL}$ , demonstrating a very high safety profile. Thus, SG2017\_200 was selected for bio-guided fractionation for *S. epidermidis* inhibition grown, the bacterium for which it obtained the best results in the biological assays.

The extract was submitted to fractionation through Medium Pressure Liquid Chromatography (MPLC), obtaining four fractions of different polarity. Specifically, polarity decreased from fraction 1 to fraction 4. The antibacterial activity of the original extract and the four fractions against *S. epidermidis* are reported in Figure 8.

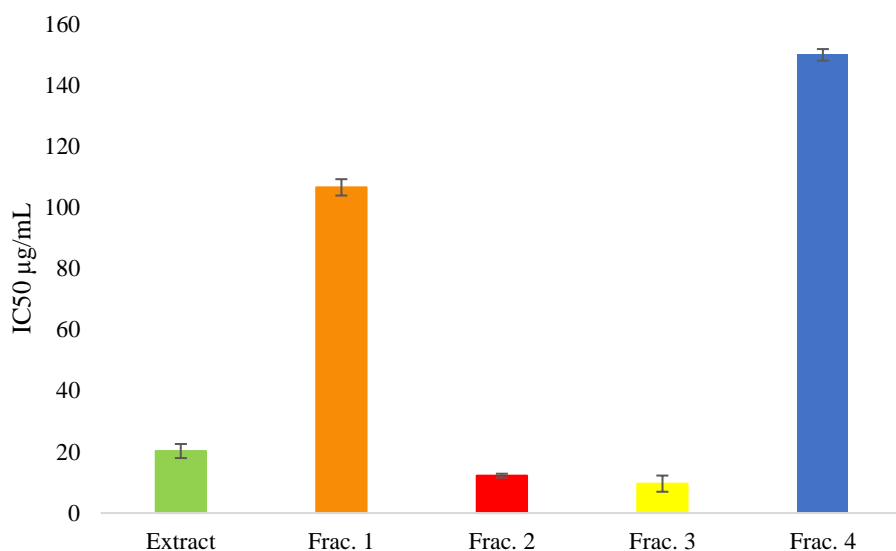


**Figure 6:** Antibacterial activity of SG2017\_200 extract and fractions against *S. epidermidis*.

By comparing the IC<sub>50</sub> values of the extract and the fractions, it was evident that the active metabolites were concentrated in fractions 2 and 3 (medium polarity). Specifically, fraction 2 possessed an IC<sub>50</sub> value of 12.3 µg/mL, while fraction 3 of 9.6 µg/mL. Fraction 3 was selected for further fractionation through MPLC to obtain sub-fractions of increased purity, yielding 15 sub-fractions which were tested for biological activity. Among the sub-fractions, two out of fifteen showed a substantial increase in antibacterial activity, resulting in a IC<sub>50</sub> value of 4.4± 0.6 µg/mL and 7.7 ± 0.3 µg/mL (Fig. 9).

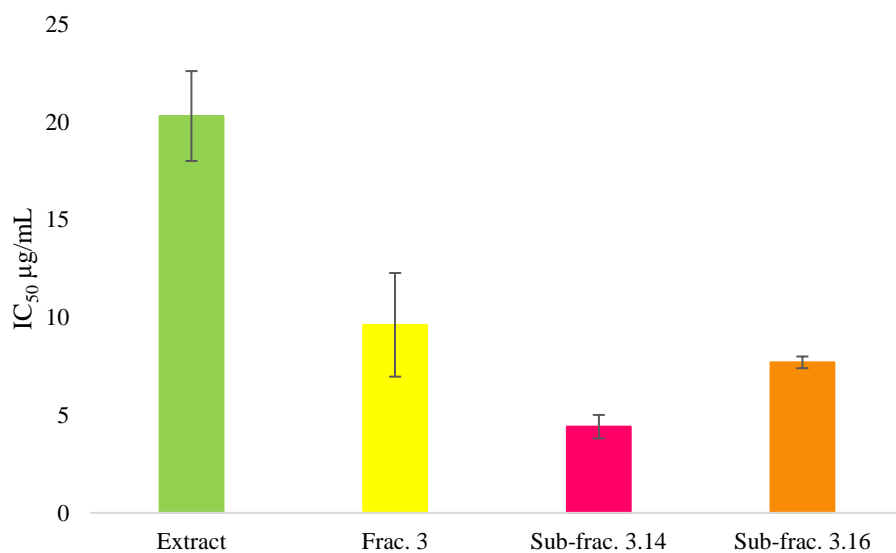


**Figure 7:** Antibacterial activity of SG2017\_200 extract, fraction 3 and sub-fraction 3.14 and 3.16 against *S. epidermidis*.

Sub-fraction 3.14 was submitted to NMR and MS analysis for the structure elucidation. It appeared to consist predominantly of one compound, although the presence of minor NMR signals indicated there were also some minor compounds at very low concentration.

UV spectrum of fraction 3.14 produced maximal absorbance peaks at  $\lambda_{\max}$  280 and 350 nm, which were characteristic of a flavonoid with a flavone skeleton. The  $^1\text{H-NMR}$  spectrum clearly showed four aromatic hydrogens,  $\delta_{\text{H}}$  7.75 and  $\delta_{\text{H}}$  6.92, which were assigned to the carbons in position 2', 3', 5' and 6' of the B ring of the flavone skeleton. The correlation in the HMBC spectrum with a carbon  $\delta_{\text{C}}$  159.54 suggested the presence of a hydroxyl group on this carbon as part of the B ring. Other two aromatic hydrogens,  $\delta_{\text{H}}$  6.19 and  $\delta_{\text{H}}$  6.37, binding the carbons  $\delta_{\text{C}}$  97.7 and  $\delta_{\text{C}}$  92.6 respectively, were assigned to the A ring. The latter carbons showed a correlation with the anomeric hydrogen signal at 5.36 in HMBC spectrum, suggesting the presence of a sugar moiety in position 3. The methyl signal at  $\delta_{\text{H}}$  0.90 binding the carbon at  $\delta_{\text{C}}$  15.54 indicated the sugar was rhamnose. Hence, the compound was identified as kaempferol-3-*O*-rhamnoside (Fig. 10), also known as afzelin. The MS analysis confirmed this hypothesis and the spectral data were in agreement with those found in the literature<sup>117</sup>.

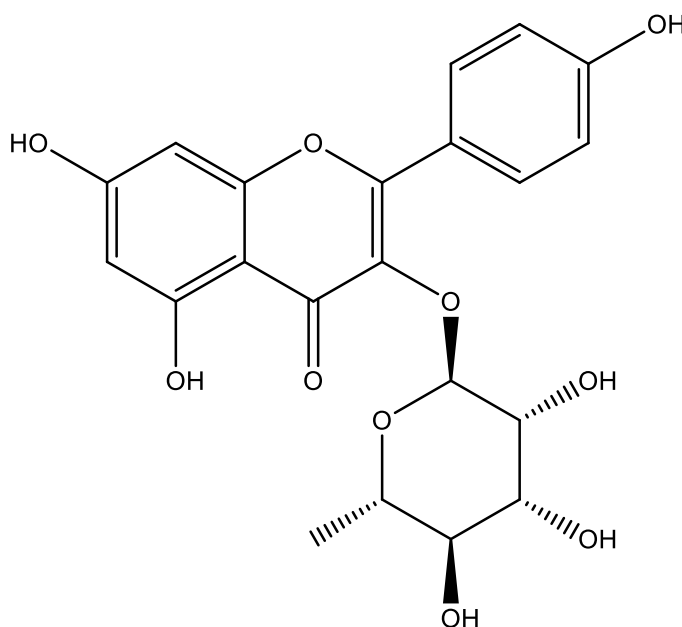


**Figure 8:** *Kaempferol-3-O-rhamnoside*

Kaempferol-3-*O*-rhamnoside was already characterized in the hydroalcoholic leaves extract of *A. unedo*<sup>118</sup>, together with the flavonoids kaempferol 3-arabinoside, quercetin 3-arabinofuranoside,

quercitrin and hyperin. This metabolite demonstrated several biological activities. Actually, it showed antiplasmodial properties against chloroquine-resistant *Plasmodium falciparum*<sup>119</sup>, anticancer activity on MCF-7 breast cancer cells and LNCaP human prostate cancer cell lines, inhibiting cell proliferation in a dose-dependent manner and promoting apoptosis by activation of the caspase signalling cascade<sup>117,120</sup>. Moreover, Kaempferol-3-*O*-rhamnoside was proved to be a competitive inhibitor of intestinal SGLT1 cotransporter, reducing glucose intestinal absorption which is an important factor in decreasing hyperglycaemia in diabetic patients<sup>121</sup>. This polyphenolic flavone also showed positive effects on allergic and inflammatory airway diseases, in fact in an asthma model mouse significantly inhibited ovalbumin-induced lung inflammation<sup>122</sup>. Kaempferol-3-*O*-rhamnoside demonstrated anti-amyloidogenic properties, counteracting cytotoxic effects due to self-assembly of the A $\beta$ 42 peptide in Alzheimer's Disease<sup>123</sup>. Regarding the antibacterial activity, the inhibition of *Staphylococcus epidermidis* growth was already reported<sup>124</sup>. Moreover, this metabolite was successfully tested against *Staphylococcus aureus*, *Pseudomonas aeruginosa* and *Salmonella typhi*. It also showed antimycotic activity against *Candida albicans* and *Candida parapsilosis*<sup>125</sup>. Further studies are ongoing for the identification of compounds with antibacterial activity against *S. epidermidis* in sub-fraction 3.16 as well as in fraction 2 of SG2017\_200 extract.

### **NMR data of Kaempferol 3-O-rhamnoside**

NMR Afzelin (Kaempferol 3-*O* rhamnoside) , (D<sub>2</sub>O, 600 MHz):  $\delta$  7.75 (d, 2,  $J$  = 8.81 Hz, H-3', H-5'), 6.92 (d, 2,  $J$  = 8.81 Hz, H-2', H-6'), 6.37 (d, 1,  $J$  = 2.16 Hz, H-8), 6.19 (d, 1,  $J$  = 2.16 Hz, H-6), 5.36 (d, 1,  $J$  = 1.74 Hz, H-1''), 4.20 (dd, 1,  $J$  = 3.42, 1.74 Hz, H-2''), 3.68 (d, 1,  $J$  = 3.42 Hz, H-3''), H-4''), 3.31 (d, 1,  $J$  = 2.69 Hz, H-5''), 0.90 (d, 3,  $J$  = 6.29 Hz, H-6''); <sup>13</sup>C NMR (CD<sub>3</sub>OD, 150 MHz):  $\delta$  159.54 (COH, C-4'), 129.79 (CH, C-3', C-5'), 120.49 (C, C-1'), 114.38 (CH, C-2', C-6'), 101.32 (CO, C-1''), 97.70 (CH, C-6), 92.64 (CH, C-8), 70.91 (CH, C-5''), 70.03 (CH, C-3'', C-4''), 69.76 (CH, C-2''), 15.56 (CH<sub>3</sub>, C-6''). Positive ESI-MS  $m/z$ : 353 [M + Na]<sup>+</sup>, 369 [M + K]<sup>+</sup>, calculated as 330.29 for C<sub>14</sub>H<sub>18</sub>O<sub>9</sub>. Negative ESI-MS  $m/z$ : 329 [M - H]<sup>-</sup>.

### 3.3.4 Conclusions

Metabolomic-chemometric approach allowed to reap the metabolomic variations of *A. unedo* leaf samples collected under different conditions. In particular, the phytochemical differences mainly concerned the expression of sugars, quinic acid and some secondary metabolites, such as arbutin and flavonoids. These differences in the metabolome also led to differences in antibacterial activity and cytotoxicity. The most promising extract was subjected to bio-guided fractionation and one of the active metabolites was identified as kaempferol-3-*O*-rhamnoside. Further studies are in progress to complete the characterisation of the other compounds responsible for the antibacterial activity.

## 4 RAPID IDENTIFICATION OF AMARYLLIDACEAE ALKALOIDS IN BULB EXTRACT OF *URCEOLINA PERUVIANA* (C. Presl) J.F. Macbr

### 4.1 Introduction

The isolation and the structure determination of new bioactive natural products (NPs) from plants is a complex process that associates extraction, fractionation of extract, fraction purification and spectrometric and spectroscopic analysis. These processes are costly and time-consuming, hence avoiding the isolation of the already known compounds is one of the most important challenges of plant-based innovation. The early identification of already discovered molecules is known as dereplication<sup>126</sup>. The second part of this thesis concerns the elaboration of a dereplication method for the identification of Amaryllidaceae alkaloids in plant extract. The Amaryllidaceae alkaloids are a large group of isoquinoline alkaloids with a wide range of biological activities and structural variability. In addition to galanthamine, marketed for the treatment of Alzheimer's disease, these isoquinoline alkaloids have demonstrated numerous biological properties, including antibacterial, antiviral, antiinflammatory, antidepressant, anticonvulsant and anticancer activities<sup>127</sup>. To date, more than 600 alkaloids were identified, hence the probability of isolating an alkaloid already known in the scientific literature is high. For this study, *Urceolina peruviana* (C. Presl) J.F. Macbr was selected. There is a scarce literature on the alkaloids in the bulbs of this species, hence in this study the alkaloids composition of the bulb extract was undertaken. The alkaloids already known in literature were quickly identified directly on the fractions of the extract, without recourse to purification processes. The only fraction which was purified was the one containing an alkaloid with an NMR profile not registered in any database, which turned out to be a new alkaloid. The dereplication method proposed in this study consists of several steps (Fig. 1): an alkaloid enriched extract is prepared, the extract is fractionated by Centrifugal Partition Chromatography (CPC), the extract fractions are analysed in Ultra Performance Liquid Chromatography coupled to High Resolution Mass Spectrometry (UPLC-HRMS) to obtain the molecular formulas of the alkaloids in the fractions, the same fractions are also analysed by Nuclear Magnetic Resonance (NMR) to obtain the 1D and 2D spectra. From the analysis of the NMR spectra a list of <sup>13</sup>C chemical shifts of carbon atoms belonging to each molecule is created. These chemical shifts are compared with the spectroscopic data present in a suitably constructed database named amaryll2\_knapsack, containing the predicted <sup>13</sup>C NMR spectra of 209 Amaryllidaceae alkaloids extracted from the web-based KNAPSAcK database by the KnapsackSearch tool [<https://github.com/nuzillard/KnapsackSearch>], and in the CSEARCH web-based tool. The molecular formula derived from the UPLC-HRMS analysis are used to reduce the

number of likely molecules, in fact the list of chemical shifts is compared only with compounds that have the indicated molecular formula. The already known alkaloids are recognized by correspondence of the list of spectroscopic data with those from databases.

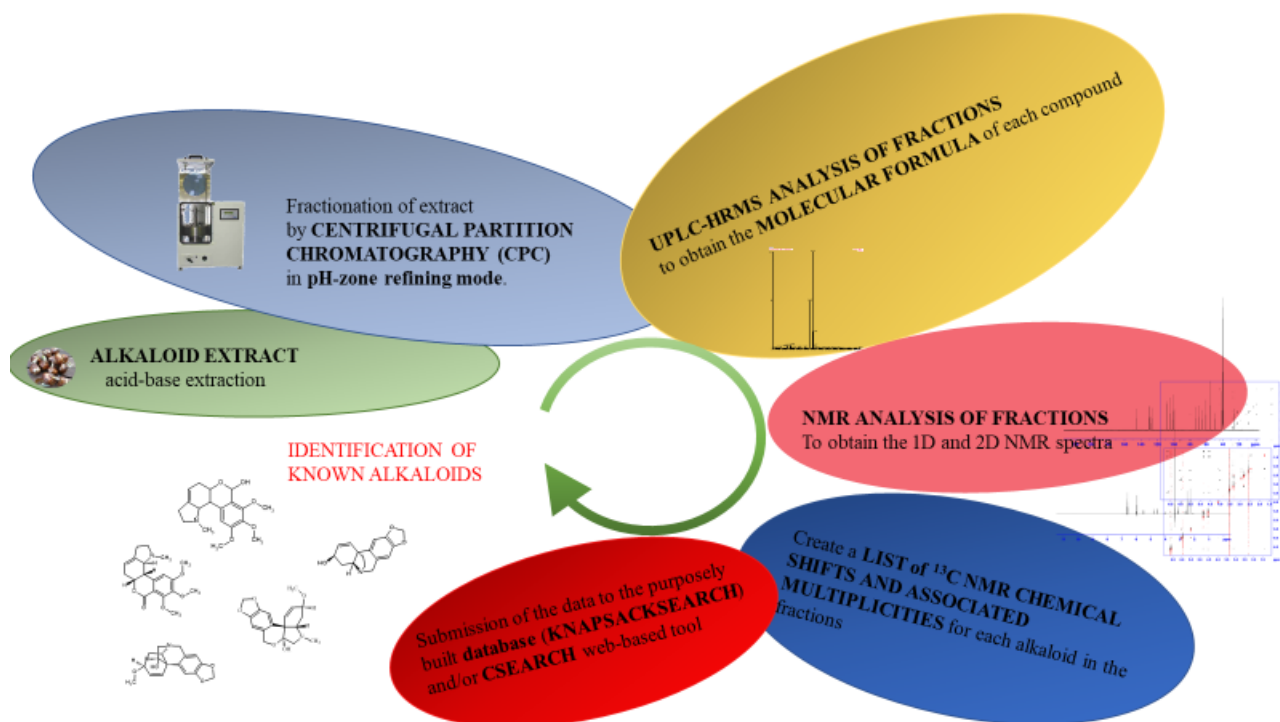


**Figure 1:** Workflow of dereplication protocol for Amaryllidaceae alkaloids

### 4.1.1 Dereplication

The dereplication concept was introduced for the first time in 1990 by Beutler *et al.* who used the term to indicate “a process of quickly identifying known chemotypes”<sup>128</sup>. In Natural Products Research, over the course of thirty years, the tools and methods for achieving this goal have changed but the concept remains the original one.

A good dereplication method allows the rapid and reliable identification of already known metabolites to avoid the time-consuming and costly isolation and characterization processes.

Several dereplication workflows can be performed in Plant-Based Drug Discovery. A first distinction can be made between targeted and untargeted workflows<sup>126</sup>.

The first one deals with the identification of determined compounds in a plant extract<sup>129–132</sup>.

The untargeted approach aims to the rapid identification of the major compounds of a plant extract or, at least, of their chemical class. An efficient dereplication strategy is based on the use of reliable, sensitive and robust analytical techniques. In this context, Nuclear Magnetic Resonance (NMR) spectroscopy and Mass Spectrometry (MS) are among the most common and powerful techniques<sup>133</sup>. In most cases the success of a dereplication method strongly depend on the availability of databases. Unfortunately, there is no universal database for NPs, on the contrary there are many different databases, most of which have no free access<sup>134</sup>.

For this study an in-home Amaryllidaceae alkaloids database, amaryll2\_knapsack, generated by KnapsackSearch from the KNApSACk database and the CSEARCH web-based tool were used. The CSEARCH web server is an online database containing several tens of million compounds, both natural products and synthetic/semi-synthetic molecules, with their predicted chemical shift values. CSEARCH accepts requests made of a list of <sup>13</sup>C NMR chemical shifts, with each value associated to a multiplicity indication (number of attached hydrogen atoms, as deduced from DEPT or multiplicity-edited 2D HSQC spectra) and returns within a few minutes a list of structures sorted in the decreasing order of likelihood. Hence, both the databases give the possibility to quickly identify the compound under examination through a simple check in the NMR spectra.

#### 4.1.2 Amaryllidoideae subfamily and Amaryllidaceae alkaloids

The Amaryllidaceae belong to a family of monocotyledonous plants traditionally placed in the order Liliales but attributed by the Angiosperm Phylogeny Group (APG) classification to the order Asparagales<sup>135,136</sup>. This plant family can be found in several climatic areas of the world, however, the distribution is particularly marked in tropical and subtropical zones. The family is essentially composed by perennial bulbous plants, renowned for the beautiful inflorescences and the countless uses in traditional medicine of many countries<sup>137</sup>. On the basis of molecular phylogenetic studies, Amaryllidaceae plant family is divided into three subfamilies: Agapanthoideae, Allioideae and Amaryllidoideae<sup>138,139</sup>, the latter is one of the most important alkaloid-containing plant taxa.

The Amaryllidoideae subfamily comprises 59 genera which include more than 800 species<sup>140</sup>. The interest for these species derives from the presence of peculiar secondary metabolites known as the Amaryllidaceae alkaloids. The Amaryllidaceae secondary metabolites are isoquinoline alkaloids renowned for the wide range of biological activities. The pharmacological properties are directly associated with the structural variety of these molecules which show different types of chemical structures. The chemical and biological variability of these compounds have arisen and still arise the interest of the scientific community. From the first study on Amaryllidaceae alkaloids in 1952, the number of publications on this issue is globally growing (Fig. 2).

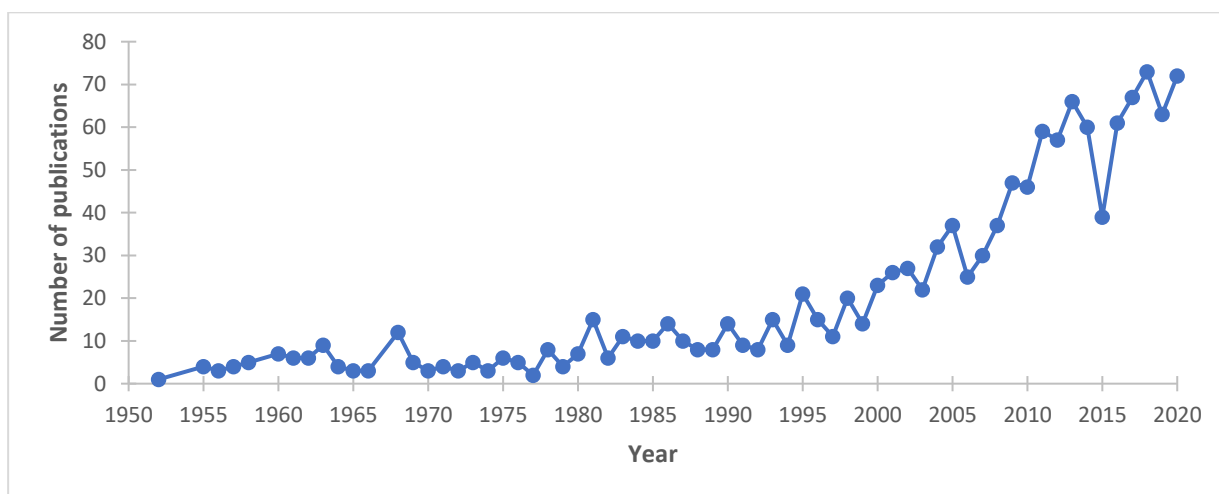


**Figure 2:** Citation report obtained with the topic “Amaryllidaceae alkaloids” from Scopus web of science. The number of publications from 1952 to October 2020 are displayed.

The biosynthetic relationship of the main alkaloids of Amaryllidaceae is schematically shown in Figure 3. Briefly, the Amaryllidaceae alkaloids derive from the amino acids L-Phenylalanine (L-Phe) and L-tyrosine (L-Tyr). L-Phe is converted into 1,2-dihydroxybenzylaldehyde (cinnamic acid pathway), while L-Tyr is converted into tyramine (by decarboxylation). The condensation of these

two derivatives results in a Schiff base, which gives norbelladine and its derivative 4'-*O*-methylnorbelladine by reduction. From the 4'-*O*-methylnorbelladine the various types of alkaloids are produced according to the type of oxidative phenol coupling (ortho-*para*', para-*para*' or para-*ortho*'). Numerous enzymes are involved in the biosynthetic pathways, many of which have not yet been identified. However, phenol oxidative reactions are probably catalysed by cytochrome P450 enzymes<sup>140,141</sup>.

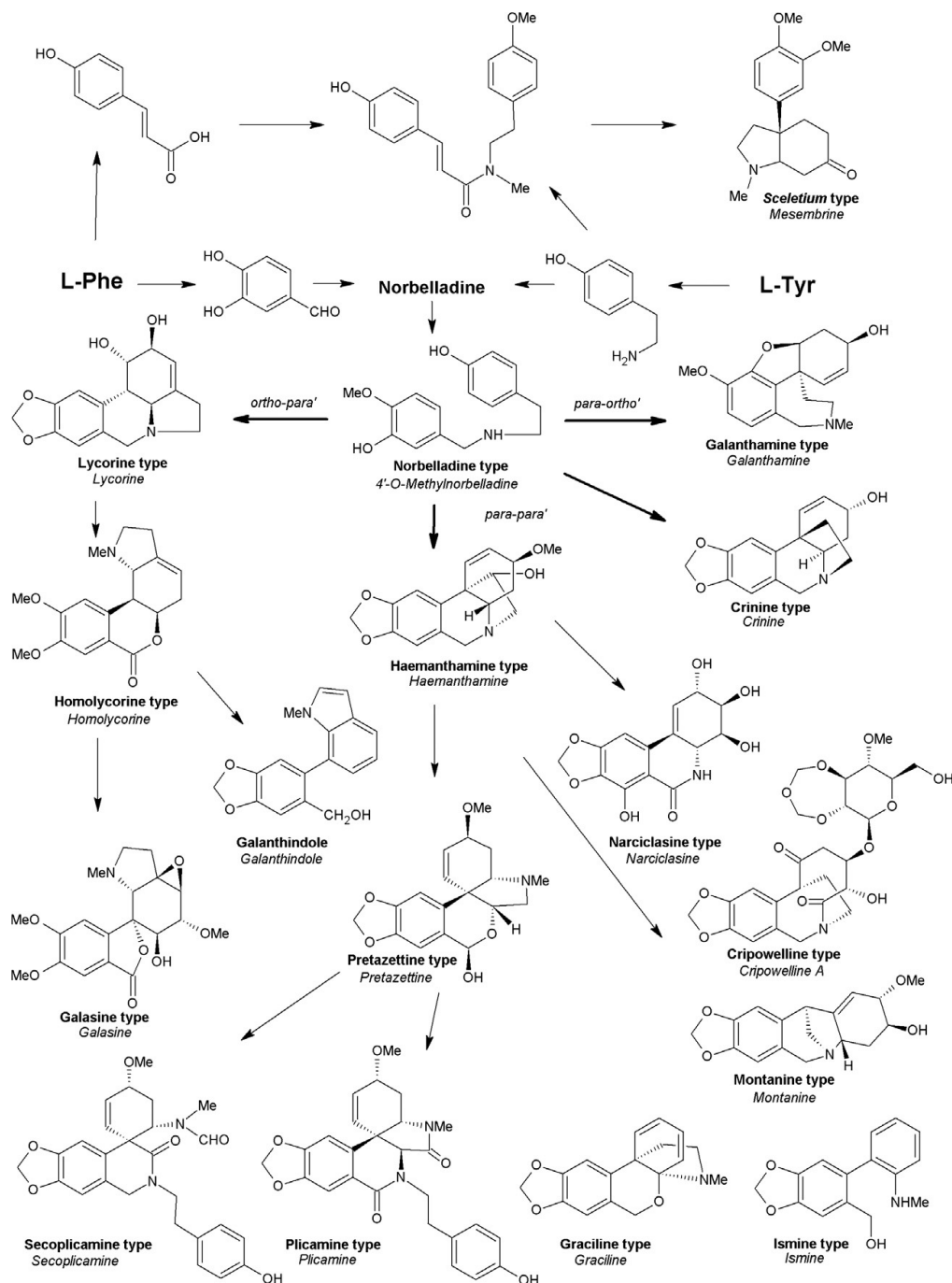


**Figure 3:** The biosynthetic relationship of the main Amaryllidaceae alkaloids. Berkov et al. 2020<sup>140</sup>

Nowadays, more than 600 alkaloids were identified and a huge amount of biological activities has been reported, including antiviral<sup>142</sup>, antibacterial<sup>143</sup>, antifungal<sup>144</sup>, antitumor, antimalarial and analgesic<sup>145</sup>. Galanthamine was marketed for the treatment of Alzheimer's disease acting as an irreversible inhibitor of the Acetylcholine Esterase enzyme (AChE)<sup>146</sup>, it has also shown other positive effects in the treatment of several pathologies such as the Metabolic Syndrome (MetS) reducing inflammation<sup>147</sup>. Pancratistatin and narciclasine showed promising anticancer activities<sup>148</sup>, these compounds together with several lycorine and haemanthamine type of alkaloids have been selected as lead molecules in the anticancer research<sup>149</sup>.

#### 4.1.3 *Urceolina peruviana* (C. Presl) J.F. Macbr

*Urceolina peruviana* (C. Presl) J.F. Macbr., also known as *Stenomesson miniatum* (Herb.) Ravenna is a bulbous perennial plant, which grows wild in the Andean regions of Peru and Bolivia. It has a scape about 40 cm high, an umbrella of six or more red or orange tubular flowers, it blooms in the spring or summer, the leaves are narrow, long until 40 cm<sup>150,151</sup> (Fig. 4).



**Figure 4:** *Urceolina peruviana* (C. Presl) J.F. Macbr flowering plant

There is scarce information on this species of Amaryllidaceae in the scientific literature. The only article about the alkaloid composition of its bulbs was written in 1957 by Boit and Döpke, who reported the identification of three alkaloids (tazettine, haemanthamine and lycorine) and two others that could be traced back to nerinine and albomaculine structures<sup>152</sup>. Regarding the ethnobotanical use of this plant, Girault, in his book "Kallawaya, guérisseurs itinérants des Andes: recherches sur les pratiques médicinales et magiques" on the uses of medicinal plants by the indigenous South Americans, mentioned *Urceolina peruviana* whose fresh bulbs were mixed with pork or llama fat for the treatment of tumours and abscesses<sup>153</sup>.

Considering the interesting ethnobotanical use and the poor documentation on its alkaloids content, *Urceolina peruviana* was selected for this study.

## 4.2 Material and methods

### Plant material

The fresh bulbs of *U. peruviana* (1090.3 g) were purchased at the horticultural nursery Quatro Estaciones (Cochabamba, Bolivia) in August 2019. Some bulbs were cultivated and the plants were identified by Dr. Umberto Mossetti, a voucher specimen (BOLO0602041) was deposited in the Herbarium of University of Bologna (SMA). The bulbs were stored in a cold room at 5 °C until the use, then they were frozen to be freeze-dried and subsequently crushed resulting in 220 g of plant material.

### Chemicals

Methyl tert-butyl ether (MtBE), acetonitrile (ACN), methanol (MeOH), ammonium hydroxide (NH<sub>4</sub>OH), chloroform (CHCl<sub>3</sub>), diethyl ether (Et<sub>2</sub>O), ethyl acetate (EtOAc) were purchased from Carlo Erba Reactifs SDS (Val de Reuil, France), sulfuric acid (H<sub>2</sub>SO<sub>4</sub>) and triethylamine (TEA) from Sigma–Aldrich (Steinheim, Germany). Deuterated dimethylsulfoxide (DMSO-*d*<sub>6</sub>) was purchased from Eurisotop (Saclay, France). Deionized water was used to prepare aqueous solutions.

### Extraction

To select the best extraction method, two extraction protocols were tested.

#### Extraction Method 1 (small-scale)

A single freeze-dried crushed bulb (1,473 g) was extracted as proposed by Lianza *et al.*<sup>154</sup> with some modifications. The plant material was extracted by maceration in 0.03 L of MeOH for 24 hours, the

solution was filtered and other MeOH was added to plant material, this operation was repeated for three days. Subsequently, the extractive solution was evaporated under reduced pressure to obtain 0.501 g of crude extract. The latter was acidified with 0.01 L of H<sub>2</sub>SO<sub>4</sub> 2% (v/v) until pH 2, 0.01 L (x4) of diethyl ether was used to remove the neutral materials. The aqueous solution was basified with NH<sub>4</sub>OH 25% (v/v) until pH 9, then was extracted with 0.01 L (x4) of EtOAc to give 0.061 g of alkaloid extract.

#### **Extraction Method 2 (small-scale)**

A single freeze-dried crushed bulb (1.294 g) was extracted according to the protocol proposed by Renault *et al.*<sup>155</sup> slightly modified. Plant material was moistened with NH<sub>4</sub>OH 2.5 M and macerated in 0.03 L of EtOAc for two days, the solution was filtered and other solvent was added to plant material for another day. The extractive solution was concentrated to 0.005 L and extracted with 0.005 L (x3) and 0.004 L (x2) of H<sub>2</sub>SO<sub>4</sub> 0.6 M. The aqueous solution was basified NH<sub>4</sub>OH 7.5 M until pH 10 and extracted with 0.005 L (x3) and 0.004 L (x2) of CHCl<sub>3</sub>. The organic solution was washed with water until pH 7 and evaporated under reduced pressure to obtain 0.02 g of alkaloid extract.

#### **Extraction Method (large-scale)**

Extractive method 2 was considered as the best protocol, hence the method was adjusted for the extraction of the whole plant material available. The crushed bulbs were moistened with NH<sub>4</sub>OH 2.5 M and macerated in 4 L of EtOAc for three days. The extractive solution was collected by lixiviation and a further 4 L of EtOAc were added for maceration for other 2 days, then the solution was concentrated to 1 L.

The EtOAc solution was extracted with 0.2 L (x3) and 0.1 L (x3) of H<sub>2</sub>SO<sub>4</sub> 0.6 M, the aqueous phase was basified with NH<sub>4</sub>OH 7.5 M until pH 10 and extracted with 0.2 L (x3) and 0.1 L (x3) of CHCl<sub>3</sub>. Finally, the chloroformic solution was washed with water until pH 7 and evaporated under reduced pressure obtaining 2.7 g of alkaloid extract.

#### **Centrifugal Partition Chromatography (CPC)**

Centrifugal Partition Chromatography (CPC) fractionation of the extract was carried out using a lab-scale FCPE300® column of 303 mL inner volume (Kromaton Technology, Angers, France). The column was composed of 7 circular partition disks, each engraved with 33 twin-cells of 1.0 mL. The liquid phases were pumped by a preparative 1800 V7115 pump (Knauer, Berlin, Germany). Fractions of 20 mL were collected by a Labocol Vario 4000 (Labomatic Instruments, Allschwil, Switzerland). 1 g of extract was fractionated by CPC in pH-zone-refining mode. MtBE, ACN and H<sub>2</sub>O were equilibrated according to the proportion 5 :2 :3 (v/v) and the two phases were separated. The lower

aqueous phase was used as stationary phase and acidified with H<sub>2</sub>SO<sub>4</sub> 10 mM (retainer). The upper organic phase was basified with TEA 8 mM (displacer) and used as mobile phase. The column was conditioned with the stationary phase at 300 rpm. The extract was solubilized in 10 mL of retainer phase (acidified aqueous phase) and 5 mL of neutral organic phase and injected, finally the mobile phase was pumped into the column in ascending mode at flow-rate of 20 mL/min and 1200 rpm. The fractions were collected from the basic organic mobile phase and pooled according to TLC analysis to give 13 fractions namely A1-A13.

CPC of fraction A12 was carried out using an apparatus adequate for the mass of the fraction (99.0 mg), assembled with FCPC-A200 column of 202 mL inner volume (Kromaton Technology, Angers, France). The column was composed of 21 circular partition disks, each engraved with 40 twin-cells of 0.24 mL. The liquid phases were pumped by a preparative 1800 V7115 pump (Knauer, Berlin, Germany) and the fractions were collected by a Labocol Vario 4000 (Labomatic Instruments, Allschwil, Switzerland). The method was the same of extract fractionation, adapting the amount of retainer and displacer to the quantity of sample, hence H<sub>2</sub>SO<sub>4</sub> 1,5 mM and TEA 2 mM were employed.

### **Thin layer chromatography (TLC)**

TLC analysis was developed on Merk TLC Silica gel 60 F254 plates, using CHCl<sub>3</sub>/ MeOH (8.5 /1.5) as mobile phase.

### **NMR analysis**

All NMR spectra were recorded on a Bruker AV III 600 NMR spectrometer (Bruker, Wissembourg, France) operating for <sup>1</sup>H NMR at 600.16 MHz. It is fitted with a TXI cryoprobe with a z-gradient coil and <sup>1</sup>H, <sup>13</sup>C, and <sup>2</sup>H cooled preamplifiers. All spectra were recorded at 298 K with samples dissolved either in DMSO-*d*<sub>6</sub> or CDCl<sub>3</sub>. Referencing of spectra recorded in DMSO-*d*<sub>6</sub> was achieved by setting the <sup>1</sup>H signal of residual DMSO-*d*<sub>5</sub> at 2.5 ppm and the <sup>13</sup>C signal of DMSO-*d*<sub>6</sub> at 39.52 ppm. Referencing of spectra recorded in CDCl<sub>3</sub> was achieved by setting the <sup>1</sup>H signal of residual CHCl<sub>3</sub> to 7.26 ppm and the <sup>13</sup>C signal of CDCl<sub>3</sub> at 77.16 ppm. All spectra were recorded using the pulse sequences from the standard library of TopSpin 3.2 (Bruker) and processed with TopSpin 4.0.5 (Bruker).

### **UPLC-HRMS analysis**

UPLC-HRMS analysis was performed using Acquity H-Class UPLC system with Diode Array detector coupled to SYNAPT G2 Si spectrometer supplied by Waters (Watford, Herts., UK). The spectrometer was composed of a positive ions electrospray source and a ToF analyser type W.

Uptisphere Strategy C18-HQ (150x2.1 mm, 2.2  $\mu\text{m}$ ; Interchim, Montluçon, France) column was employed for the chromatographic separation. A gradient elution mode was used with solvent A (ammonium acetate 1%, pH 6.6) and solvent B (ACN) at flow rate of 0.4 mL min<sup>-1</sup>. Starting from 10%B, the gradient was linearly changed to 20%B in 6 min, then to 25%B in other 6 min, after 0.2 min the percentage of B was increased to 100% keeping it constant for 1 min. Finally, the gradient returned in the initial conditions in 0.2 min and was kept constant for 2 min for equilibration. The samples were dissolved in methanol and analysed at concentration of 200 ppm with an injection volume of 1  $\mu\text{L}$ , the column temperature was set to 30°C. The alkaloids molecular formulas were proposed from accurate mass analysis of  $[\text{M-H}]^+$  ions. The UV detection wavelength was set at 287 nm, a typical value for the study of the Amaryllidaceae alkaloids.

## 4.3 Results and discussion

### Alkaloid extraction

The Amaryllidaceae alkaloids possess one or more nitrogen atoms that confer a certain basicity to the molecule. Depending on the position of nitrogen atom(s) in the chemical structure, basicity is more or less pronounced, however they can be considered weak basis<sup>156</sup>. This characteristic can be exploited for the alkaloid extraction, actually, most of the protocols rely on acid-base extraction<sup>154,155,157</sup>. Hence, the plant material is acidified and basified to have alkaloids in the salt form and the base form, respectively. In acid medium alkaloids are in the salt form and they are retained in the aqueous phase, conversely in basic medium alkaloids are retained in the organic phase. In this manner they can be separated from other types of metabolites. In this study two extraction protocols were compared to select the best one. The two methods gave different extractive yields. Specifically, method 1 by Lianza *et al.* gave an extractive yield (calculated on the freeze-dried bulb matter) of 4.14%, conversely method 2 by Renault *et al.* gave 1.54%. Both extracts, namely extract 1 (from method 1) and extract 2 (from method 2), were analysed by NMR and TLC to compare the differences in composition. As expected from the extraction yield, extract 1 showed more signals in the NMR spectra than extract 2. The most intense signals were common to both extracts, as in the carbon and proton spectrum. Extract 1 displayed a number of minor signals scattered across the spectrum (Fig 5, Fig. 6).

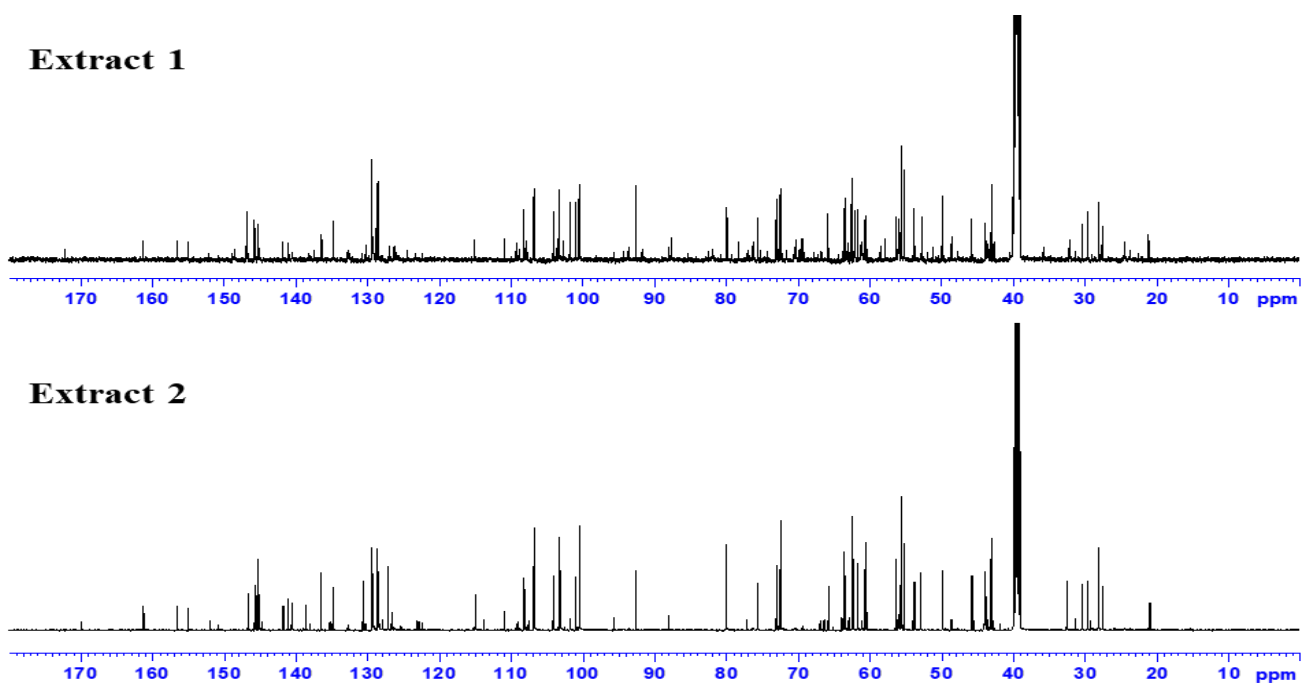


Figure 5: Comparison of  $^{13}\text{C}$ -NMR spectra of extract 1 and extract 2

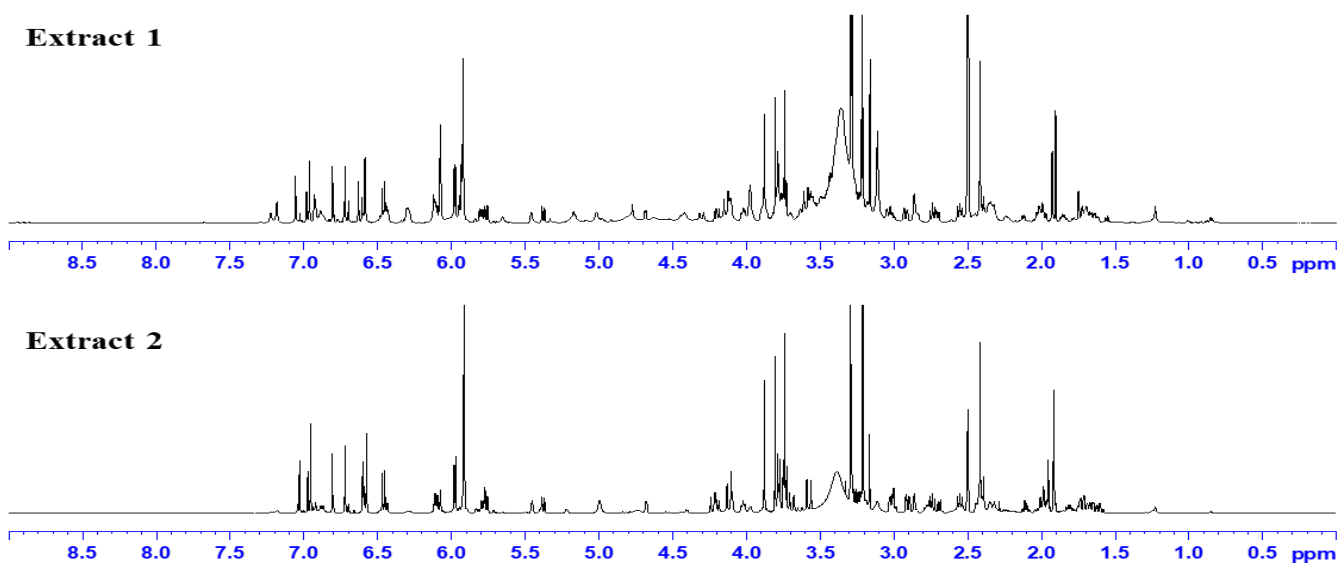
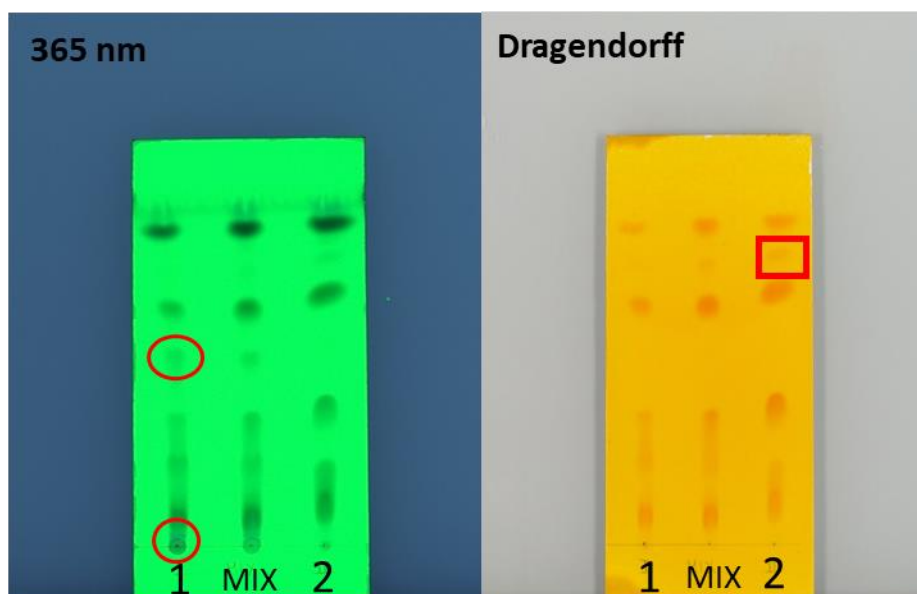


Figure 6: Comparison of  $^1\text{H}$ -NMR spectra of extract 1 and extract 2

TLC analysis showed different profiles for the extracts (Fig. 7). The plate was observed at the UV lamp at wavelength of 365 and 254 nm, then it was sprayed with Dragendorff reagent which reacts with alkaloids giving the typical orange colour. At 365 nm extract 1 showed more compounds than extract 2, however these compounds did not react with Dragendorff reagent. Moreover, extract 2 showed one more alkaloid than extract 1, hence, it is likely that the higher extraction yield of extract 1 was due to the extraction of other types of compounds (non-alkaloids).



**Figure 7:** TLC analysis of extract 1 (line 1), a mix solution of extract 1 and extract 2 (line MIX) and extract 2 (line 2). The circles on the left part indicate the compounds of extract 1 visible at 365 nm that did not react with Dragendorff reagent, the square on the right part indicate the alkaloid only present in extract 2.

Therefore, method 2 proved to be more selective for alkaloid extraction and was chosen for this study, adapting it to a large-scale extraction.

## Fractionation of extract by Centrifugal Partition Chromatography in pH-zone refining mode

Centrifugal Partition Chromatography (CPC) is a liquid–liquid partition chromatographic method, in which both the stationary and the mobile phase are liquids. The peculiarity of this separation technique is the absence of any solid support, avoiding saturation of the stationary phase and its chemical reactions with the injected material. The column is a rotor consisting of a series of stacked discs in which the cells are engraved. The separations take place in the cells which are connected by ducts. The centrifugal force makes stationary the first phase that is injected into the column while the mobile phase, injected later, is pumped through the stationary phase (Fig. 8).

This system was first designed by Murayama *et al.*<sup>158</sup>, who improved the device proposed by Ito *et al.*<sup>159</sup> originally built for the separation of lymphocytes.

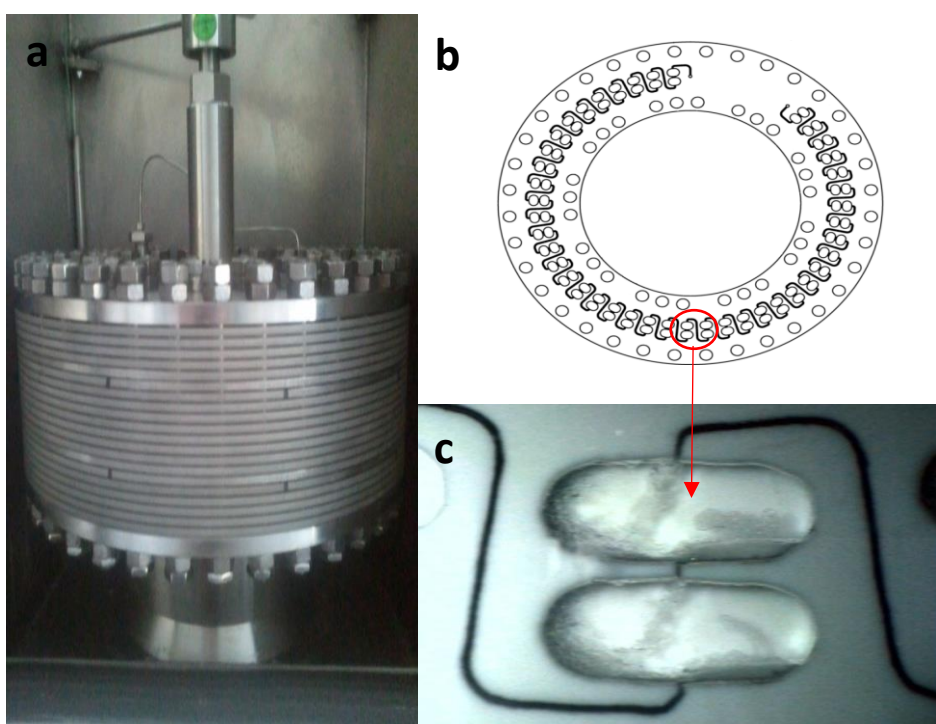


**Figure 9:** a) CPC column b) CPC disc c) CPC cells

As in all the most common liquid-liquid chromatographies this technique is also based on Nernst's distribution law, which states that the partition ratio ( $K_D$ ) of a solute between two immiscible solvent is constant at equilibrium. In CPC system both phases can be used as mobile phase since there are two elution modes: ascending mode or descending mode. The ascending mode is suitable when the less dense phase is chosen as the mobile phase, it is pumped into the column, enters the cells from the periphery and rises spontaneously through the stationary phase in the centripetal

direction, being lighter. Conversely in the descending mode the mobile phase is the densest, it enters the cells from the centre and following the centrifugal direction, it moves through the stationary phase occupying the bottom of the cell as it is heavier. In both elution modes the mobile phase moves from one cell to another through ducts until it reaches the equilibrium with the stationary phase, at this point it is possible to inject the mixture to be separated, the molecules will have different retention times depending on their affinity with the stationary phase.

CPC was successfully applied for separation of proteins, glycans, carbohydrates, phenolic acids and fatty acids<sup>160</sup>. For alkaloids separation, CPC can be used in a particular displacement mode, namely pH-zone refining<sup>161</sup>. This technique is particularly effective for molecules whose electric charge and solubility depends on pH value, so that the separation of alkaloids occurs according to their pKa values and partition coefficients<sup>162</sup>. CPC in pH-zone refining mode requires the use of an acid (or a base), named retainer, in the stationary phase to retain the alkaloids and of a base (or an acid), named displacer, in the mobile phase to elute the analytes according to their pKa and partition coefficients. The alkaloids elute in a series of contiguous blocks where their concentration and pH are constant, the blocks succeed each other with minimal overlap, in the centre of the block the analyte purity is high, while in the extreme parts normally also elute impurities and/or other alkaloids with slightly minor (or higher) pKa (Fig. 9).

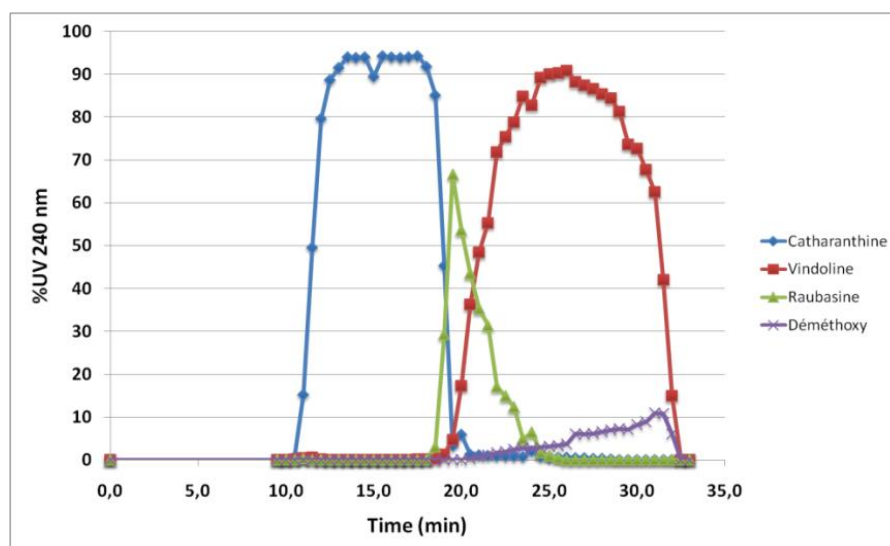


**Figure 9:** Example of alkaloids elution in CPC in pH-zone refining mode. In the central part of each block purity is high, in the extreme parts a coelution with other alkaloids or impurities is observed.

CPC in pH-zone refining mode was selected for the fractionation of *U. peruviana* bulb extract since it offers several advantages: this technique is support-free, possible chemical reactions between the analytes and the stationary phase as well as saturation of the stationary phase are avoided, high purity fractions are obtained, the sample loading capacity is high, the extract can be totally

recovered, solvent consumption is low and the separation can be monitored by measurement of the effluent pH.

CPC separations require the choice of a biphasic solvent system. It must ensure an optimal alkaloid partition into the mobile phase and the stationary phase, that means that protonated alkaloids must be totally partitioned into the aqueous phase while neutral alkaloids must be totally partitioned into the organic phase, this condition must be satisfied to achieve an effective separation. In order to select the best solvent system for CPC in pH-zone refining mode separation, several solvent systems were tested (Tab. 1).

SOLVENT SYSTEM	PROPORTION
<b>Tol/n-Hept/Ace/W</b>	24:8:10:34
<b>n-Hep/AcOEt/MeOH/W</b>	2:3:2:3
<b>MtBE/AcOEt/MeOH/W</b>	2:3:2:3
<b>n-Hep /ACN/W</b>	3:3:4
<b>MtBE/ACN/W</b>	3:3:4
<b>MtBE/ACN/W</b>	4:1:5
<b>MtBE/ACN/W</b>	5:2:3

**Table 1:** Biphasic solvent systems tested for CPC separation. Tol:toluene, n-Hept: n-heptane, Ace:acetone, W: water, AcOEt: Ethylacetate, MeOH: methanol, ACN: acetonitrile, MtBE: methyl tert-butyl ether.

The best alkaloids partition was achieved with MtBE/ACN/W solvent system in the proportion 5:2:3, thus, this biphasic solvent system was selected for CPC in pH-zone refining mode with the aqueous phase as stationary phase and the organic phase as mobile phase. The retainer ( $H_2SO_4$  10 mM) was added to the stationary phase, conversely the displacer (TEA 8 mM) was added to the mobile phase. The separation was performed in ascending mode and the fractions were collected from the organic phase to be quickly evaporated. The fractions were pooled according TLC analysis giving 13 fractions named A1-A13 (Table 2).

Fraction	A1	A2	A3	A4	A5	A6	A7	A8	A9	A10	A11	A12	A13
<b>Mass (mg)</b>	4	24	28	122	69	82	53	89	151	90	158	99	28

**Table 2:** CPC fractions with corresponding mass

## UPLC-HRMS analysis of alkaloid extract and CPC fractions

The extract and the fractions were analysed by UPLC-HRMS to obtain the molecular formulas of the isolated alkaloids. This technique was selected since UPLC-HRMS allows to perform fast analysis with high sensitivity, excellent peak resolution, low solvent consumption and excellent resolving power and mass accuracy<sup>163</sup>. Actually, UPLC system allows to work at high pressures (15000 psi) using short columns with small particles size, so that peaks of analytes appear sharp and well resolved. HRMS is able to generate distinct signals from very similar ions thanks to the technological evolution of mass analyzers. The  $m/z$  values are measured with from four to six significant digits, making HRMS particularly suitable for the differentiation of molecules with the same nominal mass, for the determination of the analytes molecular formulas and to reconstruct the ions fragmentation in detail<sup>164</sup>. Figure 10 shows the Based Peak Ion (BPI) chromatogram of the blank and the extract. The blank determination, clearly showed that the peaks between 7.15 and 9.24 min, as the peaks between 13.67 and 14.53 min, were impurities from the solvents or the column, hence these peaks were not taken into account for accurate mass analysis of  $[M-H]^+$  ions.

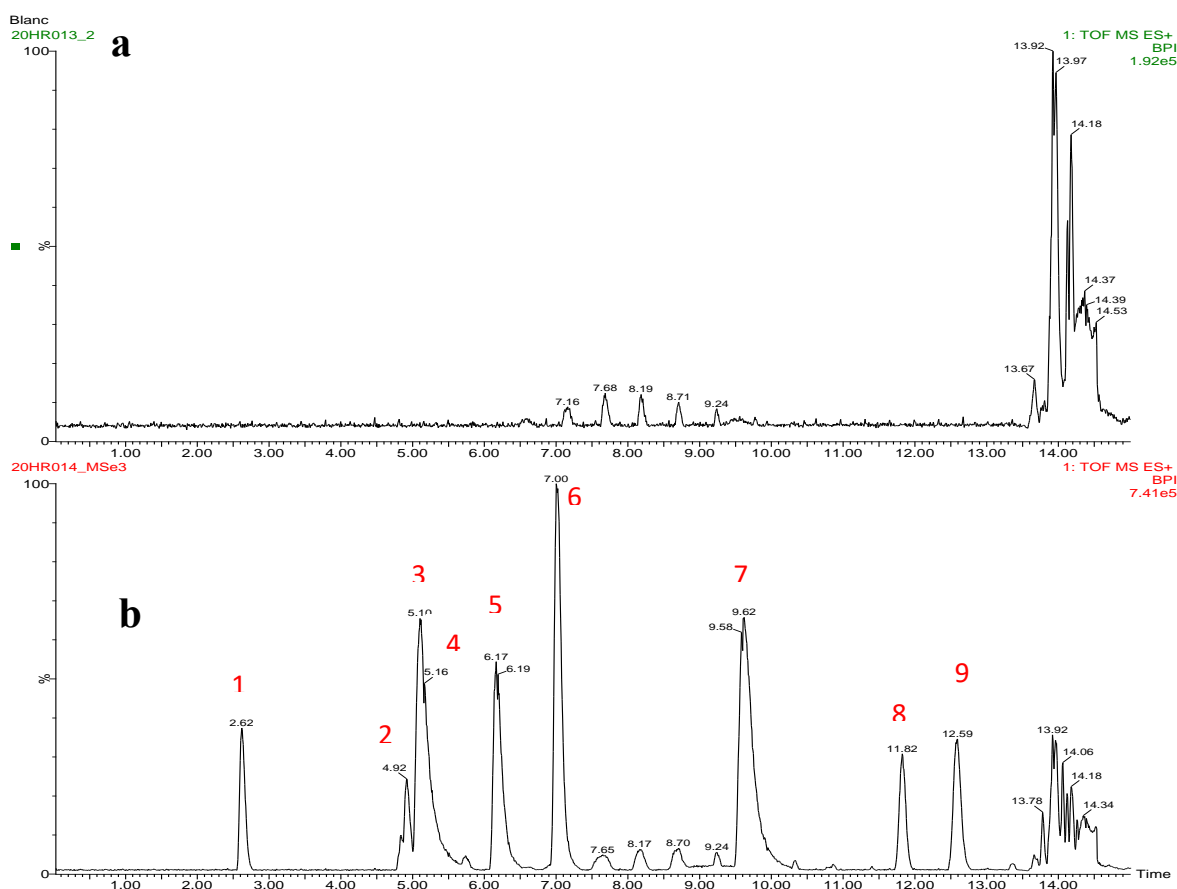


**Figure 10:** UPLC-HRMS analysis of extract. a) Blank determination b) BPI chromatogram of *U. peruviana* bulb extract

The UPLC-HRMS analysis of *U. peruviana* bulb extract led to the detection of nine compounds, with the following molecular formulas: C<sub>19</sub>H<sub>26</sub>N<sub>2</sub>O<sub>5</sub> (**1**), C<sub>19</sub>H<sub>25</sub>NO<sub>5</sub> (**2**), C<sub>18</sub>H<sub>21</sub>NO<sub>5</sub> (**3**), C<sub>21</sub>H<sub>28</sub>N<sub>2</sub>O<sub>5</sub> (**4**), C<sub>16</sub>H<sub>17</sub>NO<sub>3</sub> (**5**), C<sub>17</sub>H<sub>19</sub>NO<sub>4</sub> (**6**), C<sub>19</sub>H<sub>23</sub>NO<sub>5</sub> (**7**), C<sub>18</sub>H<sub>18</sub>N<sub>2</sub>O<sub>4</sub> (**8**) and C<sub>18</sub>H<sub>19</sub>NO<sub>4</sub> (**9**).

The UPLC-HRMS analysis of the fractions are reported in Table 3.

FRACTION	CALCULATED MOLECULAR FORMULA	RETENTION TIME [min]
A1	-----	----
A2	C <sub>18</sub> H <sub>19</sub> NO <sub>5</sub> , C <sub>15</sub> H <sub>13</sub> NO <sub>3</sub> C <sub>18</sub> H <sub>21</sub> NO <sub>5</sub> , C <sub>14</sub> H <sub>9</sub> NO <sub>2</sub>	7.00, 10.09, 12.59, 14.06
A3	C <sub>18</sub> H <sub>18</sub> N <sub>2</sub> O <sub>4</sub> , C <sub>18</sub> H <sub>21</sub> NO <sub>5</sub> , C <sub>14</sub> H <sub>9</sub> NO <sub>2</sub>	11.82, 12.59, 14.06
A4	C <sub>18</sub> H <sub>21</sub> NO <sub>5</sub>	12.59
A5	C <sub>18</sub> H <sub>21</sub> NO <sub>5</sub>	12.59
A6	C <sub>19</sub> H <sub>23</sub> NO <sub>5</sub> , C <sub>18</sub> H <sub>21</sub> NO <sub>5</sub>	9.56, 12.59
A7	C <sub>19</sub> H <sub>23</sub> NO <sub>5</sub>	9.58
A8	C <sub>17</sub> H <sub>19</sub> NO <sub>4</sub> , C <sub>19</sub> H <sub>23</sub> NO <sub>5</sub> , C <sub>16</sub> H <sub>17</sub> NO <sub>4</sub>	7.01, 9.62, 10.02
A9	C <sub>17</sub> H <sub>19</sub> NO <sub>4</sub>	6.99
A10	C <sub>19</sub> H <sub>25</sub> NO <sub>5</sub> , C <sub>16</sub> H <sub>17</sub> NO <sub>3</sub> , C <sub>17</sub> H <sub>19</sub> NO <sub>4</sub>	4.92, 6.19, 7.02
A11	C <sub>18</sub> H <sub>21</sub> NO <sub>5</sub> , C <sub>16</sub> H <sub>17</sub> NO <sub>3</sub>	5.03, 6.19
A12	C <sub>18</sub> H <sub>21</sub> NO <sub>5</sub> , C <sub>19</sub> H <sub>25</sub> NO <sub>5</sub> C <sub>21</sub> H <sub>28</sub> N <sub>2</sub> O <sub>5</sub> , C <sub>16</sub> H <sub>17</sub> NO <sub>3</sub>	4.56, 4.93 5.16, 6.20
A13	C <sub>18</sub> H <sub>21</sub> NO <sub>5</sub> , C <sub>17</sub> H <sub>19</sub> NO <sub>5</sub> C <sub>16</sub> H <sub>17</sub> NO <sub>3</sub>	5.02, 5.67, 6.19

**Table 3:** UPLC-HRMS analysis of the fractions. The table reports the molecular formulas from accurate mass analysis of [M-H]<sup>+</sup> ions and the retention time of each alkaloid detected in the fractions.

Fraction A1 had a small mass (4 mg), the UPLC-HRMS analysis showed some analytes in very low concentration, since also NMR analysis resulted of difficult interpretation due to the complexity and scarce amount of the compounds, this fraction was not further studied.

Fraction A2 chromatograms showed four alkaloids at least. For these alkaloids, the calculated molecular formulas were  $C_{18}H_{19}NO_5$ ,  $C_{15}H_{13}NO_3$ ,  $C_{18}H_{21}NO_5$  and  $C_{14}H_9NO_2$ . The latter compound was also detected in trace in fraction A3, together with the molecules with molecular formula  $C_{18}H_{18}N_2O_4$  and  $C_{18}H_{21}NO_5$  which was the most abundant.  $C_{18}H_{21}NO_5$  was also the main compound detected in the highly pure fractions A4 and A5, it also appeared in A6 in lower concentration together with the alkaloid with molecular formula  $C_{19}H_{23}NO_5$ . The latter was the major compound of fraction A7, another highly pure fraction. A residual of  $C_{19}H_{23}NO_5$  was also found in A8, which turned out to be a transition fraction, consisting of a mix of alkaloids ( $C_{17}H_{19}NO_4$ ,  $C_{19}H_{23}NO_5$ ,  $C_{16}H_{17}NO_4$ ), between two practically pure fractions, namely A7 and A9. Actually, A9 showed essentially one alkaloid, with molecular formula  $C_{17}H_{19}NO_4$ . As occurs in a typical CPC in pH-refining mode separation, this alkaloid was also detected in the next fraction at lower concentration. In addition to  $C_{17}H_{19}NO_4$ , fraction A10 resulted composed by other compounds with molecular formula  $C_{19}H_{25}NO_5$  and  $C_{16}H_{17}NO_3$ . The latter was the main alkaloid of the semi-pure fraction A11, which contained another alkaloid with molecular formula  $C_{18}H_{21}NO_5$ . This compound possessed the same molecular formula of the main alkaloid of fractions A3, A4, and A5, however the elution time was different (12.59 min in A3, A4 and A5 fractions versus 5.03 min in fraction A10), the difference in the retention time led to the hypothesis that A11 contained a constitutional isomer of the alkaloid detected in the previous fractions. The same compounds were also found in fraction A12, at different concentrations. Precisely,  $C_{18}H_{21}NO_5$  resulted the most abundant alkaloid of this fraction, which also contained a dinitrogenous alkaloid with molecular formula  $C_{21}H_{28}N_2O_5$ . Finally, fraction A13 was a complex mixture of alkaloids, the most abundant compound, with molecular formula  $C_{18}H_{21}NO_5$ , was the same of the previous fraction, a residual of the compound with molecular formula  $C_{16}H_{17}NO_3$  was also detected together with the molecule whose molecular formula was calculated as  $C_{17}H_{19}NO_5$ .

## Identification of Amaryllidaceae alkaloids by dereplication

The fractions were dissolved in DMSO- $d_6$  for NMR analysis. This solvent is not volatile at room temperature, introduces only low amounts of water in samples if correctly handled and preserves the observation of the  $^1\text{H}$  NMR signals of hydroxyl groups. Moreover, DMSO- $d_6$  can be eliminated from samples by freeze-drying. All samples were submitted to 1D  $^1\text{H}$ , 1D  $\{^1\text{H}\}$ - $^{13}\text{C}$ , 2D  $^1\text{H}$ - $^1\text{H}$  COSY, 2D multiplicity-edited  $^1\text{H}$ - $^{13}\text{C}$  HSQC, 2D  $^1\text{H}$ - $^{13}\text{C}$  HMBC, and 2D  $^1\text{H}$ - $^1\text{H}$  ROESY NMR analysis.

As already evident from the UPLC-HRMS analyses, among the 13 fractions, A4, A7, A9 and A11 contained the major compounds of the extract. These fractions showed a high degree of purity, since they were collected during the emergence of alkaloid isotachic trains, i.e. at the plateau of the contiguous compound blocks that are shaped by CPC in pH-zone refining mode. Fraction A4 and A5 were very similar both in term of purity and content, fraction A3 turned out to be semi-pure. Fraction A1, as already noted in the UPLC-HRMS analysis, had an insufficient mass and a high complexity, thus it was not studied further. Fraction A2, A6, A8, A10, A12 and A13 resulted a mixture of alkaloids, in fact these fractions were collected at the extreme parts of the contiguous blocks during the CPC separation.

The NMR spectra of the fractions were carefully studied to determine which signals belonged to each individual alkaloid. Successively, lists of  $^{13}\text{C}$  NMR chemical shifts were established, with each value associated to the corresponding multiplicity, i. e. to the number of H atoms directly bound to the C atom, symbolized by s (singlet, quaternary carbon), d (doublet, CH group), t (triplet,  $\text{CH}_2$  group), q (quadruplet,  $\text{CH}_3$  group) as required for optimal dereplication by the CSEARCH and amaryl2\_knapsacak databases. For a correct use of CSEARCH it is necessary to give some constraints that help to narrow the search field. Hence, the molecular formula of the proposed compounds was constrained to include only C, H, N, and O atoms with a molecular mass comprised between 250u and 400u, since these are the features of Amaryllidaceae alkaloids. Among the various structures proposed by the databases, only those with the molecular formula corresponding to that calculated from UPLC-HRMS analysis were taken into consideration.

- **Analysis of the purest fractions, containing the major compounds of the extract**

For the identification of the Amaryllidaceae alkaloids by dereplication, the purest fractions were those first analysed. Actually, the analysis of these fractions was easier compared to that of mixtures, since there were no overlapping signals from other molecules and allowed to rapidly characterise 58% of

extract mass. Moreover, the identification of the alkaloids in the pure or semi-pure fractions allowed to know, as least in part, the composition of the adjacent fractions composed by alkaloid mixtures.

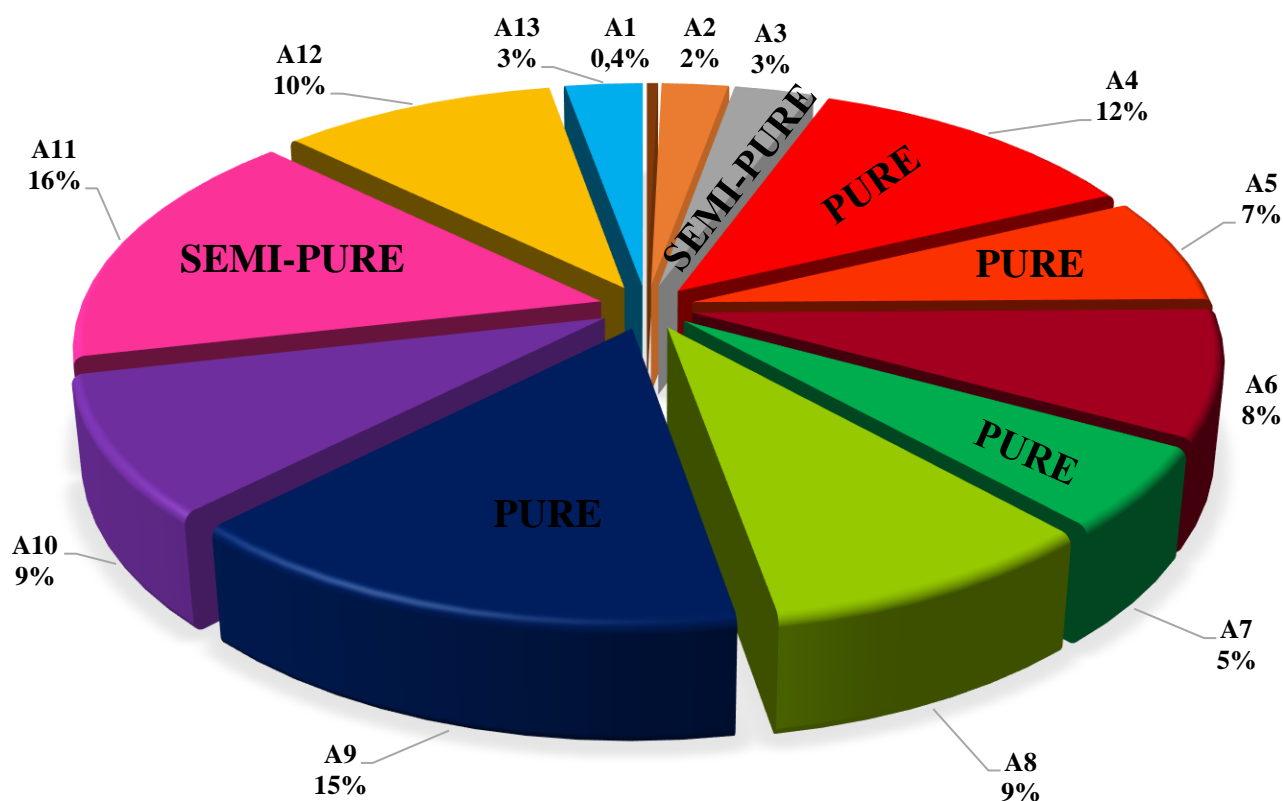


**Figure 11:** Representation of *U. peruviana* alkaloid enriched extract. The percentage of each fraction, calculated on the mass of the original extract, is reported. The pure and semi-pure fractions represented the 58% of the extract.

#### Fraction A4

In fraction A4, 18 values of  $^{13}\text{C}$  NMR chemical shifts with associated multiplicity were identified. CSEARCH proposed tazettine as the first most likely compound, the experimental chemical shift matched with those in the database, except for one value corresponding to the carbon in position 4, with  $\delta_{\text{C}}$  29.6 predicted by CSEARCH and  $\delta_{\text{C}}$  25.9 observed. The second most likely compound was criwelline, the epimer of tazettine in position 3<sup>165</sup>. The analysis of the 1D and 2D NMR spectra allowed to confirm that the planar structure was that of tazettine or criwelline. For assessing which epimer was found in fraction A4, the measurement and  $^1\text{H}$ - $^1\text{H}$  coupling constants were carried out and the ROESY spectrum was carefully examined.

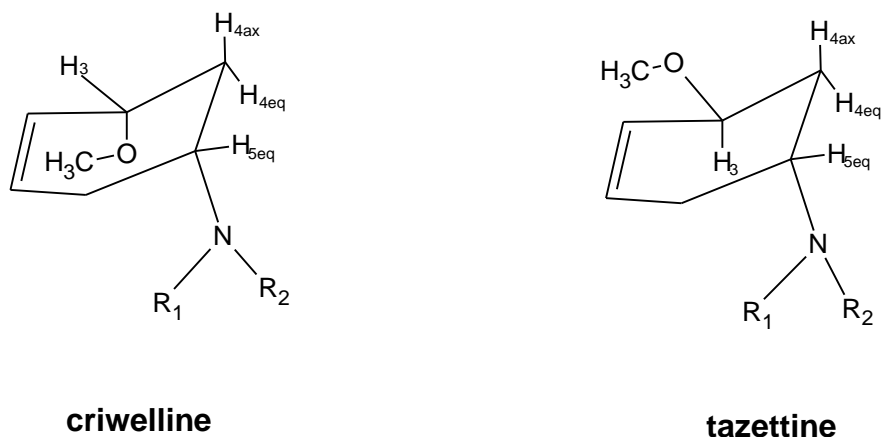


**Figure 12:** Representation of the C ring in criwelline and tazettine

With respect to the half-chair plan of the C ring (Fig. 12), the methoxyl group bound to the C-3 occurs in the equatorial position in tazettine and in axial position in criwelline. This different arrangement leads to differences in coupling constants magnitude for the protons at positions 3 and 4. Particularly, the chemical structure of tazettine results in a high coupling constant value for the interaction between  $H_3$ - $H_{4ax}$ , while  $H_3$ - $H_{4eq}$  interaction arises in a J constant of medium magnitude. Conversely, the stereochemistry of criwelline induces J constants of low and medium magnitude for  $H_3$ - $H_{4eq}$  and  $H_3$ - $H_{4ax}$  interactions, respectively. The experimental data of fraction 4 agreed with the chemical structure of tazettine, since  $J_{3,4ax}$  was 10 Hz and  $J_{3,4eq}$  was 6.4 Hz. Hence, tazettine was identified as the alkaloid of fraction A4. Tazettine was also the major alkaloid of fraction A3 and A5.

### Fraction A5

Fraction A5 was essentially composed by tazettine, it showed a degree of purity comparable to fraction A4.

### Fraction A7

In fraction A7 were identified 19  $^{13}C$  NMR chemical shift values with associated multiplicity. Among the structures proposed by amaryl12\_knapsack, only one, albomaculine, possessed three methoxy groups bound to an aromatic ring, as in the experimental spectra of fraction 7. The structure was confirmed by the analysis of NMR spectra.

### Fraction A9

The list of 17  $^{13}C$  NMR chemical shifts and associated multiplicities was submitted to a spectral similarity search in CSEARCH. Among the proposed structures only two contained an aromatic ring with a methylenedioxy substituent and hydrogens in para position, a carbon-carbon double bond between two CH groups, and a methoxy group attached to an aliphatic carbon. These structures were crinamine and haemanthamine, which are epimer in position 3 (Fig. 13).

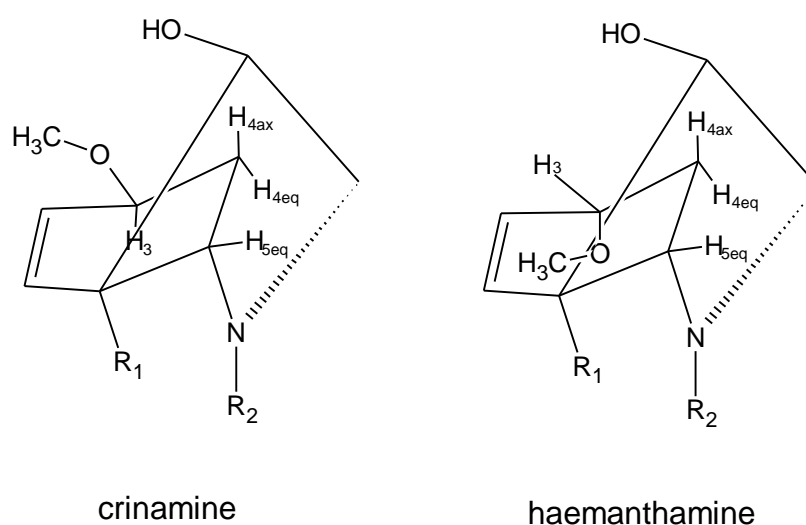


**Figure 13:** Representation of the C-ring in crinamine and haemanthamine

Haemanthamine brings the methoxyl group in axial position in the half-chair of C ring, while in crinamine is in equatorial position. Consequently, haemanthamine displays medium magnitude J constant for the coupling H3-H4<sub>ax</sub> and small J for H3-H4<sub>eq</sub> interaction. Conversely, for crinamine the coupling constant is high for H3-H4<sub>ax</sub> coupling and medium for H3-H4<sub>eq</sub> interaction. The experimental coupling constants of fraction 9 were  $J_{3,4ax} \sim 4.3$  Hz and  $J_{3,4eq} \sim 1.8$  Hz, thus it fitted with haemanthamine structure. Furthermore, the ROESY spectrum of fraction 9 clearly showed the correlation of both protons in 4 position with H3, which can only occur in the case of haemanthamine, since the detection of the interaction signal between H3 and H4<sub>ax</sub> in ROESY spectrum is unlikely for crinamine. Another signal confirming that it is haemanthamine is the interaction between H4<sub>ax</sub> and the hydroxyl group in position 11, unlikely for crinamine.

### Fraction A11

Fraction A11 showed 16 <sup>13</sup>C NMR chemical shift values belonging to the most abundant compound. Amaryll2\_knapsack contained four compounds with the molecular formula C<sub>16</sub>H<sub>17</sub>NO<sub>3</sub>, namely crinine, vittatine, epi-vittatine and epi-crinine, which differ by the configuration of stereocentres. Precisely, crinine and vittatine are two enantiomers, while epi-crinine and epi-vittatine are epimers of the former at position 3. The detailed analysis of 2D ROESY spectrum and the comparison of the <sup>13</sup>C NMR chemical shift values in A11 with those published for synthetic crinine, vittatine, epi-crinine and epivittatine<sup>166</sup>, allowed the identification of the correct epimer, which resulted crinine or vittatine. From the NMR spectra is not possible to discriminate enantiomers, for the correct identification of crinine and vittatine is necessary to carry out chiroptical methods on the pure compound. Fraction

A11 was a semi-pure fraction, since this study for dereplication aimed exactly to avoid the purification of already known compound, the alkaloid of fraction A11 was reported as crinine/vittatine.

The analysis of the purest fractions allowed to rapidly characterize the major alkaloids of the extract (Fig. 14), which were tazettine (22%), albomaculine (5%), haemanthamine (15%) and crinine/vittatine (16%) (Fig. 15).

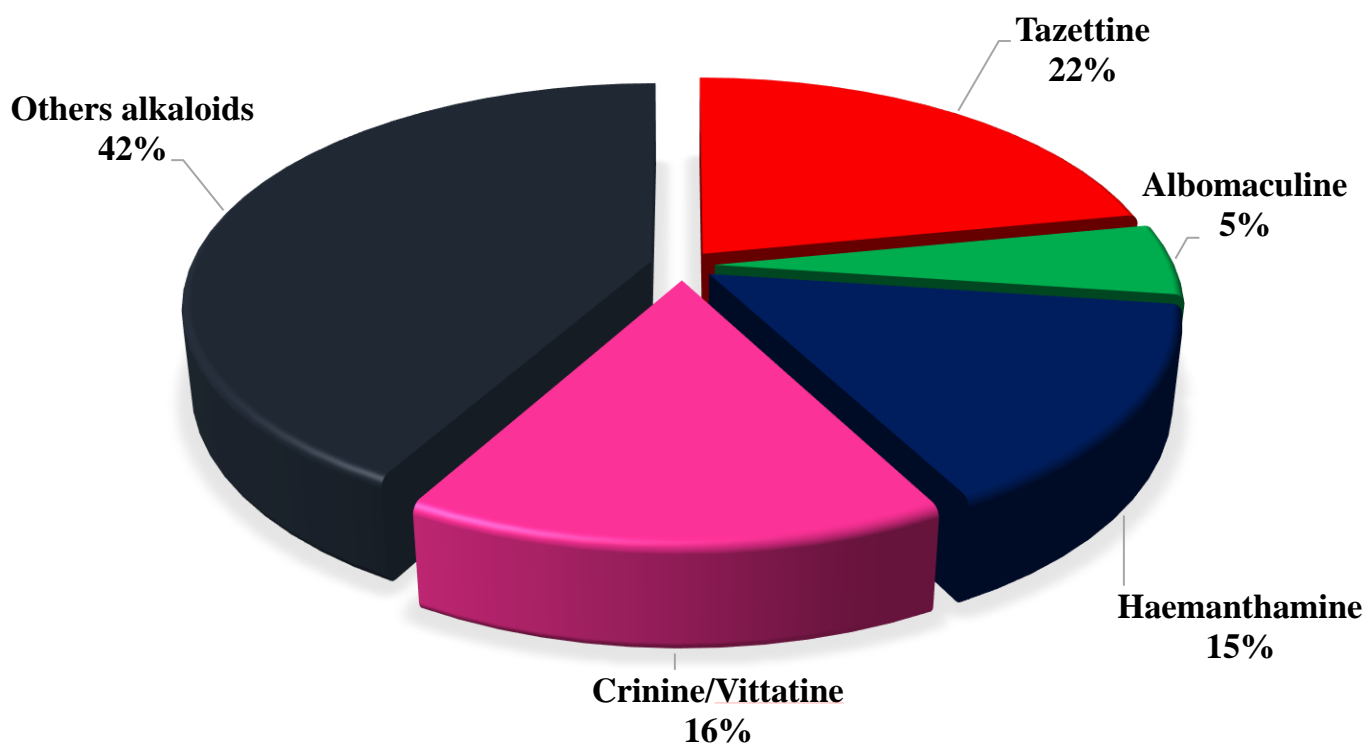


**Figure 14:** Representation of *U. peruviana* alkaloid enriched extract. The major alkaloids, which constituted the 58% of the extract, were identified as tazettine, albomaculine, haemanthamine and crinine/vittatine

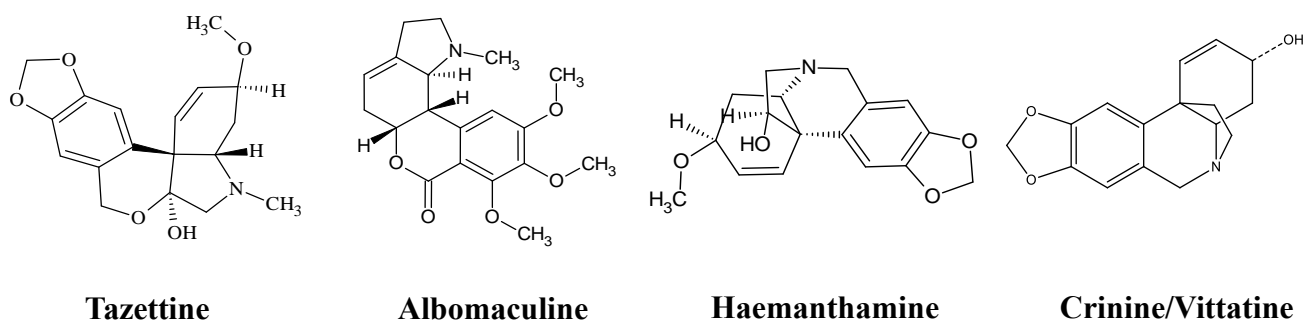


**Figure 15:** Chemical structures of the major alkaloids of *U. peruviana* bulb extract

- **Analysis of the mixed fractions, containing the minor compounds of the extract**

### **Fraction A2**

Fraction A2 resulted a mixture of alkaloids, tazettine, the major compound of fraction A3, A4 and A5, was also found in this fraction. For the other three alkaloids detected in the UPLC-HRMS analysis, the study of NMR spectra allowed to attribute the chemical shift values for each carbon of each compound. Hence, the lists were submitted to a spectral similarity search through the CSEARCH web interface and amaryll2\_knapsack, the compounds were identified as trisphaeridine ( $C_{14}H_9NO_2$ ), 3-epimacronine ( $C_{18}H_{19}NO_5$ ) and 3-methoxy-8,9-methylenedioxy-3,4-dihydrophenanthridine ( $C_{15}H_{13}NO_3$ ).

### **Fraction A3**

NMR analysis clearly showed this fraction mostly contained tazettine, the most abundant alkaloid of the extract that was found nearly pure in fractions A4 and A5. The alkaloid trisphaeridine, detected in the previous fraction, was also identified in fraction A3 at low concentration. UPLC-HRSM analysis also detected a compound with molecular formula  $C_{18}H_{18}N_2O_4$ , appearing also in the analysis of the extract, which was not possible to characterized from NMR spectra because of its low concentration.

### **Fraction A6**

The  $^{13}C$  NMR spectrum of fraction A6 showed 37 high intensity peaks whose positions are either those of A4 (18 peaks) or A7 (19 peaks). Thus, these molecules were identified as tazettine and albamaculine.  $^{13}C$  NMR spectrum also showed low intensity peaks, among which one at 169.9 ppm, that correlated in the HMBC spectrum with a singlet 1H signal at 1.95 ppm, suggested the presence of an acetate group. A low intensity HMBC correlation of this signal with one at 66.3 ppm, only possibly originating from a 4J coupling, indicated that the acetate group was bound to a methine group at  $\delta_H$  5.21, according to the HSQC spectrum. The amaryll2\_knapsack database showed twenty-four structures including a methine group linked to an acetyl group. The interpretation of COSY, HSQC and HMBC data recorded for fraction A6 lead to identify crinine acetate, starting from the signals of the acetate group.

### **Fraction A8**

The  $^{13}C$  NMR spectrum of fraction A8 displayed 18 high intensity signals possessing the same chemical shift values of albamaculine, the major alkaloid of the previous fraction A7. Other 19 high intensity signals were identified to those of haemanthamine the major alkaloid of the fraction A9. The analysis of the low intensity peaks led to isolate a set of 16  $^{13}C$ -NMR chemical shift values corresponding to an alkaloid with an NMR profile similar to crinine/vittatine, bringing a hydroxyl

group in position 6. Since the OH group may be located above or below the molecular plane, this alkaloid was identified as 6  $\alpha/\beta$ -hydroxycrinine.

### **Fraction A10**

From the analysis of the NMR spectra, fraction A10 resulted composed by the major compounds of A9 (haementamine) and A11 (crinine) and other compounds in lower amount, among which one presented two well-separated resonances at  $\delta_C$  150.8 and 152.0. The HMBC spectrum correlated this resonance with an aromatic one at  $\delta_H$  6.71, that turned correlated with three other resonances at  $\delta_C$  140.7, 132.9, and 122.4. The resonances at  $\delta_C$  150.8, 152.0, and 140.7 correlated with sharp methyl proton singlets at  $\delta_H$ , 3.77, 3.79, and 3.73 bound to carbons at  $\delta_C$  55.9, 60.8, and 60.4, respectively, according to the HSQC spectrum. These observations led to propose a fragment made of a penta-substituted aromatic ring binding three methoxy groups. The resonance at  $\delta_H$  5.83 correlated with those at  $\delta_C$  150.8, 132.9, and 122.4, thus indicating that the methoxy groups were adjacent. The proton that resonated at  $\delta_H$  4.82 (doublet) was bound to a carbon at  $\delta_C$  88.2 and correlated in the COSY spectrum with an OH proton at  $\delta_H$  6.47, indicating it belonged to a hemiacetal group bound to an aromatic carbon. 19  $^{13}C$  chemical shift values were attributed to this compound, thus the structure was individuated as the alkaloid that in UPLC-HRMS analysis possessed the molecular formula  $C_{19}H_{25}NO_5$ . Searching the amaryll2\_knapsack database for the aromatic and hemiacetal fragments as described hereabove resulted in one hit, nerinine.

### **Fraction A11 – Minor compound**

Fraction A11 contains one the major compound of the extract, crinine/vittatine, and other minor compounds since it was a semi-pure fraction. Among these, one presented an isolated and rarely observed resonance at 92.67 ppm. The analysis of COSY, HSQC and HMBC spectra led to the construction of a connected substructure that included an aromatic ring substituted by a methylenedioxy bridge, two hydrogens in para position, a quaternary carbon linked to a CH=CH group and the CH group with  $\delta_C$  92.67 and  $\delta_H$  5.92 bounded to an OH group,  $\delta_H$  6.88. The signal at  $\delta_C$  92.67 was highly compatible with a hemiacetal group bound to an aromatic ring. The substructure was searched among the compounds from Amaryllidaceae in amaryll2\_knapsack, resulting in two hits: pretazettine and 8 $\alpha$ -ethoxyprecricriwelline. The latter was left aside due to the lack of observed  $^1H$  NMR signals from a hypothetical ethoxy group. The analysis of the 2D NMR spectra lead to the identification of the planar structure of pretazettine, corresponding to the alkaloid of UPLC-HRMS analysis with molecular formula  $C_{18}H_{21}NO_5$ , which is the same as precricriwelline, the stereochemical epimer of pretazettine<sup>167</sup>. The presence of tazettine in factions A3-A5 favors the presence of pretazettine in the extract, since it is the biogenetic precursor to tazettine<sup>140</sup>.

### **Fraction A12**

Fraction A12 appeared composed by several alkaloids. Crinine/vittatine and pretazettine, alkaloids present in fraction A11, were also identified in this fraction together with traces of nerinine. In UPLC-HRMS analysis, an alkaloid with an uncommon molecular formula,  $C_{21}H_{28}N_2O_5$  was detected in this fraction. Alkaloids containing two nitrogen atoms have already been isolated from species belonging to the Amaryllidoideae subfamily<sup>168–170</sup>, however their occurrence is very limited. The  $^1H$  NMR spectrum of fraction A12 showed a highly deshielded proton at  $\delta_H$  8.84, the HSQC spectrum displayed no correlation with any carbon, the bond with an oxygen atom was highly unlikely for such deshielded proton, hence the hypothesis it was linked to a nitrogen atom was proposed. Starting from this proton a part of the molecule was characterized, the HMBC spectrum showed the correlations with three carbons  $\delta_C$  119.9, 168.4 and 71.6. The resonance of the latter carbon led to suppose it was linked to a heteroatom of the nitrogen or oxygen type, the carbon  $\delta_C$  168.9 resulted correlated with a  $CH_3$  group, thus it was thought to be part of an acetamido group, while from the carbon  $\delta_C$  119.9 a penta-substituted aromatic ring binding three methoxy groups was sketched. Searching for these fragments in the databases failed to find proposals that satisfied the molecular arrangement deduced from the NMR spectra, hence fraction A12 was selected for purification to verify it contained a new alkaloid.

### **Fraction A13**

The NMR spectra of the A13 fraction displayed many low intensity signals belonging to different molecules. Crinine/vittatine and pretazettine were identified.

The investigation of the mixed fractions allowed to enhance the characterization of *U. peruviana* bulb extract (Fig. 16). The chemical structures of the minor alkaloids of the extract are reported in Figure 17.

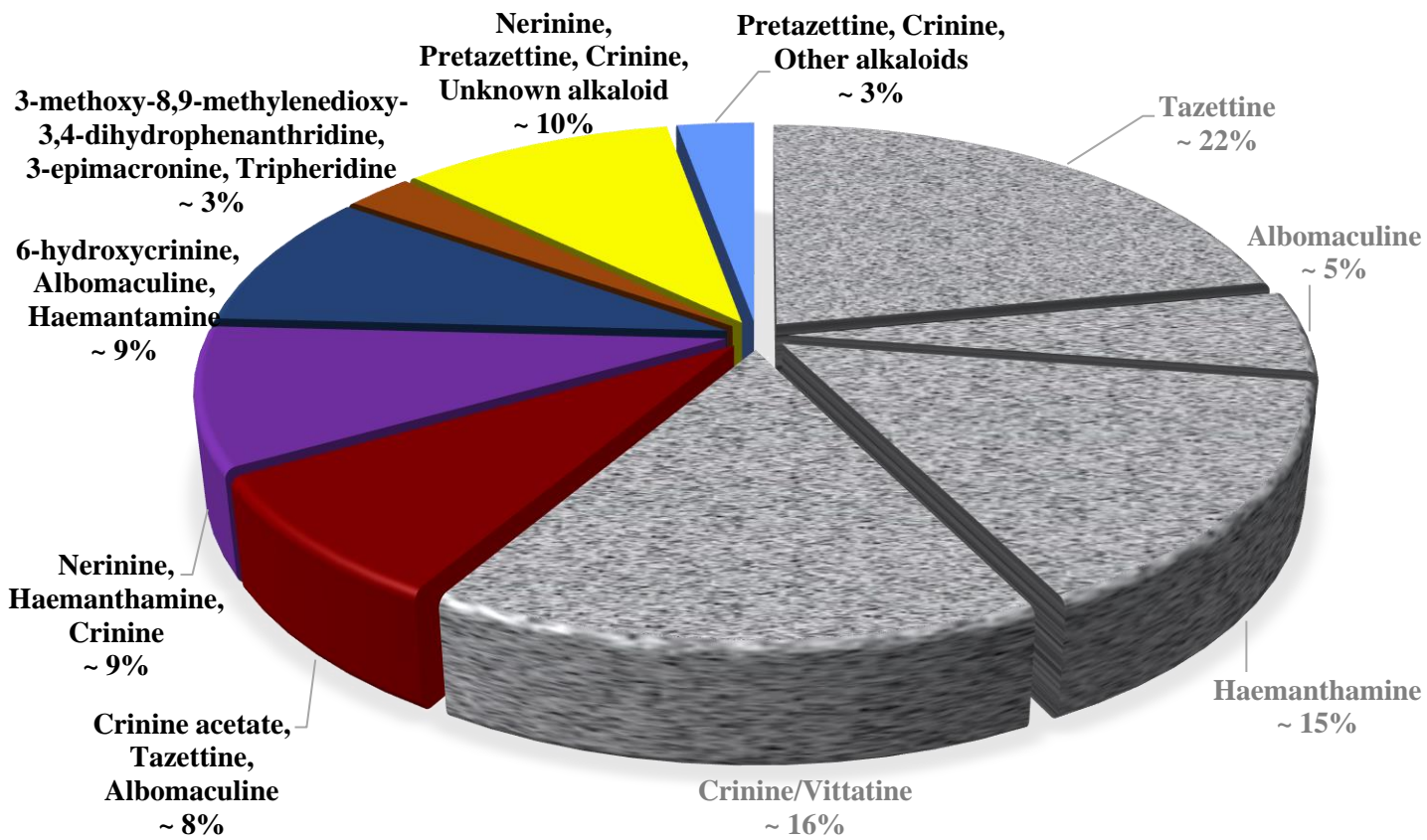


**Figure 16:** Representation of the *U. peruviana* alkaloid enriched extracts. The minor alkaloids of the extract were identified in the mixed fractions

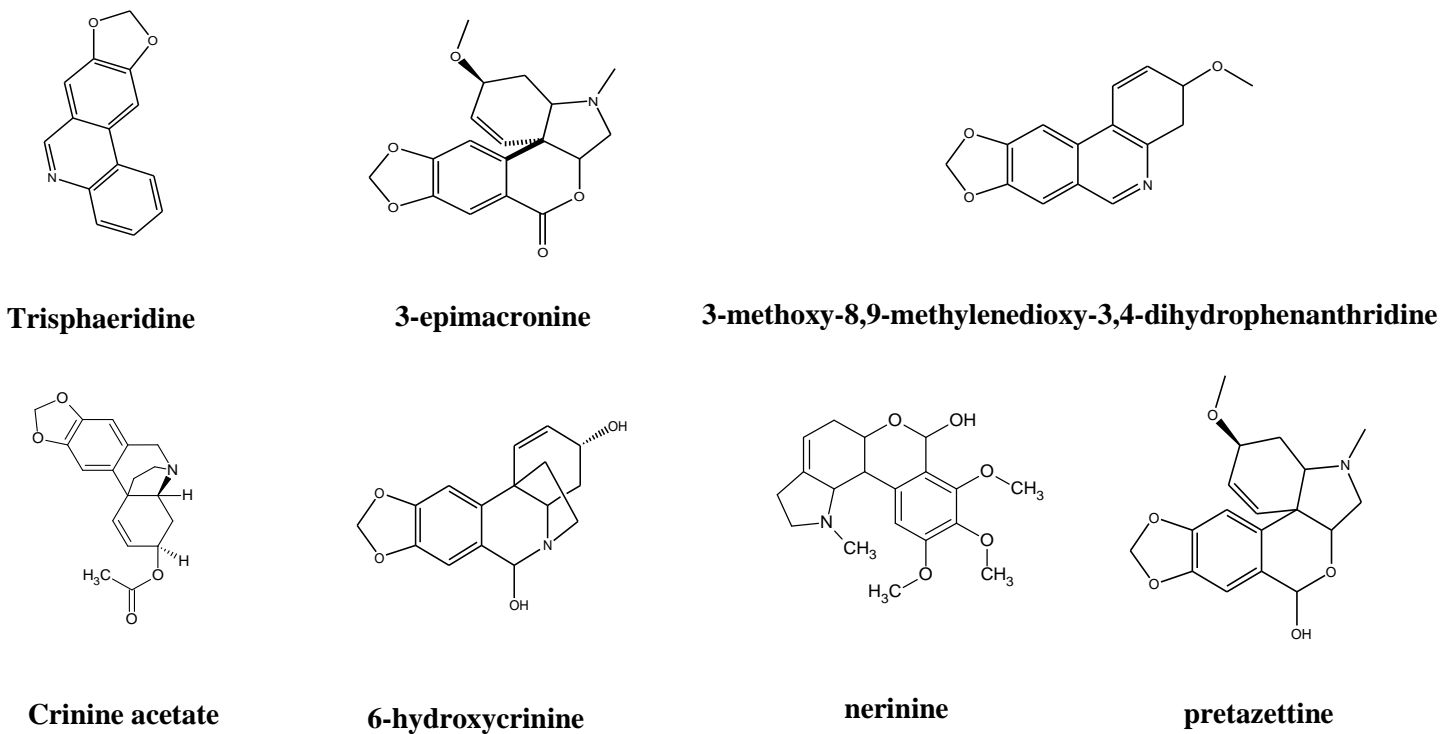


**Figure 17:** Chemical structures of the minor alkaloids of *U. peruviana* bulb extract

## Structure elucidation of the new alkaloid

Fraction A12 was again subjected to CPC in pH-zone refining mode to obtain subfractions of increased purity and elucidate the unknown alkaloid chemical structure.

Eight subfractions, namely A12\_1- A12\_8, were submitted to 1D  $^1\text{H}$ , 1D  $\{^1\text{H}\}$ - $^{13}\text{C}$ , 2D  $^1\text{H}$ - $^1\text{H}$  COSY, 2D multiplicity-edited  $^1\text{H}$ - $^{13}\text{C}$  HSQC, 2D  $^1\text{H}$ - $^{13}\text{C}$  HMBC and 2D  $^1\text{H}$ - $^1\text{H}$  ROESY NMR analysis. The unknown alkaloid was found in the last fraction.

Starting from the highly deshielded proton at  $\delta_{\text{H}}$  8.84, its correlations with three carbons  $\delta_{\text{C}}$  119.9, 168.4 and 71.6 were clearly shown in the HMBC spectrum. The quaternary carbon  $\delta_{\text{C}}$  119.9 resulted correlated with an aromatic proton  $\delta_{\text{H}}$  6.77 (J3) and an aliphatic one  $\delta_{\text{H}}$  2.27 (J3). In the HMBC spectrum the proton  $\delta_{\text{H}}$  6.77 was correlated with other four quaternary carbons  $\delta_{\text{C}}$  133.3, 152.3, 140.6, 150.1, which formed a penta-substituted aromatic ring binding three methoxy groups ( $\delta_{\text{H}}$  3.78,  $\delta_{\text{C}}$  56.0;  $\delta_{\text{H}}$  3.72,  $\delta_{\text{C}}$  60.37;  $\delta_{\text{H}}$  3.73,  $\delta_{\text{C}}$  60.17). The same proton also showed a J3 correlation with the carbon  $\delta_{\text{C}}$  43.5 binding the aliphatic proton  $\delta_{\text{H}}$  2.27. The latter resulted correlated with  $\delta_{\text{C}}$  67.0, this resonance is typically due to the proximity of a heteroatom, in this case a nitrogen atom carrying a methyl group ( $\delta_{\text{H}}$  1.89,  $\delta_{\text{C}}$  44.30). This nitrogen turned out to be part of a cyclopentane ( $\delta_{\text{H}}$  2.56,  $\delta_{\text{C}}$  67.0;  $\delta_{\text{H}}$  3.00,  $\delta_{\text{H}}$  2.19,  $\delta_{\text{C}}$  56.19;  $\delta_{\text{H}}$  2.40,  $\delta_{\text{H}}$  2.29,  $\delta_{\text{C}}$  28.14;  $\delta_{\text{C}}$  141.56). The proton  $\delta_{\text{H}}$  2.27 was also correlated to  $\delta_{\text{C}}$  65.58 binding the proton  $\delta_{\text{H}}$  4.15, the analysis of COSY and HMBC spectra for the latter proton allowed to complete the structure by placing an oxygen between the deshielded carbons  $\delta_{\text{C}}$  71.6 and 65.58, and by closing a third six-membered ring bearing an unsaturation ( $\delta_{\text{H}}$  5.37,  $\delta_{\text{C}}$  114.9;  $\delta_{\text{C}}$  141.56). Based on the resonances of the atoms close to the proton  $\delta_{\text{H}}$  8.84, the latter was inserted into an amide group with the carbonyl carbon  $\delta_{\text{C}}$  168.4 and the  $\text{CH}_3$  group  $\delta_{\text{C}}$  22.89  $\delta_{\text{H}}$  1.83. The new alkaloid (Fig. 18) was named 6-dehydroxy-6-acetamido-nerinine.

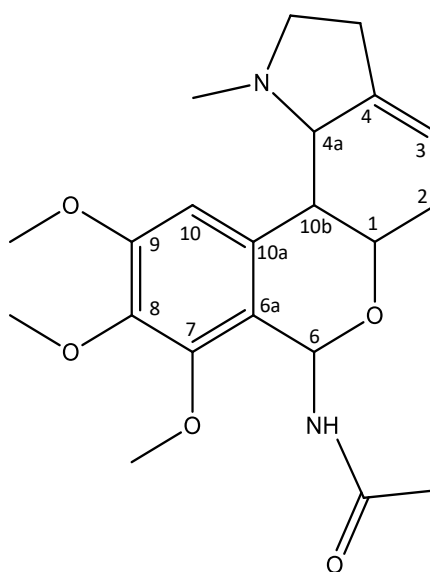


**Figure 18:** Chemical structure of the new alkaloid 6-dehydroxy-6-acetamido-nerinine

## NMR data of identified alkaloids

Position	$\delta_{\text{H}}$ (J in Hz)	$\delta_{\text{C}}$	COSY	HMBC
1	5.50 <i>ddd</i> (10.3, 1.9, 1.2)	129.2	H-2, H-3, H-4a	C-3, C-4a, C-10b, C-11
2	6.00 <i>ddd</i> (10.3, 1.9, 1.1)	129.6	H-1, H-3, H-4 <sub>ax</sub> (w)	C-4, C-10b
3	3.98 <i>ddt</i> (10.3, 6.4, 2.0)	72.6	H-1, H-2, H-4 <sub>ax</sub> , H-4 <sub>eq</sub>	C-1, C-2, C-4 (w), C-10b (w), 3-OMe
4 <sub>ax</sub>	1.39 <i>ddd</i> (13.5, 10.0, 2.1)	25.9	H-2, H-3, H-4 <sub>eq</sub> , H-4a	C-2 (w), C-3, C-4a, C-10b
4 <sub>eq</sub>	2.14 <i>dddd</i> (13.5, 6.4, 4.0, 1.1)		H-3, H-4 <sub>ax</sub> , H-4a	C-2, C-3, C-4a, C-10b
4a	2.67 <i>m</i>	69.4	H-1, H-3 (w), H-4 <sub>ax</sub> , H-4 <sub>eq</sub>	C-1, C-3, C-10b, 5-NMe
6 <sub>ax</sub>	4.80 <i>dd</i> (14.8, 1.0)	60.8	H-6 <sub>eq</sub> , H-7 (w)	C-4a (w), C-6a, C-7, C-8, C-10 (w), C-10a, C-10b, C-11
6 <sub>eq</sub>	4.54 <i>d</i> (15.0)		H-6 <sub>ax</sub> , H-7	C-4a (w), C-6a, C-7, C-8, C-10a, C-10b, C-11
6a		126.4		
7	6.66 <i>s</i>	104.2	H-6 <sub>ax</sub> , H-6 <sub>eq</sub>	C-6, C-8, C-9 (w), C10, C-10a, C-10b
8		145.8		
9		145.7		
10	6.60 <i>s</i>	108.4	H-6 <sub>ax</sub> , H-6 <sub>eq</sub>	C-1 (w), C-4a, C-6, C-6a, C-7, C-8 (w), C-9, C-10a, C-10b
10 a		128.0		
10 b		49.5		
11		101.1		
12	3.11 <i>d</i> (10.6)	65.2	H-12', 11-OH (w)	C-4a, C-6, C-10b (w), C-11, 5-NMe
12'	2.54 <i>d</i> (10.6)		H-12, 5-NMe (w)	C-4a, C-6 (w), C-10a (w), C10b, C-11, 5-NMe
3-OMe	3.33 <i>s</i>	55.3		C-3
5-NMe	2.29 <i>s</i>	41.9		C-4a, C-10b (w), C-11 (w), C-12
OCH <sub>2</sub> O	5.96 <i>d</i> (1.1) 5.95 <i>d</i> (1.1)	100.8		C-8, C-9 C-8, C-9
11-OH	6.59 <i>s</i>			C-4a, C-10b, C-11

**Table 4:** <sup>1</sup>H NMR, <sup>13</sup>C NMR, COSY and HMBC data of tazettine (600 MHz, DMSO-*d*<sub>6</sub>)

Position	$\delta_{\text{H}}$ ( <i>J</i> in Hz)	$\delta_{\text{C}}$	COSY	HMBC
1	4.68 <i>dd</i> (5.0, 1.9)	75.7	H-2 (w), H-2', H-3 (w), H-10b	C-2 (w), C-3, C-4, C-4a
2	2.34 <i>m</i>	30.4	H-1, H-2'(w), H-3	C-1, C-3, C-4, C-10b
2'	2.55 <i>m</i>		H-1, H-2 (w), H-3	C-3, C-4, C-4a (w), C-6 (w), C-10b (w)
3	5.45 <i>m</i>	115.0	H-1, H-2, H-2', H-4a	C-1, C-2 (w), C-4a, C-10b (w), C-11 (w)
4		140.7		
4a	2.43 <i>m</i>	65.9	H-3, H-10b	C-3, C-4, C-10b
6		161.4		
6a		110.9		
7		155.0		
8		141.8		
9		156.5		
10	6.97 <i>s</i>	108.2	H-10b, 9-OMe	C-6 (w), C-6a, C-7 (w), C-8, C-9, C-10a, C-10b
10 a		141.2		
10 b	2.69 <i>dd</i> (9.5, 2.0)	43.9	H-1, H-4a, H-10 (w)	C-4, C-4a, C-6a, C-10, C- 10a
11	2.42 <i>m</i>	27.6	H-11', H-12, H-12'	C-3, C-4, C-10b (w), 5- NMe (w)
11'	2.33 <i>m</i>		H-11, H-12, H-12'	C-3, C-4, C-12
12	2.10 <i>q</i> (9.2)	55.7	H-11, H-11', H-12'	C-4, C-4a, C-11, 5-NMe
12'	3.00 <i>ddd</i> (10.6, 8.3, 2.3)		H-11, H-11', H-12	C-4, C-4a, C-11, 5- NMe
7-OMe	3.80 <i>s</i>	61.6		C-7
8-OMe	3.74 <i>s</i>	60.7		C-8
9-OMe	3.88 <i>s</i>	56.4	H-10	C-9, C-10 (w)
5-N-Me	1.92 <i>s</i>	43.3		C-4a, C-12

**Table 5:**  $^1\text{H}$  NMR,  $^{13}\text{C}$  NMR, COSY and HMBC data of albomaculine (600 MHz, DMSO- $d_6$ )

Position	$\delta_{\text{H}}$ (J in Hz)	$\delta_{\text{C}}$	COSY	HMBC
1	6.46 <i>d</i> (10.1)	129.6	H-2, H-10 (w)	C-2, C-3, C-4, C-4a, C-10a, C-10b, C-11
2	6.10 <i>ddd</i> (10.1, 5.3, 1.0)	128.7	H-1, H-3, H-4 <sub>eq</sub> (w)	C-1, C-3, C-4, C-4a (w), C-10a (w), C-10b, C-11 (w)
3	3.74 <i>ddd</i> (5.3, 4.3, 1.8)	72.4	H-1 (w), H-2, H-4 <sub>eq</sub> , H-4 <sub>ax</sub> , H-4a (w)	C-1, C-2, C-4, C-4a, C-10b (w), 3-OMe
4 <sub>eq</sub>	1.72 <i>dddd</i> (13.4, 4.3, 2.0, 1.2)	28.2	H-2, H-3, H-4 <sub>ax</sub> , H-4a	C-2, C-3, C-4a, C-10b
4 <sub>ax</sub>	1.98 <i>ddd</i> (13.4, 13.4, 4.2)		H-2 (w), H-3, H-4 <sub>eq</sub> , H-4a	C-1 (w), C-3, C-4a, C-10b, 3-OMe (w)
4a	3.01 <i>dd</i> (13.4, 4.4)	62.4	H-1 (w), H-4 <sub>eq</sub> , H-4 <sub>ax</sub> , H-12'	C-3, C-4, C-6, C-10a, C-10b, C-11, C-12
6 <sub>eq</sub>	3.57 <i>d</i> (17.2)	60.7	H-6 <sub>ax</sub> , H-7, H-10	C-4a, C-6a, C-7, C-9 (w), C-10 (w), C-10a, C-10b (w), C-12
6 <sub>ax</sub>	4.12 <i>d</i> (17.1)		H-6 <sub>eq</sub> , H-7, H-10 (w), H-12 (w)	C-6a, C-7, C-9, C-10 (w), C-10a, C-10b (w), C-11, C-12
6a		127.3		
7	6.58 <i>s</i>	106.8	H-6 <sub>eq</sub> , H-6 <sub>ax</sub> , H-10 (w)	C-6, C-6a (w), C-8, C-9, C-10 (w), C-10a, C-10b (w)
8		145.3		
9		145.8		
10	6.95 <i>s</i>	103.3	H-1, H-6 <sub>eq</sub> , H-6 <sub>ax</sub> , H-7 (w)	C-6, C-6a, C-7, C-8, C-9, C-10a, C-10b, C-11
10 a		136.6		
10 b		49.9		
11	3.78 <i>ddd</i> (8.7, 3.4, 1.3)	80.1	H-4a (w), H-12, H-12', 11-OH	C-4a, C-10a, C-12
12	2.90 <i>dd</i> (13.7, 3.5)	63.6	H-6 <sub>eq</sub> (w), H-6 <sub>ax</sub> , H-11, H-12'	C-6, C-6a, C-11
12'	3.26 <i>dd</i> (13.6, 7.0)		H-11, H-12, H-4a (w)	C-4a, C-6, C-10b
3-OMe	3.21 <i>s</i>	55.6		C-3
OCH <sub>2</sub> O	5.92 <i>s</i>	100.6		C-8, C-9
11-OH	4.98 <i>d</i> (4.4)		H-11, H-12'	C-10b, C-11, C-12

**Table 6:** <sup>1</sup>H NMR, <sup>13</sup>C NMR, COSY and HMBC data of haemanthamine (600 MHz, DMSO-*d*<sub>6</sub>)

Position	$\delta_{\text{H}}$ (J in Hz)	$\delta_{\text{C}}$	COSY	HMBC
1	6.60 <i>d</i> (10.6)	130.9	H-2, H-10 (w)	C-2, C-3, C-4a, C-10a, C-10b
2	5.78 <i>ddd</i> (10.0, 5.2, 1.1)	128.5	H-1, H-3, H-4 <sub>eq</sub>	C-1, C-3, C-4, C-10b
3	4.11 <i>m</i>	62.4	H-1 (w), H-2, H-4 <sub>ax</sub> , H-4 <sub>eq</sub> , H-4a (w), 3-OH	C-1, C-2, C-4, C-4a
4 <sub>ax</sub>	1.59 <i>td</i> (13.3, 4.3)	32.7	H-3, H-4 <sub>eq</sub> , H-4a	C-2, C-3, C-4a, C-10b (w)
4 <sub>eq</sub>	1.63 <i>dddd</i> (13.3, 4.6, 2.0, 1.1)		H-2, H-3, H-4 <sub>ax</sub> , H-4a	C-2, C-3, C-4a, C-10b
4a	3.19 <i>dd</i> (12.5, 4.6)	62.5	H-1, H-4 <sub>ax</sub> , H-4 <sub>eq</sub> , H6 <sub>eq</sub> (w)	C-3, C-4, C-6, C-10a, C-11, C-12
6 <sub>eq</sub>	3.67 <i>d</i> (17.0)	61.8	H-6 <sub>ax</sub> , H-7, H-10, H-12' (w)	C-4 (w), C-4a, C-6a, C-7, C-8, C-9, C-10, C-10a, C-10b, C-12
6 <sub>ax</sub>	4.20 <i>d</i> (17.0)		H-6 <sub>eq</sub> , H-7, H-10 (w), H-12 (w)	C-4a, C-6a, C-7, C-8, C-9, C-10a, C-11, C-12
6a		127.0		
7	6.59 <i>s</i>	106.9	H-6 <sub>ax</sub> , H-6 <sub>eq</sub> , H-10	C-6, C-6a, C-7, C-8, C-9, C-10a, C-10b
8		145.1		
9		145.6		
10	7.02 <i>s</i>	103.2	H-6 <sub>ax</sub> , H-6 <sub>eq</sub> , H-7	C-6, C-6a, C-7, C-8, C-9, C-10a, C-10b, C-11
10 a		138.8		
10 b		43.9		
11	1.80 <i>m</i>	44.2	H-6 <sub>ax</sub> (w), H-11', H-12, H-12'	C-1, C-10a, C-10b, C-12
11'	1.98 <i>ddd</i> (13.3, 9.0, 4.2)		H-11, H-12, H-12'	C-4a, C-10a, C-10b, C-12
12	2.74 <i>m</i>	53.0	H-6 <sub>ax</sub> , H-11, H-11', H-12'	C-6, C-4a, C-10b, C-11
12'	3.17 <i>m</i>		H-6 <sub>ax</sub> , H-11, H-11', H-12	C-4a, C-6, C-10a, C-10b, C-11
3-OH	4.73 <i>m</i>		H-3	C-2, C-4, C-4a
OCH <sub>2</sub> O	5.90 <i>d</i> (1.1)	100.5		C-8, C-9
	5.91 <i>d</i> (1.1)			

**Table 7:** <sup>1</sup>H NMR, <sup>13</sup>C NMR, COSY and HMBC data of crinine/vittatine (600 MHz, DMSO-*d*<sub>6</sub>)

Position	$\delta_{\text{H}}$ (J in Hz)	$\delta_{\text{C}}$	COSY	HMBC
1	4.40 <i>dd</i> (6.4, 2.3)	63.8	H-2, H-2', H-3, H-10b	C-2, C-3, C-4a, C-6 (w), C-10a (w)
2	2.09 <i>m</i>	31.4	H-1, H-2', H-3	C-1, C-3, C-4, C-4a (w), C-10b
2'	2.61 <i>m</i>		H-1, H-2, H-3	C-3, C-4, C-4a, C-10b
3	5.39 <i>m</i>	114.9	H-1, H-2, H-2', H-4a	C-1, C-4a
4		141.7		
4a	2.54 <i>m</i>	66.9	H-2 (w), H-2', H-3, H-10b	
6	5.83 <i>d</i> (5.7)	88.0	H-1, H-10	C-1, C-6a, C-7 (w), C-8 (w), C-9 (w), C-10a
6a		122.5		
7		150.8		
8		140.7		
9		152.0		
10	6.70 <i>s</i>	109.2	H-10b, 9-OMe	C-4a (w), C-6, C-6a, C-7, C-8, C-9, C-10a, C-10b
10 a		132.9		
10 b	2.22 <i>dd</i> (9.5, 2.2)	43.6	H-1, H-4a, H-10	C-4, C-4a, C-6a, C-10, C-10a
11	2.29 <i>m</i>	28.1	H-3, H-4a, H-11', H-12, H-12'	
11'	2.38 <i>m</i>		H-3, H-11, H-12, H-12'	
12	2.14 <i>dt</i> (9.8, 8.5)	56.2	H-11, H-11', H-12'	C-4, C-4a, C-11, 5-NMe
12'	2.98 <i>ddd</i> (11.3, 7.7, 3.6)		H-11, H-11', H-12	C-4, C-4a, C-11, 5-NMe
6-OH	6.48 <i>d</i> (5.8)		H-6	C-6, C-6a
7-OMe	3.79 <i>s</i>	60.7		C-7
8-OMe	3.72 <i>s</i>	60.4		C-8
9-OMe	3.77 <i>s</i>	55.6	H-10	C-9, C-10
5-NMe	1.89 <i>s</i>	44.3		C-4a, C-12

**Table 8:**  $^1\text{H}$  NMR,  $^{13}\text{C}$  NMR, COSY and HMBC data of nerinine (600 MHz, DMSO- $d_6$ )

Position	$\delta_H$ (J in Hz)	$\delta_C$	COSY	HMBC
1	6.88 <i>d</i> (10.0)	135.3	H-2, H-10 (w)	C-3, C-4a, C-10a, C-10b
2	5.81 <i>ddd</i> (10.0, 5.3, 1.0)	123.1	H-1, H-3, H-4 (w), H-4'(w)	C-3, C-4, C-10b
3	5.21 <i>m</i>	66.3	H-2, H-4, H-4'	C-1, C-2, C-4a, 3-OCOR
4	1.77 <i>m</i>	29.3	H-2 (w), H-3, H-4a	C-4a, C-10b
4'	1.77 <i>m</i>		H-2 (w), H-3, H-4a	C-4a, C-10b
4a	3.13 <i>d</i> (5.1)	62.9	H-4, H-4'	C-10b, C-12
6	3.68 <i>d</i> (17.1)	61.8	H-6', H-7 (w), H-10 (w)	C-4a, C-6a, C-7, C-10a, C-12
6'	4.23 <i>d</i> (17.0)		H-6, H-7, H-10 (w), H- 12'(w)	C-6a, C-7 (w), C-10a, C- 10 b (w), C-12
6a		126.9		
7	6.60 <i>s</i>	107.0	H-6, H-6'	C-6, C-6a, C-8, C-9, C- 10, C-10a, C-10b
8		145.3		
9		145.7		
10	7.04 <i>s</i>	103.1	H-1, H-6, H-6' (w), H-7 (w)	C-6a, C-7, C-8, C-9, C- 10a, C-10b
10 a		138.1		
10 b		44.0		
11	1.86 <i>m</i>	44.2	H-11', H-12, H-12'	C-10a, C-10b, C-12
11'	2.03 <i>m</i>		H-11, H-12, H-12'	C-4a, C-10a, C-10b, C-12 (w)
12	2.79 <i>m</i>	53.0	H-11, H-11', H-12'	C-4a, C-6, C-10b
12'	3.20 <i>m</i>		H-11, H-11', H-12	C-6
3-OCOR		169.9		
3-OCOCH <sub>3</sub>	1.95 <i>s</i>	21.0		C-3, 3-OCOR
OCH <sub>2</sub> O	5.92 <i>m</i>	100.6		C-8, C-9

**Table 9:** <sup>1</sup>H NMR, <sup>13</sup>C NMR, COSY and HMBC data of crinine acetate (600 MHz, DMSO-*d*<sub>6</sub>)

Position	$\delta_H$ (J in Hz)	$\delta_C$	COSY	HMBC
1	5.38 <i>ddd</i> (10.4, 2.3, 1.3)	129.4	H-2, H-3, H-4a	C-3, C-4a, C-10b
2	5.76 <i>m</i>	128.6	H-1, H-3, H-4 <sub>ax</sub> (w)	C-4, C-10b
3	4.03 <i>m</i>	72.7	H-1, H-2, H-4 <sub>ax</sub> , H-4 <sub>eq</sub>	C-1, C-2, 3-OMe
4 <sub>eq</sub>	1.69 <i>m</i>	29.7	H-3, H-4 <sub>ax</sub> , H-4a	C-3
4 <sub>ax</sub>	2.41 <i>m</i>		H-2, H-3, H-4 <sub>eq</sub> , H4a	C-2, C-3, C-4a, C-10b, C-12
4a	2.86 <i>m</i>	63.5	H-1, H-4 <sub>ax</sub> , H-4 <sub>eq</sub>	C-1, C-3, C-10a, C-10b, 5-NMe
6	5.92 <i>m</i>	92.7	H-7, 6-OH	
6a		129.4		
7	6.81 <i>s</i>	108.3	H-6	C-6, C-6a, C-8, C-9, C10, C-10a, C-10b
8		145.8		
9		146.8		
10	6.72 <i>s</i>	104.2	H-6	C-6a, C-7, C-8, C-9, C-10b
10 a		134.8		
10 b		45.8		
11	4.20 <i>d</i> (16.9)	73.2	H-12, H-12'	C-6, C-10a, C-12, 5-NMe
12	2.74 <i>m</i>	53.8	H-11, H-12'	C-4a, C-10b, C-11, 5-NMe
12'	2.55 <i>m</i>		H-11, H-12	C-4a, C10b, C-11, 5-NMe
3-OMe	3.29 <i>s</i>	55.2		C-3
5-NMe	2.42 <i>s</i>	43.0	H-2, H-3, H-4 <sub>ax</sub> , H-4 <sub>eq</sub> , H4a	C-2 (w), C-4a, C-10b (w), C-12
OCH <sub>2</sub> O	5.97 <i>d</i> (1.1) 5.98 <i>d</i> (1.1)	101.0		C-8, C-9
6-OH	6.88 <i>s</i>		H-6	C-8, C-9 C-6, C-6a

**Table 10:** <sup>1</sup>H NMR, <sup>13</sup>C NMR, COSY and HMBC data of pretazettine (600 MHz, DMSO-*d*<sub>6</sub>)

Position	$\delta_{\text{H}}$ (J in Hz)	$\delta_{\text{C}}$	COSY	HMBC
1	8.68 <i>dd</i> (8.3, 1.5)	123.0	H-2 (w), H-4 (w), H-7, H-10	C-2 (w), C-3, C-4, C-4a
2	7.65 <i>m</i>	126.7	H-1, H-3, H-4	C-4, C-10b
3	7.71 <i>ddd</i> (8.4, 6.8, 1.4)	128.0	H-1, H-4	C-1, C-4a, C-10b (w)
4	8.03 <i>dd</i> (8.1, 1.4)	129.5	H-1, H-3	C-2, C-10b
4a		143.9		
6	9.16 <i>s</i>	151.8	H-7, H-10	C-4a, C-6a, C-7, C-10, C-10a, C-10b
6a		122.8		
7	7.67 <i>s</i>	105.4	H-6, H-10	C-6, C-9, C-10a, C-10b
8		148.1		
9		151.5		
10	8.32 <i>s</i>	100.4	H-6, H-7	C-6, C6a, C-7, C-8, C-9, C-10b
10 a		129.6		
10 b		124.0		
OCH <sub>2</sub> O	6.28 <i>s</i>	102.2		C-8, C-9

**Table 11:** <sup>1</sup>H NMR, <sup>13</sup>C NMR, COSY and HMBC data of trisphaeridine (600 MHz, DMSO-*d*<sub>6</sub>)

Position	$\delta_H$ (J in Hz)	$\delta_C$	COSY	HMBC
1	5.29 <i>m</i>	125.9	H-2, H-3, H-4a	C-3, C-4a, C-10b
2	5.92 <i>m</i>	131.7	H-1, H-3, H-4 <sub>eq</sub>	C-4, C-10b
3	4.04 <i>m</i>	72.33	H-1, H-2, H-4 <sub>ax</sub> , H-4 <sub>eq</sub>	C-1, C-2, 3-OMe
4 <sub>ax</sub>	1.72 <i>m</i>	28.9	H-3, H-4 <sub>eq</sub> , H-4a	C-3, C-4a
4 <sub>eq</sub>	2.43 <i>m</i>		H-2, H-3, H-4 <sub>ax</sub> , H-4a	C-2, C-3, C-4a, C-10b
4a	3.11 <i>m</i>	69.4	H-1, H-4 <sub>ax</sub> , H-4 <sub>eq</sub>	C-3, 5-NMe
6		164.9		
6a		118.0		
7	7.39 <i>s</i>	109.9	H-10	C-6, C-6a, C-8, C-9, C10, C-10a
8		146.8		
9		152.2		
10	6.97 <i>s</i>	104.0	H-7	C-6, C-6a, C-7, C-8, C- 9, C-10a
10 a		142.1		
10 b		45.7		
11	4.62 <i>dd</i> (10.9, 7.7)	101.1	H-1, H-12, H-12'	C-1, C-10a, C-10b, C-12
12	2.92 <i>m</i>	52.9	H-11, H-12'	C-4a, C-10b, C-11, 5- NMe
12'	2.76 <i>m</i>		H-11, H-12, 5-NMe (w)	C-4a, C10b, C-11, 5- NMe
3-OMe	3.30 <i>s</i>	55.3	H-3 (w)	C-3
5-NMe	2.44 <i>s</i>	42.5	H-2, H-3, H-4 <sub>ax</sub> , H-4 <sub>eq</sub>	C-3, C-4a
OCH <sub>2</sub> O	6.15 <i>d</i> (1.0) 6.13 <i>d</i> (1.0)	102.4		C-8, C-9

**Table 12:** <sup>1</sup>H NMR, <sup>13</sup>C NMR, COSY and HMBC data of 3-epimacronine (600 MHz, DMSO-*d*<sub>6</sub>)

Position	$\delta_{\text{H}}$ (J in Hz)	$\delta_{\text{C}}$	COSY	HMBC
1	7.35 <i>m</i>	124.1	H-2, H-3	C-3, C-4a, C-10a, C-10b
2	6.31 <i>dd</i> (9.8, 4.3)	128.4	H-1, H-3	C-3, C-4, C-10b
3	4.19 <i>m</i>	72.10	H-2, H-4	C-1, C-2, C-4a, 3-OMe
4	3.16 <i>m</i>	35.9	H-3	C-2, C-3, C-4a, C-10b
4'	3.16 <i>m</i>		H-3	C-2, C-3, C-4a, C-10b
4a		147.1		
6	8.81 <i>s</i>	148.2	H-7	C-4a, C-6a, C-7, C-10a, C-10b
6a		124.8		
7	7.42 <i>s</i>	103.2	H-6, H-10	C-6, C-8, C-9, C-10a, C-10b
8		147.4		
9		151.3		
10	7.67 <i>s</i>	98.1	H-7	C6a, C-8, C-9, C-10a, C-10b
10 a		130.0		
10 b		120.5		
3-OMe	3.25 <i>s</i>	54.9	H-3	C-3
OCH <sub>2</sub> O	6.200 <i>d</i> (0.8) 6.205 <i>d</i> (0.8)	101.9		C-8, C-9

**Table 13:** <sup>1</sup>H NMR, <sup>13</sup>C NMR, COSY and HMBC data of 3-methoxy-8,9-methylenedioxy-3,4-dihydrophenanthridine (600 MHz, DMSO-*d*<sub>6</sub>)

## 4.4 Conclusion

The dereplication protocol for Amaryllidaceae alkaloids developed in this study allowed to characterize *U. peruviana* bulb extract. Twelve alkaloids were identified, eleven out of them, namely tazettine, albomaculine, haemanthamine, crinine/vittatine, trisphaeridine, 3-epimacronine, 3-methoxy-8,9-methylenedioxy-3,4-dihydrophenanthridine, 6 $\alpha$ / $\beta$ -hydroxycrinine, crinine acetate, nerinine and pretazettine, were already known in scientific literature. Their identification was carried out directly on the fractions of the extract, without resorting in purification processes, saving time and resources.

One alkaloid showed an NMR profile not found in any database, hence, the fraction containing it was subjected to a second fractionation to obtain sub-fractions of increased purity in order to elucidate its structure. The new alkaloid presented a peculiar structure, with two nitrogen atoms, which is very rare. The new alkaloid was called 6-dehydroxy-6-acetamido-nerinine.

## 5 CONCLUSIONS

Plant-based drug discovery continues to play a central role in finding new bioactive molecules. In recent years many techniques were developed for overcoming some of the typical difficulties of this branch of research. Among these, metabolomics coupled to chemometrics and the procedures for dereplication are particularly effective for the analysis of plant extracts.

The metabolomic-chemometric approach allowed the selection of the most promising extracts in a screening for antibacterial activity by simultaneously considering different data in a PCA model. NMR-based metabolomics led to reap the metabolomic changes of *Arbutus unedo* L. leaf samples collected under different conditions. This approach guided the selection of the most phytochemically diverse samples which demonstrated considerable variations in biological activities. One the antibacterial agents of *A. unedo* leaf extract was identified as Kaempferol-3-*O*-rhamnoside.

Further studies will be carried out to complete the characterisation of the antibacterial agents in *A unedo* leaf extract.

The procedure for dereplication of Amaryllidaceae alkaloids led to the characterization of *Urceolina peruviana* (C. Presl) J.F. Macbr bulb extract, without employing costly purification processes, saving resources and time. The method allowed the rapid identification of the known alkaloid and the recognition of the only fraction containing an unknown molecule. Hence, only this fraction was purified and the structure of new alkaloid was elucidated. This dinitrogenous alkaloid was named 6-dehydroxy-6-acetamido-nerinine.

## REFERENCES

- (1) Dias, D. A., Urban, S., & Roessner, U. A historical overview of natural products in drug discovery. *Metabolites*. **2012** 2(2), 303-336.
- (2) Akula, R.; Ravishankar, G. A. Influence of Abiotic Stress Signals on Secondary Metabolites in Plants. *Plant Signal. Behav.* **2011**, 6 (11), 1720–1731.
- (3) Pagare, S.; Bhatia, M.; Tripathi, N.; Pagare, S.; Bansal, Y. K. Secondary Metabolites of Plants and Their Role: Overview. **2015**, 9, 12.
- (4) Chappell, J. Biochemistry and Molecular Biology of the Isoprenoid Biosynthetic Pathway in Plants. *Annu. Rev. Plant Physiol. Plant Mol. Biol.* **1995**, 46 (1), 521–547.
- (5) Cho, K. S.; Lim, Y.; Lee, K.; Lee, J.; Lee, J. H.; Lee, I.-S. Terpenes from Forests and Human Health. *Toxicol. Res.* **2017**, 33 (2), 97–106.
- (6) Tetali, S. D. Terpenes and Isoprenoids: A Wealth of Compounds for Global Use. *Planta* **2019**, 249 (1), 1–8.
- (7) Julkunen-Tiitto, R. Assessing the Response of Plant Flavonoids to UV Radiation: An Overview of Appropriate Techniques. *Phytochem. Rev.* **2015**, v. 14 (2), 273–297.
- (8) Zaynab, M.; Fatima, M.; Abbas, S.; Sharif, Y.; Umair, M.; Zafar, M. H.; Bahadar, K. Role of Secondary Metabolites in Plant Defense against Pathogens. *Microb. Pathog.* **2018**, 124, 198–202.
- (9) Cheynier, V.; Comte, G.; Davies, K. M.; Lattanzio, V.; Martens, S. Plant Phenolics: Recent Advances on Their Biosynthesis, Genetics, and Ecophysiology. *Plant Physiol. Biochem.* **2013**, 72, 1–20.
- (10) Khan, M. I. R.; Asgher, M.; Iqbal, N.; Khan, N. A. Potentiality of Sulphur-Containing Compounds in Salt Stress Tolerance. *Ecophysiology and responses of plants under salt stress*. **2013** Springer, New York, NY. 443-472.
- (11) Ahmed, E.; Arshad, M.; Khan, M. Z.; Amjad, M. S.; Sadaf, H. M.; Riaz, I.; Ahmad, N. Secondary Metabolites and Their Multidimensional Prospective in Plant Life. *J. Pharmacogn. Phytochem.* **2017**, 6, 205-214.
- (12) Debnath, B.; Singh, W. S.; Das, M.; Goswami, S.; Singh, M. K.; Maiti, D.; Manna, K. Role of Plant Alkaloids on Human Health: A Review of Biological Activities. *Mater. Today Chem.* **2018**, 9, 56–72.
- (13) McChesney, J. D., Venkataraman, S. K., & Henri, J. T. Plant natural products: back to the future or into extinction? *Phytochemistry* **2017** 68(14), 2015-2022.
- (14) Petersen, F., & Amstutz, R. *Natural Compounds as Drugs, Volume II*. **2008** (Vol. 66) Springer Science & Business Media.
- (15) David, B.; Wolfender, J.-L.; Dias, D. A. The Pharmaceutical Industry and Natural Products: Historical Status and New Trends. *Phytochem. Rev.* **2015**, 14 (2), 299–315.
- (16) Newman, D. J.; Cragg, G. M. Natural Products as Sources of New Drugs over the Nearly Four Decades from 01/1981 to 09/2019. *J. Nat. Prod.* **2020**, 83 (3), 770–803.

- (17) Lautié, E., Russo, O., Ducrot, P., & Boutin, J. A. Unraveling plant natural chemical diversity for drug discovery purposes. *Frontiers in Pharmacology*. **2020**, *11*, 397.
- (18) Harvey, A. L., Edrada-Ebel, R., & Quinn, R. J. The re-emergence of natural products for drug discovery in the genomics era. *Nature reviews drug discovery*. **2015**, *14*(2), 111-129.
- (19) Katiyar, C.; Kanjilal, S.; Gupta, A.; Katiyar, S. Drug Discovery from Plant Sources: An Integrated Approach. *AYU Int. Q. J. Res. Ayurveda* **2012**, *33* (1), 10.
- (20) Newman, D. J.; Cragg, G. M. Plant Endophytes and Epiphytes: Burgeoning Sources of Known and “Unknown” Cytotoxic and Antibiotic Agents? *Planta Med.* **2020**, *86* (13/14), 891–905.
- (21) Joshi, B.; Panda, S. K.; Jouneghani, R. S.; Liu, M.; Parajuli, N.; Leyssen, P.; Neyts, J.; Luyten, W. Antibacterial, Antifungal, Antiviral, and Anthelmintic Activities of Medicinal Plants of Nepal Selected Based on Ethnobotanical Evidence. *Evid. Based Complement. Alternat. Med.* **2020**, *2020*, 1–14.
- (22) McMurray, R. L.; Ball, M. E. E.; Tunney, M. M.; Corcionivoschi, N.; Situ, C. Antibacterial Activity of Four Plant Extracts Extracted from Traditional Chinese Medicinal Plants against *Listeria Monocytogenes*, *Escherichia Coli*, and *Salmonella Enterica* Subsp. *Enterica* Serovar *Enteritidis*. *Microorganisms* **2020**, *8* (6), 962.
- (23) Das, B.; Mahalik, G. Ethnobotanical Survey and Antimicrobial Activity of Medicinal Plants Used To Cure Various Diseases in Kaptipada and Udala Block of Odisha, India: A Review. **2020**, No. 60, 13.
- (24) Wolfensberger, A.; Kuster, S. P.; Marchesi, M.; Zbinden, R.; Hombach, M. The Effect of Varying Multidrug-Resistance (MDR) Definitions on Rates of MDR Gram-Negative Rods. *Antimicrob. Resist. Infect. Control* **2019**, *8* (1), 193.
- (25) Abolhasan Choobdar, F., Khalesi, N., Haghghi Aski, B., Behdadmehr, S., Safari, A., & Kalantar, S. Determination of Antibiotic Resistance Pattern of Bacteria Isolated from Blood, Cerebrospinal Fluid and Urine Samples in Neonatal Intensive Care Units at Ali Asghar Hospital during 2013-2015. *Iran. J. Neonatol. IJN* **2020**, *11*(3), 38-43.
- (26) Van Duin, D., & Paterson, D. L. Multidrug-resistant bacteria in the community: trends and lessons learned. *Infect. Dis. Clin. North Am.* **2016**, *30* (2), 377–390.
- (27) Klemm, E. J.; Wong, V. K.; Dougan, G. Emergence of Dominant Multidrug-Resistant Bacterial Clades: Lessons from History and Whole-Genome Sequencing. *Proc. Natl. Acad. Sci.* **2018**, *115* (51), 12872–12877.
- (28) Rolo, J.; De Lencastre, H.; Miragaia, M. Strategies of Adaptation of *Staphylococcus Epidermidis* to Hospital and Community: Amplification and Diversification of SCC mec. *J. Antimicrob. Chemother.* **2012**, *67* (6), 1333–1341.
- (29) May, L.; Klein, E. Y.; Rothman, R. E.; Laxminarayan, R. Trends in Antibiotic Resistance in Coagulase-Negative *Staphylococci* in the United States, 1999 to 2012. *Antimicrob. Agents Chemother.* **2014**, *58* (3), 1404–1409.
- (30) Chitemerere, T. A.; Mukanganyama, S. Evaluation of Cell Membrane Integrity as a Potential Antimicrobial Target for Plant Products. *BMC Complement. Altern. Med.* **2014**, *14* (1), 278.

- (31) Zhao, X.; Zhao, F.; Zhong, N. Quorum Sensing Inhibition and Anti-Biofilm Activity of Traditional Chinese Medicines. In *Food Safety - Some Global Trends*; El-Samragy, Y., Ed.; InTech, 2018.
- (32) Radulovic, N. S.; Blagojevic, P. D.; Stojanovic-Radic, Z. Z.; Stojanovic, N. M. Antimicrobial Plant Metabolites: Structural Diversity and Mechanism of Action. *Curr. Med. Chem.* **2013**, *20* (7), 932–952.
- (33) Anand, U.; Jacobo-Herrera, N.; Altemimi, A.; Lakhssassi, N. A Comprehensive Review on Medicinal Plants as Antimicrobial Therapeutics: Potential Avenues of Biocompatible Drug Discovery. *Metabolites* **2019**, *9* (11), 258.
- (34) Fiehn, O. Metabolomics — the Link between Genotypes and Phenotypes. In *Functional Genomics*; Town, C., Ed.; Springer Netherlands: Dordrecht, **2002**; pp 155–171.
- (35) Schripsema, J.; Dagnino, D. Metabolomics: Experimental Design, Methodology and Data Analysis. In *Encyclopedia of Analytical Chemistry*; Meyers, R. A., Ed.; John Wiley & Sons, Ltd: Chichester, UK, **2014**; pp 1–17.
- (36) Schrimpe-Rutledge, A. C.; Codreanu, S. G.; Sherrod, S. D.; McLean, J. A. Untargeted Metabolomics Strategies—Challenges and Emerging Directions. *J. Am. Soc. Mass Spectrom.* **2016**, *27* (12), 1897–1905.
- (37) Madsen, R.; Lundstedt, T.; Trygg, J. Chemometrics in Metabolomics—A Review in Human Disease Diagnosis. *Anal. Chim. Acta* **2010**, *659* (1–2), 23–33.
- (38) Sun, J.; Schnackenberg, L.; Beger, R. Studies of Acetaminophen and Metabolites in Urine and Their Correlations with Toxicity Using Metabolomics. *Drug Metab. Lett.* **2009**, *3* (3), 130–136.
- (39) Wishart, D. S. Metabolomics: Applications to Food Science and Nutrition Research. *Trends Food Sci. Technol.* **2008**, *19* (9), 482–493.
- (40) Hegeman, A. D. Plant Metabolomics--Meeting the Analytical Challenges of Comprehensive Metabolite Analysis. *Brief. Funct. Genomics* **2010**, *9* (2), 139–148.
- (41) Zhang, A.; Sun, H.; Wang, P.; Han, Y.; Wang, X. Modern Analytical Techniques in Metabolomics Analysis. *The Analyst* **2012**, *137* (2), 293–300.
- (42) Markley, J. L., Brüschweiler, R., Edison, A. S., Eghbalnia, H. R., Powers, R., Raftery, D., & Wishart, D. S. The future of NMR-based metabolomics. *Current opinion in biotechnology* **2017**, *43*, 34-40.
- (43) Kim, H. K.; Choi, Y. H.; Verpoorte, R. NMR-Based Plant Metabolomics: Where Do We Stand, Where Do We Go? *Trends Biotechnol.* **2011**, *29* (6), 267–275.
- (44) Kim, H. K.; Choi, Y. H.; Verpoorte, R. NMR-Based Metabolomic Analysis of Plants. *Nat. Protoc.* **2010**, *5* (3), 536–549.
- (45) Khoo, L. W.; Mediani, A.; Zolkeflee, N. K. Z.; Leong, S. W.; Ismail, I. S.; Khatib, A.; Shaari, K.; Abas, F. Phytochemical Diversity of Clinacanthus Nutans Extracts and Their Bioactivity Correlations Elucidated by NMR Based Metabolomics. *Phytochem. Lett.* **2015**, *14*, 123–133.

- (46) Maulidiani, M.; Sheikh, B. Y.; Mediani, A.; Wei, L. S.; Ismail, I. S.; Abas, F.; Lajis, N. H. Differentiation of *Nigella Sativa* Seeds from Four Different Origins and Their Bioactivity Correlations Based on NMR-Metabolomics Approach. *Phytochem. Lett.* **2015**, *13*, 308–318.
- (47) Kuhnen, S.; Bernardi Ogliari, J.; Dias, P. F.; da Silva Santos, M.; Ferreira, A. G.; Bonham, C. C.; Wood, K. V.; Maraschin, M. Metabolic Fingerprint of Brazilian Maize Landraces Silk (Stigma/Styles) Using NMR Spectroscopy and Chemometric Methods. *J. Agric. Food Chem.* **2010**, *58* (4), 2194–2200.
- (48) Minoja, A. P.; Napoli, C. NMR Screening in the Quality Control of Food and Nutraceuticals. *Food Res. Int.* **2014**, *63*, 126–131.
- (49) Gad, H. A., El-Ahmady, S. H., Abou-Shoer, M. I., & Al-Azizi, M. M. Application of chemometrics in authentication of herbal medicines: a review. *Phytochem. Anal.* **2013**, *24*(1), 1-24.
- (50) Heyman, H. M., & Meyer, J. J. M. NMR-based metabolomics as a quality control tool for herbal products. *S. Afr. J. Bot.* **2012**, *82*, 21-32.
- (51) Clausen, M. R.; Edelenbos, M.; Bertram, H. C. Mapping the Variation of the Carrot Metabolome Using <sup>1</sup>H NMR Spectroscopy and Consensus PCA. *J. Agric. Food Chem.* **2014**, *62* (19), 4392–4398.
- (52) Wu, H.; Liu, X.; Zhao, J.; Yu, J.; Pang, Q.; Feng, J. Toxicological Effects of Environmentally Relevant Lead and Zinc in Halophyte Suaeda Salsa by NMR-Based Metabolomics. *Ecotoxicology* **2012**, *21* (8), 2363–2371.
- (53) Lankadurai, B. P.; Nagato, E. G.; Simpson, M. J. Environmental Metabolomics: An Emerging Approach to Study Organism Responses to Environmental Stressors. *Environ. Rev.* **2013**, *21* (3), 180–206.
- (54) Hendriks, M. M. W. B.; Eeuwijk, F. A. van; Jellema, R. H.; Westerhuis, J. A.; Reijmers, T. H.; Hoefsloot, H. C. J.; Smilde, A. K. Data-Processing Strategies for Metabolomics Studies. *TrAC Trends Anal. Chem.* **2011**, *30* (10), 1685–1698.
- (55) Worley, B.; Powers, R. Multivariate Analysis in Metabolomics. *Curr Metabolomics.* **2013**, *1*(1): 92–107.
- (56) J. Ellinger, J.; A. Chylla, R.; L. Ulrich, E.; L. Markley, J. Databases and Software for NMR-Based Metabolomics. *Curr. Metabolomics* **2012**, *1* (1), 28–40.
- (57) Brennan, L. NMR-Based Metabolomics: From Sample Preparation to Applications in Nutrition Research. *Prog. Nucl. Magn. Reson. Spectrosc.* **2014**, *83*, 42–49.
- (58) Girish, H. V., & Satish, S. Antibacterial activity of important medicinal plants on human pathogenic bacteria-a comparative analysis. *World Appl. Sci. J.* **2008**, *5*(3), 267-271.
- (59) Abreu, A. C.; Paulet, D.; Coqueiro, A.; Malheiro, J.; Borges, A.; Saavedra, M. J.; Choi, Y. H.; Simões, M. Antibiotic Adjuvants from *Buxus Sempervirens* to Promote Effective Treatment of Drug-Resistant *Staphylococcus Aureus* Biofilms. *RSC Adv.* **2016**, *6* (97), 95000–95009.
- (60) Abreu, A. C.; Coqueiro, A.; Sultan, A. R.; Lemmens, N.; Kim, H. K.; Verpoorte, R.; van Wamel, W. J. B.; Simões, M.; Choi, Y. H. Looking to Nature for a New Concept in Antimicrobial Treatments: Isoflavonoids from *Cytisus Striatus* as Antibiotic Adjuvants against MRSA. *Sci. Rep.* **2017**, *7* (1), 3777.

- (61) Fois, M.; Fenu, G.; Cañadas, E. M.; Bacchetta, G. Disentangling the Influence of Environmental and Anthropogenic Factors on the Distribution of Endemic Vascular Plants in Sardinia. *PLOS ONE* **2017**, *12* (8), e0182539.
- (62) Marignani, M.; Bruschi, D.; Astiaso Garcia, D.; Frondoni, R.; Carli, E.; Pinna, M. S.; Cumo, F.; Gugliermetti, F.; Saatkamp, A.; Doxa, A.; Queller, E. M.; Chaieb, M.; Bou Dagher-Kharrat, M.; El Zein, R.; El Jeitani, S.; Khater, C.; Mansour, S.; Al-Shami, A.; Harik, G.; Alameddine, I.; el-Fadel, M.; Blasi, C. Identification and Prioritization of Areas with High Environmental Risk in Mediterranean Coastal Areas: A Flexible Approach. *Sci. Total Environ.* **2017**, *590–591*, 566–578.
- (63) Migheli, Q.; Balmas, V.; Komoń-Zelazowska, M.; Scherm, B.; Fiori, S.; Kopchinskiy, A. G.; Kubicek, C. P.; Druzhinina, I. S. Soils of a Mediterranean Hot Spot of Biodiversity and Endemism (Sardinia, Tyrrhenian Islands) Are Inhabited by Pan-European, Invasive Species of *Hypocrea/Trichoderma*. *Environ. Microbiol.* **2009**, *11* (1), 35–46.
- (64) Venditti, A.; Maggi, F.; Quassinti, L.; Bramucci, M.; Lupidi, G.; Ornano, L.; Ballero, M.; Sanna, C.; Bruno, M.; Rosselli, S.; Bianco, A. Bioactive Constituents of *Juniperus Turbinata* GUSS. from La Maddalena Archipelago. *Chem. Biodivers.* **2018**, *15* (8), e1800148.
- (65) Venditti, A.; Sanna, C.; Lorenzetti, L. M.; Ballero, M.; Bianco, A. New Coumarinyl Ethers in *Daphne Oleoides* SCHREB. Collected from Sardinia Island. *Chem. Biodivers.* **2017**, *14* (6), e1700072.
- (66) Bobo-Pinilla, J.; Barrios de León, S. B.; Seguí Colomar, J.; Fenu, G.; Bacchetta, G.; Peñas de Giles, J.; Martínez-Ortega, M. M. Phylogeography of *Arenaria Balearica* L. (Caryophyllaceae): Evolutionary History of a Disjunct Endemic from the Western Mediterranean Continental Islands. *PeerJ* **2016**, *4*, e2618.
- (67) Mandrone, M.; Bonvicini, F.; Lianza, M.; Sanna, C.; Maxia, A.; Gentilomi, G. A.; & Poli, F. Sardinian plants with antimicrobial potential. Biological screening with multivariate data treatment of thirty-six extracts. *Ind. Crop. Prod.* **2019**, *137*, 557-565.
- (68) Bonvicini, F.; Antognoni, F.; Mandrone, M.; Protti, M.; Mercolini, L.; Lianza, M.; & Poli, F. Phytochemical analysis and antibacterial activity towards methicillin-resistant *Staphylococcus aureus* of leaf extracts from *Argania spinosa* (L.) Skeels. *Plant Biosyst.* **2017**, *v. 151* (4), 649–656.
- (69) Bonvicini, F.; Lianza, M.; Mandrone, M.; Poli, F.; Gentilomi, G. A.; Antognoni, F. *Hemidesmus indicus* (L.) R. Br. extract inhibits the early step of herpes simplex type 1 and type 2 replication. *New Microbiol.* **2018**, *41*, 187-194.
- (70) Coppo, E.; Marchese, A. Antibacterial Activity of Polyphenols. *Curr. Pharm. Biotechnol.* **2014**, *15* (4), 380–390.
- (71) Luís, Â.; Silva, F.; Sousa, S.; Duarte, A. P.; Domingues, F. Antistaphylococcal and Biofilm Inhibitory Activities of Gallic, Caffeic, and Chlorogenic Acids. *Biofouling* **2014**, *30* (1), 69–79.
- (72) Cueva, C.; Mingo, S.; Muñoz-González, I.; Bustos, I.; Requena, T.; del Campo, R.; Martín-Álvarez, P. J.; Bartolomé, B.; Moreno-Arribas, M. V. Antibacterial Activity of Wine Phenolic Compounds and Oenological Extracts against Potential Respiratory Pathogens: Wine Phenolics against Respiratory Pathogens. *Lett. Appl. Microbiol.* **2012**, *54* (6), 557–563.
- (73) Rodriguez Vaquero, M. J. Phenolic Compound Combinations on Escherichia Coli Viability in a Meat System. *J. Agric. Food Chem.* **2010**, *v. 58* (10), 2010 v.58 no.10.

- (74) Magesh, H.; Kumar, A.; Alam, A.; Sekar, U.; Sumantran, V. N.; Vaidyanathan, R. Identification of Natural Compounds Which Inhibit Biofilm Formation in Clinical Isolates of *Klebsiella Pneumoniae*. *Indian J Exp Biol.* **2013**, *9*.
- (75) Potapovich, A. I., & Kostyuk, V. A. Comparative study of antioxidant properties and cytoprotective activity of flavonoids. *Biochemistry (Moscow)*, **2003**, *68*(5), 514-519.
- (76) Hosseinzadeh, H.; Nassiri-Asl, M. Review of the Protective Effects of Rutin on the Metabolic Function as an Important Dietary Flavonoid. *J. Endocrinol. Invest.* **2014**, *37* (9), 783–788.
- (77) Loi, M. C., Frailis, L., & Maxia, A. Le piante utilizzate nella medicina popolare nel territorio di Gesturi (Sardegna centro-meridionale). *Atti Soc Tosc Sci Nat Mem Serie B*, **2003**, *109*, 167-176.
- (78) Ballero, M.; Sacchetti, G.; & Poli, F. Plants in folk medicine in the territory of Perdasdefogu (Central Sardinia, Italy). *Allionia* **1997**, 157-164.
- (79) Zucca, P.; Pintus, M.; Manzo, G.; Nieddu, M.; Steri, D.; Rinaldi, A. C. Antimicrobial, Antioxidant and Anti-Tyrosinase Properties of Extracts of the Mediterranean Parasitic Plant *Cytinus Hypocistis*. *BMC Res. Notes* **2015**, *8* (1), 562.
- (80) Maisetta, G.; Batoni, G.; Caboni, P.; Esin, S.; Rinaldi, A. C.; Zucca, P. Tannin Profile, Antioxidant Properties, and Antimicrobial Activity of Extracts from Two Mediterranean Species of Parasitic Plant *Cytinus*. *BMC Complement. Altern. Med.* **2019**, *19* (1), 82.
- (81) Magiatis, P.; Pratsinis, H.; Kalpoutzakis, E.; Konstantinidou, A.; Davaris, P.; Skaltsounis, A.-L. Hydrolyzable Tannins, the Active Constituents of Three Greek *Cytinus* Taxa against Several Tumor Cell Lines. *Biol. Pharm. Bull.* **2001**, *24* (6), 707–709.
- (82) Buzzini, P.; Arapitsas, P.; Goretti, M.; Branda, E.; Turchetti, B.; Pinelli, P.; Ieri, F.; Romani, A. Antimicrobial and Antiviral Activity of Hydrolysable Tannins. *Mini-Rev. Med. Chem.* **2008**, *8* (12), 1179–1187.
- (83) Cakilcioglu, U.; Turkoglu, I. An Ethnobotanical Survey of Medicinal Plants in Sivrice (Elazığ-Turkey). *J. Ethnopharmacol.* **2010**, *132* (1), 165–175.
- (84) Agelet, A.; Vallès, J. Studies on Pharmaceutical Ethnobotany in the Region of Pallars (Pyrenees, Catalonia, Iberian Peninsula). Part III. Medicinal Uses of Non-Vascular Plants. *J. Ethnopharmacol.* **2003**, *84* (2–3), 229–234.
- (85) Duru, M. E.; Cakir, A.; Kordali, S.; Zengin, H.; Harmandar, M.; Izumi, S.; Hirata, T. Chemical Composition and Antifungal Properties of Essential Oils of Three *Pistacia* Species. *Fitoterapia* **2003**, *74* (1–2), 170–176.
- (86) Kavak, D. D.; Altiok, E.; Bayraktar, O.; Ülkü, S. *Pistacia Terebinthus* Extract: As a Potential Antioxidant, Antimicrobial and Possible  $\beta$ -Glucuronidase Inhibitor. *J. Mol. Catal. B Enzym.* **2010**, *64* (3–4), 167–171.
- (87) Pulaj, B.; Mustafa, B.; Nelson, K.; Quave, C. L.; Hajdari, A. Chemical Composition and in Vitro Antibacterial Activity of *Pistacia Terebinthus* Essential Oils Derived from Wild Populations in Kosovo. *BMC Complement. Altern. Med.* **2016**, *16* (1), 147.

- (88) Piras, A. Chemical Characterisation and Biological Activity of Leaf Essential Oils Obtained from *Pistacia Terebinthus* Growing Wild in Tunisia and Sardinia Island. *Nat. Prod. Res.* **2017**, v. 31 (22), 2684–2689.
- (89) Sanna, C.; Rigano, D.; Corona, A.; Piano, D.; Formisano, C.; Farci, D.; Franzini, G.; Ballero, M.; Chianese, G.; Tramontano, E.; Tagliatalata-Scafati, O.; Esposito, F. Dual HIV-1 Reverse Transcriptase and Integrase Inhibitors from *Limonium Morisianum* Arrigoni, an Endemic Species of Sardinia (Italy). *Nat. Prod. Res.* **2019**, 33 (12), 1798–1803.
- (90) Chiocchio, I.; Mandrone, M.; Sanna, C.; Maxia, A.; Tacchini, M.; Poli, F. Screening of a Hundred Plant Extracts as Tyrosinase and Elastase Inhibitors, Two Enzymatic Targets of Cosmetic Interest. *Ind. Crops Prod.* **2018**, 122, 498–505.
- (91) Daino, G. L.; Frau, A.; Sanna, C.; Rigano, D.; Distinto, S.; Madau, V.; Esposito, F.; Fanunza, E.; Bianco, G.; Tagliatalata-Scafati, O.; Zinzula, L.; Maccioni, E.; Corona, A.; Tramontano, E. Identification of Myricetin as an Ebola Virus VP35–Double-Stranded RNA Interaction Inhibitor through a Novel Fluorescence-Based Assay. *Biochemistry* **2018**, 57 (44), 6367–6378.
- (92) Khan, N. A.; Nazar, R.; Iqbal, N.; Anjum, N. A. *Phytohormones and Abiotic Stress Tolerance in Plants*; Springer Science & Business Media, **2012**.
- (93) Celikel, G.; Demirsoy, L.; Demirsoy, H. The Strawberry Tree (*Arbutus Unedo* L.) Selection in Turkey. *Sci. Hortic.* **2008**, 118 (2), 115–119.
- (94) Ruiz-Rodríguez, B.-M.; Morales, P.; Fernández-Ruiz, V.; Sánchez-Mata, M.-C.; Cámara, M.; Díez-Marqués, C.; Pardo-de-Santayana, M.; Molina, M.; Tardío, J. Valorization of Wild Strawberry-Tree Fruits (*Arbutus Unedo* L.) through Nutritional Assessment and Natural Production Data. *Food Res. Int.* **2011**, 44 (5), 1244–1253.
- (95) Morgado, S.; Morgado, M.; Plácido, A. I.; Roque, F.; Duarte, A. P. *Arbutus Unedo* L.: From Traditional Medicine to Potential Uses in Modern Pharmacotherapy. *J. Ethnopharmacol.* **2018**, 225, 90–102.
- (96) Smeekens, S.; Ma, J.; Hanson, J.; Rolland, F. Sugar Signals and Molecular Networks Controlling Plant Growth. *Curr. Opin. Plant Biol.* **2010**, 13 (3), 273–278.
- (97) Sami, F., Yusuf, M., Faizan, M., Faraz, A., & Hayat, S. Role of sugars under abiotic stress. *Plant Physiol. Bioc.* **2016**, 109, 54–61.
- (98) Van Doorn, W. G. Is the Onset of Senescence in Leaf Cells of Intact Plants Due to Low or High Sugar Levels? *J. Exp. Bot.* **2008**, 59 (8), 1963–1972.
- (99) León, P. Sugar and Hormone Connections. *Trends Plant Sci.* **2003**, 8 (3), 110–116.
- (100) Ciereszko, I. Sucrose metabolism in plant tissues under stress conditions: key enzymes, localization and function. *Compartmentation of responses to stresses in higher plants, true or false. Kerala: Transworld Research Network*, **2009**, 193–218.
- (101) Ciereszko, I. Regulatory Roles of Sugars in Plant Growth and Development. *Acta Soc Bot Pol* **2018**, 13.

- (102) Santos-Sánchez, N. F., Salas-Coronado, R., Hernández-Carlos, B., & Villanueva-Cañongo, C. Shikimic acid pathway in biosynthesis of phenolic compounds. In *Plant Physiological Aspects of Phenolic Compounds*. **2019** IntechOpen.
- (103) Marsh, K. B.; Bolding, H. L.; Shilton, R. S.; Laing, W. A. Changes in Quinic Acid Metabolism during Fruit Development in Three Kiwifruit Species. *Funct. Plant Biol.* **2009**, *36* (5), 463.
- (104) Correia, P. J. Changes in the Concentration of Organic Acids in Roots and Leaves of Carob-Tree under Fe Deficiency. *Funct. Plant Biol.* **2014**, *v. 41* (5), 496–504.
- (105) Passarinho, J. A., Lamosa, P., Baeta, J. P., Santos, H., & Ricardo, C. P. Annual changes in the concentration of minerals and organic compounds of *Quercus suber* leaves. *Physiologia Plantarum*, **2006** *127*(1), 100-110.
- (106) Das, N. M., Mohan, R., & Parthipan, B. P. Isolation, Purification and Characterization of Arbutin from *Cleidion nitidum* (Muell.–Arg.) Thw. ex Kurz. (Euphorbiaceae). *Int. J. Sci. Res.* **2016** *5*(1), 1549-1554.
- (107) Thongchai, W., Liawruangrath, B., & Liawruangrath, S. High-performance liquid chromatographic determination of arbutin in skin-whitening creams and medicinal plant extracts. *J. Cosmet. Sci.* **2007**, *58*(1), 35-44.
- (108) Migas, P.; Krauze-Baranowska, M. The Significance of Arbutin and Its Derivatives in Therapy and Cosmetics. *Phytochem. Lett.* **2015**, *13*, 35–40.
- (109) Takebayashi, J.; Ishii, R.; Chen, J.; Matsumoto, T.; Ishimi, Y.; Tai, A. Reassessment of Antioxidant Activity of Arbutin: Multifaceted Evaluation Using Five Antioxidant Assay Systems. *Free Radic. Res.* **2010**, *44* (4), 473–478.
- (110) Pavlović, R. D.; Lakušić, B.; Došlov-Kokoruš, Z.; & Kovačević, N. Arbutin content and antioxidant activity of some Ericaceae species. *Pharmazie* **2009**, No. 10, 656–659.
- (111) Taha, M. M. E. Gastroprotective Activities of *Turnera Diffusa* Willd. Ex Schult. Revisited: Role of Arbutin. *J. Ethnopharmacol.* **2012**, *9*.
- (112) Cheng, S.-L.; Liu, R. H.; Sheu, J.-N.; Chen, S.-T.; Sinchaikul, S.; Tsay, G. J. Toxicogenomics of A375 Human Malignant Melanoma Cells Treated with Arbutin. *J. Biomed. Sci.* **2007**, *14* (1), 87–105.
- (113) EMA. Assessment Report on *Arctostaphylos Uva-Ursi* (L.) Spreng., Folium. *Eur. Med. Agency* **2012**, *44*, 1–34.
- (114) Nenadis, N.; Llorens, L.; Koufogianni, A.; Díaz, L.; Font, J.; Gonzalez, J. A.; & Verdager, D. Interactive effects of UV radiation and reduced precipitation on the seasonal leaf phenolic content/composition and the antioxidant activity of naturally growing *Arbutus unedo* plants. *J. Photochem. Photobiol. B.* **2015**, *153*, 435-444.
- (115) Maleš, Ž.; Šarić, D.; Bojić, M. Quantitative Determination of Flavonoids and Chlorogenic Acid in the Leaves of *Arbutus Unedo* L. Using Thin Layer Chromatography. *J. Anal. Methods Chem.* **2013**, *2013*, 1–4.

- (116) Šic Žlabur, J.; Bogdanović, S.; Voća, S.; Skendrović Babojelić, M. Biological Potential of Fruit and Leaves of Strawberry Tree (*Arbutus Unedo* L.) from Croatia. *Molecules* **2020**, *25* (21), 5102.
- (117) Diantini, A.; Subarnas, A.; Lestari, K.; Halimah, E.; Susilawati, Y.; Julaeha, E.; Achmad, T. H.; Suradji, E. W.; Yamazaki, C.; Kobayashi, K.; Koyama, H.; Abdulah, R. Kaempferol-3-O-Rhamnoside Isolated from the Leaves of *Schima Wallichii* Korth. Inhibits MCF-7 Breast Cancer Cell Proliferation through Activation of the Caspase Cascade Pathway. *Oncol. Lett.* **2012**, *5*.
- (118) Fiorentino, A.; Castaldi, S.; D'Abrosca, B.; Natale, A.; Carfora, A.; Messere, A.; Monaco, P. Polyphenols from the Hydroalcoholic Extract of *Arbutus Unedo* Living in a Monospecific Mediterranean Woodland. *Biochem. Syst. Ecol.* **2007**, *35* (11), 809–811.
- (119) Barliana, M. I.; Suradji, E. W.; Abdulah, R.; Diantini, A.; Hatabu, T.; Nakajima-Shimada, J.; Subarnas, A.; Koyama, H. Antiplasmodial Properties of Kaempferol-3-O-Rhamnoside Isolated from the Leaves of *Schima Wallichii* against Chloroquine-Resistant *Plasmodium Falciparum*. *Biomed. Rep.* **2014**, *2* (4), 579–583.
- (120) Halimah, E.; Diantini, A.; Destiani, D. P.; Pradipta, I. S.; Sastramihardja, H. S.; Lestari, K.; Subarnas, A.; Abdulah, R.; Koyama, H. Induction of Caspase Cascade Pathway by Kaempferol-3-O-Rhamnoside in LNCaP Prostate Cancer Cell Lines. *Biomed. Rep.* **2015**, *3* (1), 115–117.
- (121) Rodríguez, P.; González-Mujica, F.; Bermúdez, J.; Hasegawa, M. Inhibition of Glucose Intestinal Absorption by Kaempferol 3-O- $\alpha$ -Rhamnoside Purified from Bauhinia Megalandra Leaves. *Fitoterapia* **2010**, *81* (8), 1220–1223.
- (122) Chung, M. J.; Pandey, R. P.; Choi, J. W.; Sohng, J. K.; Choi, D. J.; Park, Y. I. Inhibitory Effects of Kaempferol-3-O-Rhamnoside on Ovalbumin-Induced Lung Inflammation in a Mouse Model of Allergic Asthma. *Int. Immunopharmacol.* **2015**, *25* (2), 302–310.
- (123) Sharoar, M.; Thapa, A.; Shah Nawaz, M.; Ramasamy, V.; Woo, E.-R.; Shin, S.; Park, I.-S. Kaempferol-3-O-Rhamnoside Abrogates Amyloid Beta Toxicity by Modulating Monomers and Remodeling Oligomers and Fibrils to Non-Toxic Aggregates. *J. Biomed. Sci.* **2012**, *19* (1), 104.
- (124) Fouseki, M. M.; Damianakos, H.; Karikas, G. A.; Roussakis, C.; Gupta, M.; Chinou, I. Chemical Constituents from *Cordia Alliodora* and *C. Collococa* (Boraginaceae) and Their Biological Activities. *Fitoterapia* **2016**, *115*, 9–14.
- (125) Tatsimo, S. J. N.; Tamokou, J. de D.; Havyarimana, L.; Csupor, D.; Forgo, P.; Hohmann, J.; Kuate, J.-R.; Tane, P. Antimicrobial and Antioxidant Activity of Kaempferol Rhamnoside Derivatives from *Bryophyllum Pinnatum*. *BMC Res. Notes* **2012**, *5* (1), 158.
- (126) Hubert, J.; Nuzillard, J.-M.; Renault, J.-H. Dereplication Strategies in Natural Product Research: How Many Tools and Methodologies behind the Same Concept? *Phytochem. Rev.* **2017**, *16* (1), 55–95.
- (127) Cimmino, A.; Masi, M.; Evidente, M.; Superchi, S.; & Evidente, A. Amaryllidaceae alkaloids: Absolute configuration and biological activity. *Chirality* **2017**, *29*(9), 486–499.
- (128) Beutler, J. A.; Alvarado, A. B.; Schaufelberger, D. E.; Andrews, P.; McCloud, T. G. Dereplication of Phorbol Bioactives: Lyngbya Majuscula and Croton Cuneatus. *J. Nat. Prod.* **1990**, *53* (4), 867–874.

- (129) Nothias-Scaglia, L.-F.; Dumontet, V.; Neyts, J.; Roussi, F.; Costa, J.; Leyssen, P.; Litaudon, M.; Paolini, J. LC-MS2-Based Dereplication of *Euphorbia* Extracts with Anti-Chikungunya Virus Activity. *Fitoterapia* **2015**, *105*, 202–209.
- (130) Messaili, S.; Colas, C.; Fougère, L.; Destandau, E. Combination of Molecular Network and Centrifugal Partition Chromatography Fractionation for Targeting and Identifying *Artemisia Annua* L. Antioxidant Compounds. *J. Chromatogr. A* **2020**, *1615*, 460785.
- (131) Cabral, R. S.; Allard, P.-M.; Marcourt, L.; Young, M. C. M.; Queiroz, E. F.; Wolfender, J.-L. Targeted Isolation of Indolopyridoquinazoline Alkaloids from *Conchocarpus Fontanesianus* Based on Molecular Networks. *J. Nat. Prod.* **2016**, *79* (9), 2270–2278.
- (132) Qiu, F.; McAlpine, J. B.; Lankin, D. C.; Burton, I.; Karakach, T.; Chen, S.-N.; Pauli, G. F. 2D NMR Barcoding and Differential Analysis of Complex Mixtures for Chemical Identification: The *Actaea* Triterpenes. *Anal. Chem.* **2014**, *86* (8), 3964–3972.
- (133) Zani, C. L.; Carroll, A. R. Database for Rapid Dereplication of Known Natural Products Using Data from MS and Fast NMR Experiments. *J Nat Prod* **2017**, *9*.
- (134) Sorokina, M.; Steinbeck, C. *On the Redundancy of Natural Products Public Databases and Where to Find Data in 2020 - A Review on Natural Products Databases*; Preprint; **2019** Life Sciences.
- (135) Haston, E.; Richardson, J. E.; Stevens, P. F.; Chase, M. W.; Harris, D. J. The Linear Angiosperm Phylogeny Group (LAPG) III: A Linear Sequence of the Families in APG III. *Bot. J. Linn. Soc.* **2009**, *161* (2), 128–131.
- (136) THE ANGIOSPERM PHYLOGENY GROUP. An Update of the Angiosperm Phylogeny Group Classification for the Orders and Families of Flowering Plants: APG III: APG III. *Bot. J. Linn. Soc.* **2009**, *161* (2), 105–121.
- (137) Nair, J. J.; van Staden, J.; Bonnet, S. L.; Wilhelm, A. Distribution and Diversity of Usage of the Amaryllidaceae in the Traditional Remediation of Infectious Diseases. *Nat. Prod. Commun.* **2017**, *12* (4), 1934578X1701200.
- (138) Chase, M. W.; Christenhusz, M. J. M.; Fay, M. F.; Byng, J. W.; Judd, W. S.; Soltis, D. E.; & Stevens, P. F. An update of the Angiosperm Phylogeny Group classification for the orders and families of flowering plants: APG IV. *Bot. J. Linn. Soc.* **2016** *181*(1), 1-20.
- (139) Chase, M. W.; Reveal, J. L.; Fay, M. F. A Subfamilial Classification for the Expanded Asparagalean Families Amaryllidaceae, Asparagaceae and Xanthorrhoeaceae: Asparagales subfamilial classification. *Bot. J. Linn. Soc.* **2009**, *161* (2), 132–136.
- (140) Berkov, S.; Osorio, E.; Viladomat, F.; & Bastida, J. Chemodiversity, chemotaxonomy and chemoecology of Amaryllidaceae alkaloids. In *The Alkaloids: Chemistry and Biology* **2020** (Vol. 83, pp. 113-185). Academic Press.
- (141) Kilgore, M. B.; Kutchan, T. M. The Amaryllidaceae Alkaloids: Biosynthesis and Methods for Enzyme Discovery. *Phytochem. Rev.* **2016**, *15* (3), 317–337.
- (142) Chen, H.; Lao, Z.; Xu, J.; Li, Z.; Long, H.; Li, D.; Lin, L.; Liu, X.; Yu, L.; Liu, W.; Li, G.; Wu, J. Antiviral Activity of Lycorine against Zika Virus *in Vivo* and *in Vitro*. *Virology* **2020**, *546*, 88–97.

- (143) Elgorashi, E. E.; Zschocke, S.; van Staden, J.; Eloff, J. N. The Anti-Inflammatory and Antibacterial Activities of Amaryllidaceae Alkaloids. *South Afr. J. Bot.* **2003**, *69* (3), 448–449.
- (144) Nair, J. J., & van Staden, J. Antifungal constituents of the plant family Amaryllidaceae. *Phytother. Res.* **2018**, *32*(6), 976–984.
- (145) He, M.; Qu, C.; Gao, O.; Hu, X.; Hong, X. Biological and Pharmacological Activities of Amaryllidaceae Alkaloids. *RSC Adv.* **2015**, *5* (21), 16562–16574.
- (146) Narahashi, T.; Moriguchi, S.; Zhao, X.; Marszalec, W.; Yeh, J. Z. Mechanisms of Action of Cognitive Enhancers on Neuroreceptors. *Biol. Pharm. Bull.* **2004**, *27* (11), 1701–1706.
- (147) Consolim-Colombo, F. M.; Sangaletti, C. T.; Katayama, K. Y.; Angelis, K. Y. D.; Moraes, T. L. de; Araújo, A. A.; Lopes, H. F.; Camacho, C. Y.; Bortolotto, L. M.; Michelini, L. M.; Irigoyen, M. M.; Barnaby, D. P.; Tracey, K. J.; Pavlov, V. A. The Acetylcholinesterase Inhibitor Galantamine Ameliorates Oxidative Stress in Subjects with the Metabolic Syndrome. *FASEB J.* **2020**, *34* (S1), 1–1.
- (148) Kornienko, A.; Evidente, A. Chemistry, Biology, and Medicinal Potential of Narciclasine and Its Congeners. *Chem. Rev.* **2008**, *108* (6), 1982–2014.
- (149) Van Goietsenoven, G.; Mathieu, V.; Lefranc, F.; Kornienko, A.; Evidente, A.; & Kiss, R. Narciclasine as well as other Amaryllidaceae isocarboxystyryls are promising GTP-ase targeting agents against brain cancers. *Med. res. rev.* **2013**, *33*(2), 439–455.
- (150) Meerow, A. W. A New Species of Eucrosia and a New Name in Stenomesson (Amaryllidaceae). *Brittonia* **1985**, *37* (3), 305.
- (151) Meerow, A.; Jost, L.; Oleas, N. Two New Species of Endemic Ecuadorean Amaryllidaceae (Asparagales, Amaryllidaceae, Amarylloideae, Eucharideae). *PhytoKeys* **2015**, *48*, 1–9.
- (152) Boit, H.-G.; Döpke, W. Alkaloide aus *Urceolina*-, *Hymenocallis*-, *Elisena*-, *Calostemma*-, *Eustephia*- und *Hippeastrum*-Arten. *Chem. Ber.* **1957**, *90* (9), 1827–1830.
- (153) Girault, L. *Kallawaya, guérisseurs itinérants des Andes: recherches sur les pratiques médicinales et magiques.* **1984** (No. 107). IRD Editions.
- (154) Lianza, M.; Verdan, M. H.; de Andrade, J. P.; Poli, F.; de Almeida, L.; Costa-Lotufo, L.; Cunha Neto, Á.; Oliveira, S.; Bastida, J.; Batista, A.; Batista Jr., J.; Borges, W. Isolation, Absolute Configuration and Cytotoxic Activities of Alkaloids from *Hippeastrum Goianum* (Ravenna) Meerow (Amaryllidaceae). *J. Braz. Chem. Soc.* **2020**.
- (155) Renault, J.-H.; Nuzillard, J.-M.; Maciuk, A.; Zeches-Hanrot, M. Use of Centrifugal Partition Chromatography for Purifying Galanthamine. **2009** U.S. Patent Application No. 11/722,004.
- (156) Knolker, H. J. *The Alkaloids.* **2017** Academic Press.
- (157) Cahlíková, L.; Macáková, K.; Zavadil, S.; Jiroš, P.; Opletal, L.; Urbanová, K.; Jahodář, L. Analysis of Amaryllidaceae Alkaloids from *Chlidanthus Fragrans* by GC-MS and Their Cholinesterase Activity. *Nat. Prod. Commun.* **2011**, *6* (5), 1934578X1100600.
- (158) Murayama, W.; Kobayashi, T.; Kosuge, Y.; Yano, H.; Nunogaki, Y.; Nunogaki, K. A New Centrifugal Counter-Current Chromatograph and Its Application. *J. Chromatogr. A* **1982**, *239*, 643–649.

- (159) Ito, Y.; Weinstein, M.; Aoki, I.; Harada, R.; Kimura, E.; & Nunogaki, K. The coil planet centrifuge. *Nature*. **1966**, *212*(5066), 985-987.
- (160) Bojczuk, M.; Żyżelewicz, D.; Hodurek, P. Centrifugal Partition Chromatography - A Review of Recent Applications and Some Classic References. *J. Sep. Sci.* **2017**, *40* (7), 1597–1609.
- (161) Weisz, A.; Scher, A. L.; Shinomiya, K.; Fales, H. M.; & Ito, Y. A new preparative-scale purification technique: pH-zone-refining countercurrent chromatography. *J. Am. Chem. Soc.* **1944**, *116*(2), 704-708.
- (162) Fang, L.; Liu, Y.; Yang, B.; Wang, X.; & Huang, L. Separation of alkaloids from herbs using high-speed counter-current chromatography. *J. sep. sci.* **2011**, *34*(19), 2545-2558.
- (163) Nováková, L.; Matysová, L.; & Solich, P. Advantages of application of UPLC in pharmaceutical analysis. *Talanta*, **2006**, *68*(3), 908-918.
- (164) Arrebola-Liébanas, F. J.; Romero-González, R.; & Frenich, A. G. HRMS: Fundamentals and Basic Concepts. In *Applications in High Resolution Mass Spectrometry 2017* (pp. 1-14).
- (165) Danishefsky, S.; Morris, J.; Mullen, G.; & Gammill, R. Total synthesis of dl-tazettine. *J. Am. Chem. Soc.* **1980**, *102*(8), 2838-2840.
- (166) Das, M. K.; Kumar, N.; & Bisai, A. Catalytic asymmetric total syntheses of naturally occurring Amaryllidaceae alkaloids, (–)-crinine, (–)-epi-crinine, (–)-oxocrinine, (+)-epi-elwesine, (+)-vittatine, and (+)-epi-vittatine. *Org. lett.* **2018**, *20*(15), 4421-4424.
- (167) Danishefsky, S.; Morris, J.; Mullen, G.; & Gammill, R. Total synthesis of dl-tazettine. *J. Am. Chem. Soc.* **1980**, *102*(8), 2838-2840.
- (168) Brine, N. D.; Campbell, W. E.; Bastida, J.; Herrera, M. R.; Viladomat, F.; Codina, C.; Smith, P. J. A Dinitrogenous Alkaloid from *Cyrtanthus Obliquus*. *Phytochemistry* **2002**, *61* (4), 443–447.
- (169) Ünver, N.; Gözler, T.; Walch, N.; Gözler, B.; Hesse, M. Two Novel Dinitrogenous Alkaloids from *Galanthus Plicatus* Subsp. *Byzantinus* (Amaryllidaceae). *Phytochemistry* **1999**, *50* (7), 1255–1261.
- (170) de Andrade, J. P.; Pigni, N. B.; Torras-Claveria, L.; Berkov, S.; Codina, C.; Viladomat, F.; Bastida, J. Bioactive Alkaloid Extracts from *Narcissus Broussonetii*: Mass Spectral Studies. *J. Pharm. Biomed. Anal.* **2012**, *70*, 13–25.

